MONTHLY NOTICES

OF THE

ROYAL ASTRONOMICAL SOCIETY

Vol. 94 No. 5

MEETING OF 1934 MARCH 9

Prof. F. J. M. Stratton, President, in the Chair.

The following candidates were proposed for election as Fellows of the Society, the names of the proposers from personal knowledge being appended :—

Marcel de Kerolyr, Assistant-observateur, Station d'Astrophysique de l'Observatoire de Paris, Forcalquier (B.A.), France (proposed by Mrs. Isaac Roberts) ;

B. S. Madhava Rao, M.Sc., Professor at the College of Engineering, Mysore University, Bangalore, India (proposed by K. B. Madhava) ; and

Cecil Frederick Wickes, 113 Ninth Avenue, Durban, S. Africa (proposed by W. N. Roseveare).

One hundred and fifteen presents were announced as having been received since the last ordinary meeting, including :—

Ch. Fabry, "Les Principes de la Photométrie en Astronomie et en Physique."

Paris Observatory, "Catalogue des étoiles doubles de la zone $+24^{\circ}$ de la carte photographique du ciel."

Mrs. Isaac Roberts, "Isaac Roberts' Atlas of 52 regions." Supplement to the edition commemorating Isaac Roberts' Centenary.

In connection with the communications read by Professor Zernike and Mr. Burch, a demonstration was held on the first floor during the second half of the meeting.

ERNEST WILLIAM HOBSON was one of the most distinguished Fellows of the Society. Beginning his career at Cambridge at a time when some knowledge of lunar and planetary theory was expected of all its mathematical residents, he gave considerable study to the subject over many years ; and his interest in the logical formulation of dynamical theory never left him. Senior Wrangler in 1878, he was very soon engaged as a Mathematical Lecturer at Christ's College ; in 1884 he was chosen as one of the four who were distinguished by the title of University Lecturers, the other three being Mr. Glazebrook, Mr. J. J. Thomson and Mr. Forsyth (*Reporter*, June 3). He became a member of the London Mathematical Society in 1887, and published the first of his papers in their Journal in 1888. This, on the conduction of heat, indicates the character of his work in those days, which became a study of the functions used in the mathematical physics and astronomical theory of that time. To mathematicians, the acumen and thoroughness with which, up to the end of his life, he influenced the analytical theory of such modes of expression needs no remark. But already, in the last decade of the century, his mind was turning from the applications of these functions to the logical theory of the functions themselves. In 1893 Dr. Forsyth, who as the Senior Wrangler of 1881 was specially distinguished for his knowledge of Hydrodynamics, had created a school of Mathematical Analysis in Cambridge, by the publication of his volume, of more than 600 royal octavo pages, on functions of a complex variable. In 1902 Hobson carried the change still further back to fundamentals, by his Presidential Address to the London Mathematical Society, on the Infinite and Infinitesimal in Mathematical Analysis. Those who were present must still remember the silence as he solemnly pronounced the words, " This was the first breach in the Infinite " ; and those who knew him had often heard of the impression which the volume of Louis Couturat, *De l'infini mathématique* (1896), had made upon him. In 1903 Hobson became Stokes lecturer. In 1910 he became Sadleirian Professor of Pure Mathematics ; and added, to the subjects on which he gave lectures, that of Calculus of Variations, which his predecessor in the Chair had introduced ; this office he resigned in 1931. In 1907 he published one large volume, *The Theory of Functions of a Real Variable* ; the second edition of this in two volumes, 1920 and 1925, contains in all 1450 royal octavo pages ; another volume, *The Theory of Spherical and Ellipsoidal Harmonics*, published in 1931 (500 pp., royal 8vo), applied to these functions the results of one of his great original papers, on the "Theory of Convergence." Less fundamental are his *Treatise on Plane Trigonometry* (1891), and his little volume on *Squaring the Circle* (57 pp., 1913), and two lectures delivered respectively at University College and at King's College, London. His Gifford Lectures at Aberdeen, on the Domain of Natural Science (1921–22), has reached a second edition ; it illustrates well the catholicity of his interest and the penetration of his intellect ; its earlier part is a careful exposition of his judgment of the limitations to which the contribution of natural science to our knowledge of the universe is necessarily subject. In 1912 he was a Secretary of the International Mathematical Congress held at Cambridge ; in the same year he

was President of Section A, at the meeting of the British Association in Sheffield.

He died on 1933 April 18.

He was elected a Fellow of the Society on 1895 June 14.

DIFFRACTION THEORY OF THE KNIFE-EDGE TEST AND ITS IMPROVED FORM, THE PHASE-CONTRAST METHOD.

F. Zernike.

(Communicated by Professor F. J. M. Stratton)

1. The well-known knife-edge test was introduced by Foucault in 1856, and its principle explained by geometrical optics.* It is clear, however, that for a mirror having deviations comparable with the wave-length, the wave theory must necessarily be used, and it thus provides the only possible way to find the limit of sensibility.† A simple example will show at once the peculiarities of the wave treatment, and suggest an improved form of test.

Let a spherical mirror be tested in the usual way by placing an artificial star near its centre of curvature, the mirror-surface being observed with the eye just behind the star-image. Suppose the mirror-surface to be slightly wavy, *i.e.* to deviate from the ideal spherical form by a train of sine waves having an amplitude of a fraction of a wave-length. For the present, these will be taken as depending on one co-ordinate only, and the whole mirror be treated as one-dimensional. This mirror will evidently act as a diffraction grating, giving only first-order spectra on both sides of the central image of the star. Let it be called a *phase grating*. It is clear that the three light cones emerging from the three star-images will give two systems of interference fringes, the first one resulting from the left-hand cone with part of the central one, the second in the same way from the right-hand cone. On a screen some distance behind the star-image these cones will give an illuminated circle that may roughly be considered as an image of the mirror-surface. Strictly speaking, a lens is used to produce a sharp image, on the retina or otherwise, but this is not essential.

The effect of the wavy surface may be compared with the case of a mirror made into a diffraction grating by waves of a different kind, viz. of periodically changing reflecting power. Let this be called an *amplitude grating*. Evidently we shall not need any knife-edge or other device to see the bright and dark stripes on this mirror. In agreement with this, the diffraction theory shows that in this case the three images of the light-source have equal phase, causing the two fringe systems mentioned above to coincide. Now the phase grating gives small differences of phase to the

* *Annal. Obs. Paris*, **5**, 203, 1859 ; *M.N.*, **19**, 284, 1859.

† Lord Rayleigh, *Phil. Mag.*, **33**, 161, 1917 ; S. Banerji, *Ap. J.*, **48**, 50, 1918, applied the wave theory to the knife-edge test in the case of discontinuities of the surface.

reflected vibrations, but this is equivalent to adding small vibrations 90° in advance of the main vibration. Therefore the diffraction images will be 90° in advance of the central star-image. This 90° change of phase will shift the first fringe system, caused by the left-hand spectrum, a quarter fringe to the right, the second system the same distance to the left. If no knife-edge is used, both systems appear, with the result that their differences of intensity cancel exactly. Therefore the wavy deviations of the mirror-surface remain invisible.

The simplest way to detect the deviations will be to intercept one of the lateral diffraction images by a knife-edge, the other one remaining to form interference fringes with the central image. Because of the quarter-fringe displacement, however, these fringes, as seen projected on the mirror-surface, will not coincide with the surface waves that cause them, but the maxima and minima will fall on the slopes of the wave, which thus appear alternately brightened and darkened.

If the knife-edge is brought in from the other side, the other system remains, and the waves on the mirror are seen shaded on the other side. This explanation of the well-known relief effect of the knife-edge is clearly quite different from the ordinary geometrical treatment.

The surface waves will also appear when one of the systems of interference fringes is shifted by half a fringe with respect to the other. We may attain this by reversing the phase of one of the lateral spectra by means of a glass plate with two halves of slightly different thicknesses. Such a "phase reversing plate" will evidently have the same effect as a knife-edge, as it leaves one of the systems of fringes unchanged.

Clearly it will be much better, however, to make a symmetrical arrangement, changing the phase of the central image by 90°. This is the newly proposed *method of phase contrast.* By this both systems of fringes are shifted a quarter fringe in opposite directions, bringing them into coincidence with each other and with the maxima and minima of the waves on the surface. Indeed, the diffraction images are in this way brought into phase with the central image, and the eye will see the phase grating as if it were an amplitude grating. The same phase-changing device will clearly make an amplitude grating appear as a phase grating. Indeed, as an experimental test of our diffraction theory, a wire grating may be put in front of a mirror, and the phase of the central image changed by 90°. The opaque bars of the grating are then hardly visible.

Changes of phase in adjacent parts of the light are in all cases easily attained by glass plates, of which one surface has been partly etched away. As Lord Rayleigh indicated long ago, dilute hydrofluoric acid removes the glass surface very evenly, leaving a flat surface lying a fraction of a wave-length, or even a few wave-lengths, below the original surface. The depth attained is easily tested by means of Newton's rings.

The test case of a mirror with a single sine wave on its surface having shown that the phase-contrast method renders the deviations of the surface as an exactly corresponding sine wave of intensity, it is to be expected that the same method will render small deviations of arbitrary arrangement as

proportional changes of intensity. By the following quite different treatment we shall find the effect of arbitrarily large deviations of the surface.

2. The optical arrangement for testing mirrors, or optical systems generally, by observing the surface of the mirror, or generally the aperture of the system, may be considered as a case of optical image formation of a non-luminous object—the surface of the mirror, etc.—with the aid of waves from a point-source. The exact theoretical treatment of the case is provided by the diffraction theory which Abbe proposed for microscopic images. As a general result of this theory, Lummer states that "if all the diffraction spectra of the light source can pass unmodified, the image will be exactly similar to the object in structure and phase." *

The principle of the phase-contrast method will now be elucidated by a vector diagram of the vibrations as they leave the mirror. Let each vibration be represented in the usual way by a vector, the length of the vector representing the amplitude, its angle with a fixed direction the phase angle of the vibration. The advantage of this kind of representation lies in the fact that composition of vibrations (interference) corresponds to composition (addition) of the vectors in the diagram.

Imagine the mirror to be divided into a large number N of surface elements of equal size. Let N vectors be drawn from the origin to represent the vibrations from all the elements. In the figure their terminal points only have been inserted. For an ideal mirror these points would all coincide, *e.g.* in M differences of reflecting power would give points on OM, while in our case—differences of height, changing the phases only—the N terminal points will lie on the circle through M, higher and lower parts of the mirror-surface corresponding respectively to points like P and P'. According to the statement of Lummer, quoted above, the same diagram will represent the amplitudes and phases in the image of the mirror, when no modification of the diffraction images has been introduced as yet. Now if the light from the central star-image only were admitted to form the image, this would be uniformly illuminated. As the light-paths to the central image are all equal, its representing vector will be found by adding all N vectors. In order to find the vector representing the vibration in the uniform image, the resulting sum must be divided by a certain factor. From the case of the perfect mirror which forms no lateral diffraction spectra, it is clear that this factor must be equal to N. This means that the effect of the central image alone is represented in the image of the mirror by a vector OG, where G is the centre of gravity of the N terminal points. Interception of the central image will therefore result in a subtraction of the vector OG from every vibration in the image, *i.e.* the origin of the vector diagram is shifted to G. In the phase-contrast method, however, the central pencil is not removed, but changed in phase, *e.g.* by 90°. The effect of this will be found by subtracting OG and adding the vector O_1G, if the phase has been advanced, or O_2G if the phase has been retarded. As a result the origin of the diagram is shifted to O_1 or to O_2. As the eye or the photographic plate can merely perceive the intensity and not the phase, observation

* *Handwörterbuch d. Naturw.*, I, 35, 1912.

will yield the squares of the distances from the new origin. Therefore higher parts of the mirror will appear brighter, and lower parts darker than the mean illumination in the first case (O_1), and reversely in the second case (O_2).

The diagram shows at once that this method will be very sensitive. Thus if MP' be one-tenth of the radius, the change of intensity will be about 20 per cent. and still visible. The retardation corresponding to this is only one-tenth radian or $\lambda/60$. The method will indeed be specially suitable to make very accurate surfaces, for which the centre of gravity G will lie near M. On the other hand, a surface with large deviations will give terminal points all around the circle, and this may result in a position of G near O. In such a case the method will not be of much use. It is different, however, if only the smaller part of the mirror deviates largely from the

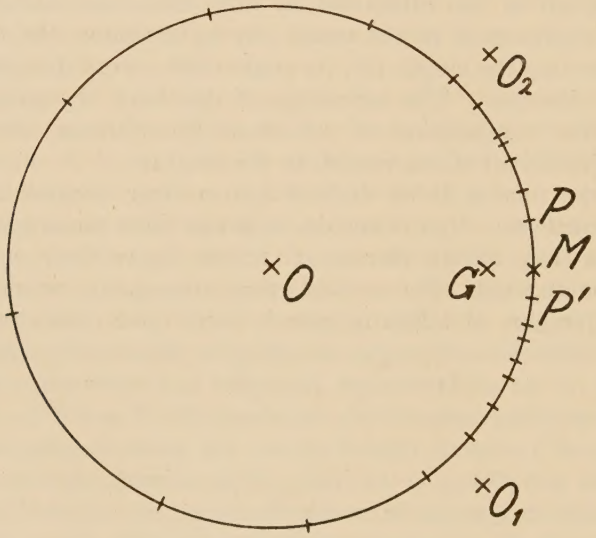

FIG. 1.

perfect form. The larger part will then assure that G and therefore O_1 lie far enough from O. Points on the mirror corresponding to the point on the circle nearest to O_1 will then appear with minimum brightness. The smaller, deviating part of the mirror will therefore be seen crossed by dark lines of equal deviation, the error in light-path increasing by one wave-length on going from one line to the next. This is exactly the same effect as Newton's rings that would be seen by applying a test glass to the mirror.

3. In the foregoing exposition of the principles of the phase-contrast method we have tacitly assumed that the central star-image can be changed in phase without influencing the diffraction spectra. This cannot be strictly true, as the star-image is not a sharply limited disc, but a diffraction pattern with concentric rings. This must especially be taken into account when the spectra lie near the central image, *i.e.* in the case of deviations of long period. An exact mathematical treatment of the problem has been worked out in the case of deviations small compared with the wave-length. We shall here give a short account of this treatment and of the relatively simple resulting

formulæ, referring for the proofs to the elaborate paper shortly to appear in *Physica*, where also a fuller treatment of the knife-edge test will be found.

In the following we shall denote by x, y, or r, ϕ the rectangular or polar co-ordinates on the surface of the mirror or in its image, by ξ, η, or ρ, ψ the co-ordinates in the plane of the star-image, and by $\mathfrak{J}_n$ the Bessel function of nth order.

The diffraction image of a point-source formed by a perfect mirror was calculated by Airy with the well-known result that the amplitude is given by $\mathfrak{J}_1(\rho)/\rho$ if the unit of ρ is adequately chosen. Our first problem is to determine the small changes of this function caused by small deviations of the mirror-surface that are given as an arbitrary function of x and y. The second problem will be to find the diffraction effect in the image plane caused by the vibrations in the focal plane.

We develop the arbitrary function that determines the errors of the mirror-surface in a series of functions that are adapted to our problem. There can be little doubt that these functions should be polynomials in x and y. Indeed, the simplest errors are polynomials of low degree, *e.g.* astigmatism (2nd degree), spherical aberration (4th degree), etc. Instead of using a power series, however, it will prove more expedient to develop in a series of *orthogonal* polynomials. Clearly these should be orthogonal on the circular area of the mirror. Expressed in terms of r and ϕ, these *circle polynomials* were found to have the form $R_n^m(r)\sin m(\phi-\alpha)$ where $n-m$ is even, $m \leq n$, and R is a finite hypergeometric series (Jacobi polynomial):

$$R_n^m(r) = (-)^{\frac{n-m}{2}} \binom{\frac{n+m}{2}}{m} r^m F\left(\frac{n+m+2}{2}, -\frac{n-m}{2}, m+1, r^2\right)$$

$$= \frac{r^{-m}}{\left(\frac{n-m}{2}\right)!}\left(\frac{d}{d(r^2)}\right)^{\frac{n-m}{2}}\left\{r^{n+m}(r^2-1)^{\frac{n-m}{2}}\right\}$$

the constant being chosen in such a way that $R_n^m(1) = 1$.*

For the lowest degrees we give the polynomials explicitly :

m \ n	0	1	2	3	4	5	6
0	1	...	$2r^2-1$	...	$6r^4-6r^2+1$	...	$20r^6-30r^4+12r^2-1$
1	...	r	...	$3r^3-2r$	...	$10r^5-12r^3+3$	...
2	...	...	r^2	...	$4r^4-3r^2$	...	$15r^6-20r^4+6r^2$
3	...	...	...	r^3	...	$5r^5-4r^3$	...
4	...	...	...	...	r^4	...	$6r^6-5r^4$
5	...	...	...	...	...	r^5	...
6	...	...	...	...	...	...	r^6

* These formulæ and the properties of the circle polynomials as used in the calculations would seem to be new. The polynomials were found to be a kind of zonal harmonics in four dimensions. A different set of polynomials orthogonal on a circle was investigated by F. Didon, *Ann. Ec. Norm.*, **7**, 247, 1870.

If now the arbitrary deviation of the mirror-surface is represented by a series of these polynomials, it will be found that the terms with $r \sin \phi$, $r \cos \phi$, and $2r^2 - 1$ do not represent real errors, but can be made to vanish by adjusting the mirror. Except these three, every term of the general

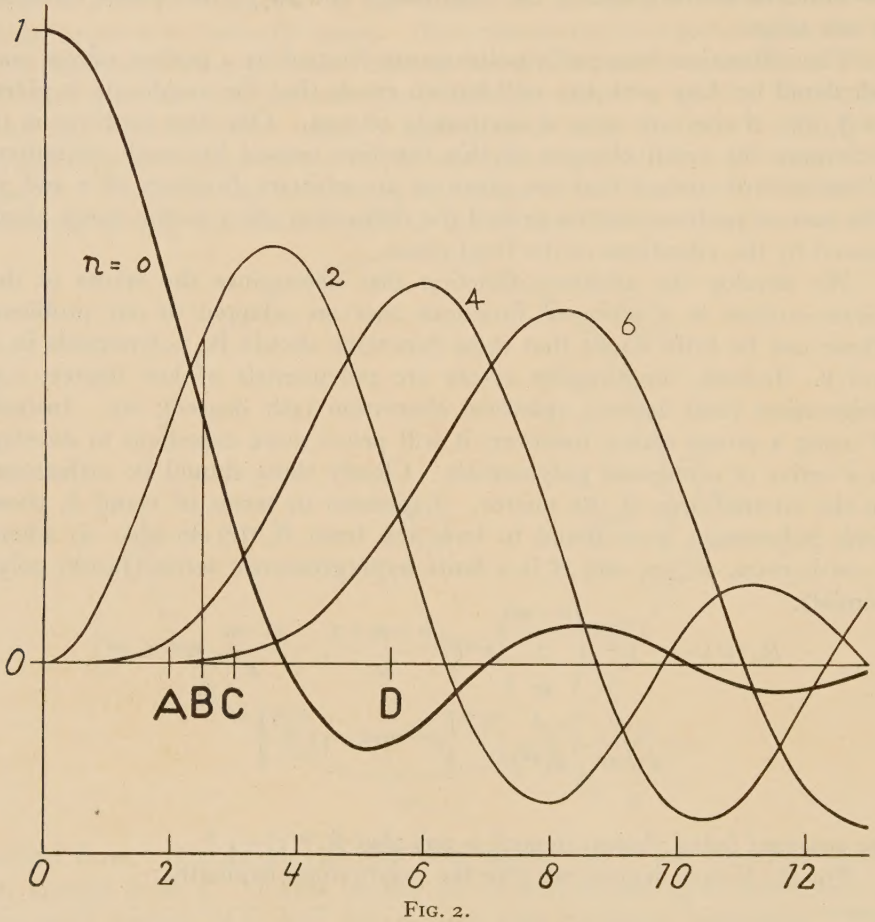

FIG. 2.

form $C_{nm}R_n{}^m(r) \begin{matrix}\sin m\phi \\ \cos m\phi\end{matrix}$ may be said to represent an "error" of nth order, the magnitude of which is given by the coefficient C_{nm}.

The diffracted amplitude caused by the error $C_{nm}R_n{}^m \cos m\phi$ is found for n even, by calculating

$$C_{nm}\int_0^1\int_0^{2\pi} \cos\{r\rho\cos(\phi-\psi)\}R_n{}^m(r)\cos m\phi\, r dr d\phi = (-)^{\frac{n}{2}} 2\pi C_{nm}\rho^{-1}J_{n+1}(\rho)\cos m\psi$$

and similarly for n odd and for $\sin \phi$. In this result the radial factor is independent of m. In fig. 2 the functions $(2n+2)\rho^{-1}J_{n+1}(\rho)$ are represented for $n = 2, 4, 6$ together with the pattern for the perfect mirror ($n = 0$).

The curves of fig. 2 show that the central part—the spurious disk—of the diffraction pattern of the perfect mirror is not changed by small errors

of any order, and that such changes as occur lie farther and farther from the centre as the order is increased.

Clearly the pattern for a perfect mirror corresponds to the central star-image in the test case of § 1, while the changes of the pattern caused by deviations of the surface correspond to the diffraction spectra. The phase-contrast method, which requires us to change the phase of the central image only, can therefore be used without difficulty in the case of errors of higher orders. For the lowest orders it will be necessary to use a glass plate with a minute circular disk of differing thickness—a phase disk—of a size adapted

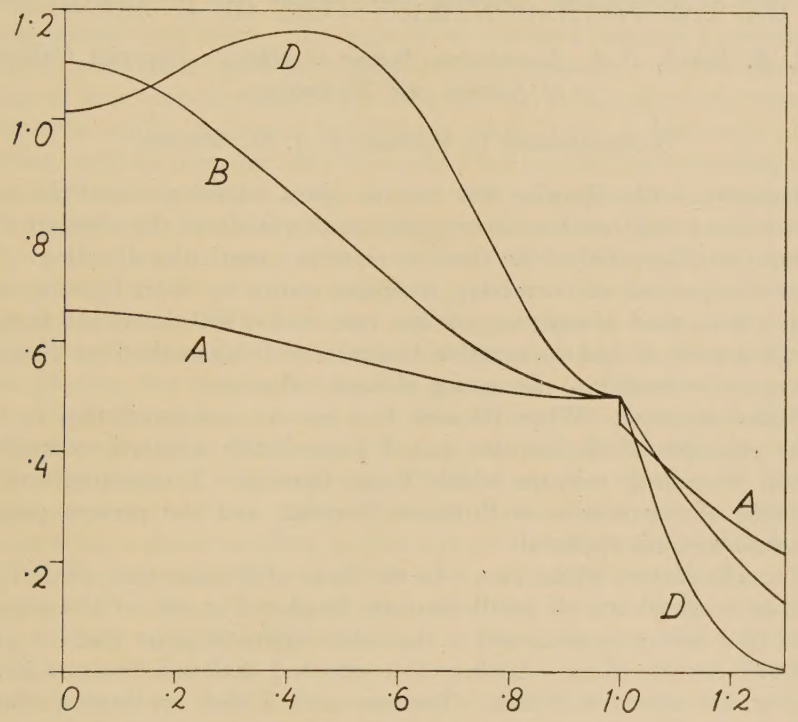

Fig. 3.

to the case. To detect astigmatism, the radius of the phase disk should be taken as 2·5 in the units of fig. 2 (point B); for spherical aberration, and any higher orders as well, the radius might be as large as 5·5 (point D). Of course the central image is more or less disturbed by such phase disks. This means that even a perfect mirror will no longer be seen as a uniformly illuminated circle, as it is without the disk. This effect of the change of phase can be calculated by a second integration of much the same kind as the first one. Fig. 3 shows the resulting intensity for phase disks of different radii. Any radius between A and C in fig. 2 will give practically the same uniform intensity, the increase of intensity towards the centre (curve B) being automatically compensated by a slightly different adjustment of focus. Larger phase disks, as D, give a somewhat higher intensity, but would seem less good in all other respects. The unit in fig. 2 being $\lambda F/\pi D$ for a relative

aperture D/F, the diameter of the phase disk should be less than $2\lambda F/D$, and preferably from 60 to 90 per cent. of this value (range $A - C$). In all cases part of the light is thrown outside the image of the mirror, forming broad diffraction rings round it. Their appearance gives a sensitive criterion for the exact centring of the phase disk on the star-image.

ON THE PHASE-CONTRAST TEST OF F. ZERNIKE.

C. R. Burch, B.A., Leverhulme Fellow in Optics: Imperial College of Science and Technology.

(Communicated by Professor F. J. M. Stratton)

Summary.—The Zernike test has the great advantage over the knife-edge test, as a null test for mirror systems, that it shows the absolute error, and not the differential of the absolute error in a particular direction. This makes the process of correcting irregular errors by local figuring much easier. A method of carrying out the test, which will detect 0·1 fringe of error, is described, and the practical limitations of this method are discussed, with special reference to the testing of large reflectors.

Acknowledgment.—When I learnt, in a private communication in 1933, of the principle of the Zernike test, I immediately resolved to apply the method to testing mirrors which I am figuring. I communicated the substance of my results to Professor Zernike, and the present paper is published with his approval.

§ 1. *The Nature of the Test.*—In the form of Zernike test which I have used, an artificial star of small diameter is placed at one of the stigmatic points of a mirror system, and at the other stigmatic point there is placed the small circular phase-retarding disk, which I shall refer to as a Zernike disk, or, for short, a Z-disk. The star and Z-disk are both preferably somewhat smaller than the Airy disks of the system at the points at which they are respectively placed. The eye of the observer is placed close behind the Z-disk, and he looks either directly at the mirror under test, or at its image in any auxiliary mirrors which may come between it and him. He then sees interference fringes formed between the wave leaving the mirror and the supplementary wave to which its passage through the Z-disk gives rise. If the Z-disk is not larger than the Airy disk produced by the system, that part of the supplementary wave lying within the cone of light proceeding from the mirror will be substantially spherical, so that since the wave-front leaving the mirror system departs from sphericity only by the errors of the mirror under test, the fringe system seen (in a given colour) will be substantially the Newton-ring system which would be seen if a true-figure test-plate were laid on, or very close to, the mirror under test. The colour-sequence of the fringes will be determined by the chromatic dispersion of phase retardation of the Z-disk, and can be ascertained from the colour

changes which occur when the Z-disk is moved out of focus, and when it is decentred.

§ 2. *Making Zernike Disks.*—In setting up the test, the making of suitable Z-disks was the first problem. Their diameter must be comparable with that of the Airy disk (·01 mm. for an F/8 image) : their thickness must be a small number of wave-lengths in order that the Zernike fringes shall show a good colour contrast. Clearly the best thickness will be comparable in magnitude with the best thickness for a phase-retarding knife-edge, and material giving good dispersion for such a knife-edge will also give good dispersion for a Z-disk. I therefore first made phase-retarding knife-edges of collodion, Canada balsam and resin. The resin films—pressed between a microscope slide and cover-glass—gave the strongest colour contrast : the best thickness was that at which interference fringes in the air film at the edge of the resin just ceased to be visible at normal incidence in white light. I then made phase-retarding strips by pressing resin fibres, for I had noticed that exceedingly fine fibres can be drawn from a blend of resin with a few per cent. of turpentine which I had used for polishing tools. The procedure is to dip two rods into the molten resin : touch them together and jerk them apart. Fibres ·01 mm. diameter can be drawn in this way easily, and I succeeded in drawing one ·002 mm. diameter. When laid on a slide and capped with a cover-glass, the fibres could be pressed into strips at room temperature. It is advisable, before pressing the fibre, to let down a spring clip gently on to one edge of the cover-glass, and then to tack the other edge to the slide with balsam, to prevent lateral motion during the pressing, which is done under the microscope, with a metal rod, and repeated all along the fibre, until Newton fringes are seen (in white light) while the pressure is applied. The fibre does not stick to the cover-glass, so that it is not torn if the cover-glass springs up when the pressure is relaxed. I found it necessary to re-press some fibres a few days after they were made, but after that they no longer tended to return to their original cylindrical shape. Obviously the next step was to make spheres of resin and press them into disks. Spheres of all sizes from ·05 mm. down to ·001 mm. or less are precipitated when a 5 per cent. solution of resin in acetone is poured into twenty times its volume of water. (The addition of turpentine is only necessary for drawing fibres.) Those that remain in suspension for 12 hours may be rejected as too small : those that settle in one hour are too big. I have tried distributing the globules over a slide with a needle : the difficulty is that they tend to stick to each other in chains, and also to stick to the needle, which one must "twang" to release them. By the time I had parted the chains, I had smeared and cracked many of the globules. However, even the fragments became reasonably circular on pressing. I find it better to distribute them in water. The procedure is : Dilute the suspension until it looks only faintly milky ; pour a few drops on to a slide : shake off the excess, and allow the remaining film to dry before putting the cover-glass on. If you put the cover-glass on while the film is wet, the surface tension of the water pulls the globules into chains as it dries. The cover-glass is then tacked with balsam and pressed, under the microscope. Precautions should be taken to keep out dust while

assembling the slide, and it is advisable first of all to obtain Newton rings between slide and cover-glass—in doing so one crushes foreign matter which the cleaning process has failed to remove. In this way one produces a slide containing perhaps 100 Z-disks, ranging from ·02 mm. to ·002 mm. diameter, many of them of the right order of thickness, and reasonably circular.

§ 3. *The Focussing Carriage and "Star."*—The slide of Z-disks is mounted on a focussing carriage which is a geometrical slide running on bicycle balls, and fitted with three micrometer screws, controlling the vertical and horizontal and focal position of the slide. The carriage is clamped to a levelling table, so that the focussing track can be pointed exactly parallel to the optic axis. As "star" I use a pinhole, on which is focussed through a right-angle prism the filament of a 16-watt gas-filled lamp of the type used in railway signalling. The image is the same size as the filament, the diameter of which exceeds the diameter—·013 mm.—of the largest pinhole I have used. The filament is coiled in a fairly close helix, so that even with an uncorrected condensing lens the star gives a practically uniform cone of light up to F/8. The intensity is sufficient for testing with two reflections from silver plus two from unsilvered glass at normal incidence. The smallest pinhole I have used is ·005-mm. diameter (just small enough for testing at F/4): it gives enough light for testing with one reflection from unsilvered glass, but not with two. The ·005-mm. pinhole was made by resting the point of a mounted needle, which had been honed on an Arkansas hone, on a sheet of aluminium foil ("tinfoil") lying on a glass plate. Only a few per cent. of piercings are successful, most producing slots at least two widths long. Even the best piercing did not approximate to a circle more closely than does a square. One can also find natural holes of this order of smallness in "tinfoil."

§ 4. *The Test Procedure.*—The slide of Z-disks is set several mm. out of focus, and the observer, with his eye close behind the image, looks at the illuminated mirror. As he moves the centring screws, so as to traverse the slide across the cone of light, he will see circular patches, surrounded by rings, moving across the mirror. Each of these is the system of interference fringes created by a Z-disk: there is no difficulty in finding them, because the slide contains very many Z-disks. One is centred, and the focussing track is levelled and adjusted in azimuth so that the fringe system stays central when the Z-disk is taken through focus. It will be noticed that the Z-disks are not all identical, the fringe systems which they give differing in the colour of the central patch, which may be almost any colour, weak or strong, or neutral tint, or simply brighter than the general level of intensity of the rest of the mirror. They differ also in the number of rings which can be discerned surrounding the central patch.

In making the Zernike test for the first time, one is naturally tempted to select, out of the many Z-disks whose fringes can be seen when the slide is out of focus, that one which gives the most vividly coloured fringes. But consider what the conditions are for the production of brilliant fringes some distance out of focus. They are (*a*) that the chromatic dispersion of phase

retardation of the Z-disk shall be good, (*b*) that the supplementary wave created by the passage of light through the Z-disk should be comparable in amplitude with the wave leaving the mirror; this can only be so if an appreciable part of the light leaving the mirror traverses the Z-disk—that is, if the diameter of the Z-disk is an appreciable fraction of the diameter of the cone of light at the plane of the Z-disk ; this implies again, if the Z-disk is some distance out of focus, that its diameter should *not* be as small as that of the Airy disk formed at focus. Now the only circumstances under which we can be sure that the sphericity of the supplementary wave created by the Z-disk will be inappreciably affected by the errors of the mirror, and at the same time that the amplitude of the supplementary wave will be comparable with that of the wave leaving the mirror—so that the mirror errors shall show up in strong interference contrast—are that the Z-disk should be comparable in size with the Airy disk, and that it should be situated thereon, very nearly at focus. Such a Z-disk will necessarily give a weak supplementary wave when some distance out of focus, and its interference fringes will then be heavily diluted with uncoloured light. We must therefore reject those Z-disks which show brilliant colours some distance off focus, and choose one which shows very faint and ghostly fringes.

It is convenient to specify the distance of the Z-disk from focus in terms of the apparent error of the mirror in interference fringes (half wave-lengths), temporarily assuming "true figure" to be that which would focus where the Z-disk happens to be : the merit of this specification is that the fringe system given by a Z-disk depends essentially on its number of fringes off focus, whatever may be the focal ratio of the image. [To convert mm. axial distance off focus into fringes off focus, divide 250 by the square of the focal number of the image : the quotient is the number of fringes off focus per mm. off focus—thus F/16 gives one fringe per mm. This assumes $\lambda = 5 \times 10^{-5}$ cm.]

We can now apply a second check that the Z-disk is small enough, for if we put it a *small* number, *n*, of fringes inside or outside focus, it ought to show just *n* concentric fringes on the mirror (unless the mirror errors exceed one fringe). If we make *n* large, we shall not see *n* fringes for two reasons : first, because the source is not monochromatic, and the scale of the fringes depends on wave-length; and, second, because of the finite size of the source, which destroys the visibility of the higher-order fringes. One can just see the second fringe with a ·013-mm. source and an F/8 image (for which ·013 mm. is really rather too large). With an F/16 image about 4 fringes are visible.

At the same time, we can check that the Z-disk is sufficiently circular. If the fringe system is circular both inside and outside focus, then the Z-disk is circular, and the mirror has no astigmatism. An elliptical fringe system can be due to astigmatism or to an elliptical Z-disk. But if the ellipticity is due to astigmatism, the major axis of the ellipse will be perpendicular to the focal line to which the Z-disk is nearest, so that if the ellipse is elongated vertically inside focus it will be elongated horizontally outside focus : on the other hand, if the ellipticity is due to the Z-disk, the

major axis of the ellipse will have the same direction as the major axis of the Z-disk, and the fringe system will be elongated in the same direction both inside and outside focus. Finally, we have yet another check that the Z-disk is sufficiently small : if the Z-disk is smaller than the Airy disk of the mirror, the supplementary wave to which it gives rise will spread through a wider cone than does the light from the mirror, so that we shall see the mirror surrounded by a halo of light, the outer diameter of which may be 50–70 per cent. greater than the diameter of the mirror. The intensity of the halo is proportional to that of the light traversing the Z-disk, so that the halo is only visible when the Z-disk is within a fringe or two of focus, and if the mirror errors exceed a fringe or two (so that "focus" is indefinite) the halo may be too faint to be seen. A Z-disk that is too large gives a very narrow halo, unless it has inclusions or cracks : these may give a wide halo, but because of their irregularity they give a secondary interference pattern in the halo, making it patchy. A large Z-disk with a small circular concentric inclusion would pass the "halo" test of suitability, but would have been rejected on the previous tests. (I have not found a Z-disk of this type.) Some Z-disks produce a coloured halo—blue, green or red. This, then, is the colour of the supplementary wave which they are creating : they are, in fact, absorbing selectively. I think this is due to interference in the air film between the Z-disk and the cover-glass, for some Z-disks look coloured under the microscope. It is presumably wise to reject a Z-disk giving a deeply coloured halo, for a Z-disk which produces absorption alone (without phase shifting) will show errors of opposite signs in the same colour, giving the same colour-sequence inside and outside focus (such a Z-disk should be rejected), and presumably one which produces absorption plus phase shifting will not give so good a colour contrast between "high" and "low" errors as one producing phase shifting alone.

We can now consider the colours developed by the Z-disk on the mirror. When the Z-disk is, say, 3 fringes out of focus, the fringes will be faint and neutral tinted. But as it is brought nearer focus, colours will develop if it is of the right thickness. It will in general be found that the central colour of the fringe system is not the same inside and outside focus : for example, we may get blue and yellow, or green and red, depending on the thickness of the Z-disk : this is the effect that a Z-disk which retards the phase of some colours by $m \pm \frac{1}{4}$ periods produces. If the phase retardation is $\frac{1}{4}$ period for all colours, the central inside and outside focus colours will be black and white respectively : such a Z-disk can be used for the test, but I prefer to work with one giving a contrast of tint rather than of amplitude. Select then a Z-disk showing a good contrast between its inside- and outside-focus colours, but, above all, do not select a Z-disk on account of its good colours unless the preceding tests have shown that it is sufficiently small. I cannot too strongly emphasise this point. If one uses a Z-disk that is too large, it will create a supplementary wave containing a part of the short-period error and nearly the whole of the long-period error of the mirror, so that while it will show up local irregularities nearly as well as a smaller Z-disk, it will fail to show up long-period errors—simple spherical aberra-

tion, and more especially the two errors of longest period, astigmatism and error of absolute focal position. A test with a Z-disk that is too large is, in fact, exactly like testing a flat with a straight-edge that sags under its own weight: the local humps show up, but slow curvature does not. Therefore, even if one is not interested in determining the absolute focal position, it is essential to verify that it can be determined with precision—that a change of, say, $\frac{1}{2}$ fringe in the focal position does change the fringe system by $\frac{1}{2}$ fringe, as a proof that the Z-disk is small enough.

The foregoing considerations, then, provide a means of ascertaining from the appearances seen on the test itself whether a given Z-disk is a good one or not, so that while it is convenient to inspect the Z-disks with a microscope during their manufacture, it is by no means essential to pick out a good one with a microscope, and to ensure that that Z-disk, and no other, is used for the test.

§ 5. *The Interpretation of the Test.*—If the errors do not exceed $\frac{1}{4}$ to $\frac{1}{2}$ fringe, the interpretation of the test presents no difficulty, for by putting the Z-disk a fringe or so out of focus, one can superpose a general spherical error larger than the residual errors without making the colours too faint to identify, and one can even superpose an error of tilt by decentring the Z-disk when it is slightly out of focus: this is equivalent to the process of lifting one edge of a contact interference test-plate, to see how the colour-sequence runs; but there is the slight difference that if the Z-disk is inside focus we must imagine a hypothetical test-plate with its centre attached to the Z-disk to be making contact to the outside of the mirror-surface, this test-plate being slightly convex with respect to the mirror; so that as the Z-disk is decentred, it rolls the hypothetical test-plate over the mirror, and the fringe system moves in the same direction as the Z-disk, expanding as it approaches a hill and contracting when it gets to the top: contracting when it approaches a hollow and expanding when it gets to the bottom. If the Z-disk is outside focus, we must imagine the hypothetical test-plate to be slightly concave with respect to the mirror, and to be making contact to the inside of the mirror-surface from the back; so that as it is rolled over the back of the mirror-surface, the fringe system moves in the opposite direction to the Z-disk, and the pattern contracts when it approaches a hill, expanding when it gets to the top: expands when it approaches a hollow and contracts when it gets to the bottom.

If one decentres the Z-disk at focus, the visibility of the fringes fades very rapidly, as the Z-disk approaches the first zero of the Airy rings, and the supplementary wave is no longer created.

We have, further, the rule that the primary colour developed centrally inside focus will be the colour in which areas up to about $\frac{1}{4}$ fringe high will show when the Z-disk is at focus, and the primary outside focus colour will be that in which areas up to about $\frac{1}{4}$ fringe low will show.

Let us take as an example a test on a spherical speculum 12·5 cm. diameter, 200 cm. radius of curvature. When the chosen Z-disk was set 3 fringes inside focus, 3 fringes showed in faint nondescript colours, the third being so faint as to be only just distinguishable. When it was set $\frac{1}{2}$ fringe

inside focus it produced a halo round the mirror, extending to about 18 cm. diameter. The fringe system on the mirror consisted of a blue central patch outside which the colour shaded through neutral tint into a tawny yellow, which in turn shaded into a very pale yellow near the edge of the mirror. The fringe system was not exactly circular—traces of the residual errors could, in fact, be seen "through" the $\frac{1}{2}$-fringe focussing error. When the Z-disk was set $\frac{1}{2}$ fringe outside focus, the central patch was deep tawny yellow, surrounded by neutral tint shading into blue-white, and to very pale yellow near the edge of the mirror: traces of residual error marred the precise regularity of the system.

When the Z-disk was set at focus neither the blue nor the deep tawny yellow were fully developed on any part of the mirror: there were, however, irregular patches where the neutral tint which covered most of the mirror shaded into a very weak blue or tawny yellow.

From the appearances $\frac{1}{2}$ fringe inside and outside focus, I interpret the colour-sequence for this Z-disk when at focus as follows:—

Very pale yellow to deep tawny yellow ...	$\frac{1}{2}$ to $\frac{1}{4}$ fringe low.
Deep tawny yellow to neutral tint ...	$\frac{1}{4}$,, 0 ,, ,,
Neutral tint to blue	0 ,, $\frac{1}{4}$,, high.
Blue to very pale yellow	$\frac{1}{4}$,, $\frac{1}{2}$,, ,,

The patches, where with the Z-disk at focus the neutral tint changes to weak blue or tawny yellow, I interpret as being about $\frac{1}{8}$ fringe high or low. I have done a Michelson test on this mirror, and did not find more than about $\pm 0{\cdot}1$ fringe error. I had, of course, seen the existence of these errors on the knife-edge test, and indeed had reduced them to their present value by local figuring, testing with vertical and horizontal knife-edges in succession. But the interpretation of irregular error from a pair of knife-edge tests is by no means easy, especially when one is nearing the limit of sensitivity of the test, and I was not sufficiently certain of the interpretation to continue the local figuring. The great value of the Zernike test is not that it may be somewhat more sensitive, nor even that it is free from the disadvantage of producing logarithmically infinite illumination at the edge of the mirror (the "Rayleigh ring" of the knife-edge test), but that no matter how complicated the errors may be, the colours indicate the errors themselves, and not the slope of error in some particular direction.

To check the Zernike test on a system whose error could be easily measured by other methods, I made a mirror of the alloy Cu_4Sn, 7·5 cm. diameter, 75 cm. radius of curvature, with $\pm \frac{1}{4}$ fringe of oblate error, the centre and edge being $\frac{1}{4}$ fringe high and the intermediate zone $\frac{1}{4}$ fringe low (as determined by zonal knife-edge measurements). When the Z-disk was set at the mean focal position, it showed a patch of primary inside focus colour (blue) at the centre, and a ring of blue round the edge, with a ring of yellow (primary outside focus colour) in between. This mirror has since provided a remarkable demonstration of the development of irregular error: after a few weeks the knife-edge shadows showed mottled patches superposed on the spherical aberration: clearly the mirror had become irregular,

but the precise shape of the individual irregularities was extremely difficult to deduce from a pair of knife-edge tests. The Zernike test now shows patches, about 4 mm. diameter with sharply defined edges, contrasting markedly in colour with their surroundings. When one so focusses the Z-disk that the surroundings show primary low colour, the patches in general show primary high colour : they must be about $\frac{1}{2}$ fringe high. Apparently blocks of crystals in the casting have slipped. The casting was not a good one : it has flaws which seem to penetrate right through it, and I would not have used it for any other than a "pathological" mirror. I have not seen this effect with any other metal mirror.

§ 6. *Interpretation of the Test with Large Errors.*—When the mirror has several fringes error, the visibility of the fringes with a small Z-disk may be reduced, owing to the spread of the image, to substantially nil, and it may be necessary, in order to see fringes at all, to use a Z-disk so large that that part of the supplementary wave which it creates from the contribution to the incident wave arising from a given small portion of the mirror is not spread over the solid angle fed by the whole mirror, but has appreciable amplitude only in the neighbourhood of that part of the incident wave that produced it. The fringes seen on any part of the mirror then approximate to those which would be seen on that part if the remoter parts of the mirror did not exist, and an area shows the primary inside or outside focus colours (which, were the Z-disk small, we would interpret as meaning up to $\frac{1}{4}$ fringe high or low respectively), not because it is high or low with respect to the true figure, but because the Z-disk is inside or outside the focus of the area in question. The primary colours appear, in fact, at those parts of the mirror which make internal or external contact with any parallel to the true figure. Thus, so far as removal of the errors by figuring is concerned, we may safely polish any zone which shows primary inside focus colour when the Z-disk is set in the desired focal position, but it will not necessarily be possible to attain the true figure without polishing some zone that shows primary outside focus colours at the beginning of the figuring process, for some zone, although above the true figure, may be surrounded by a zone which is higher still.

Secondary colours—orders of interference higher than the first, which are usually of nondescript tint—will surround the primary colours, and will move with them when the Z-disk is decentred, and it is possible for the secondary fringes associated with the primary inside focus colour (interferences of the $+1$st, $+2$nd . . . $+n$th order) to move through the fringes associated with the primary outside focus colour (interferences of the -1st, -2nd . . . $-n$th order) when the Z-disk is decentred : we may expect visibility to be lost rapidly in the process.

As an example of this let us consider a Zernike test which I made on a slightly astigmatic prolate spheroid 11·2 cm. diameter, 231 cm. radius of curvature, before I realised the importance of choosing the smallest Z-disks with which the Zernike fringes are visible.

Starting well inside focus (for all zones of the mirror), I chose a Z-disk giving a fringe system consisting of a blue centre, bordered by neutral tint and then pink, followed by nondescript-coloured fringes of second and

higher orders. The blue patch increased in size as the Z-disk was centred, showing that the centre had a shorter focal length—in fact, that the mirror was prolate. On approaching mean focus the blue patch expanded, until when it was 3–4 cm. diameter it began to develop a pink centre : clearly the Z-disk was now just outside the focus of the central zone. There were then three bright and two dark fringes surrounding the outer pink border of the blue patch : the whole pattern was quite circular. Thus it seemed that the aspherical error of this mirror must be simply $2\frac{1}{2}$ fringes (of some visible wave-length) of prolate departure from the sphere of closest fit to the centre. On moving the Z-disk farther out, the pink centre expanded to 4 cm. diameter and a dark border developed between it and the blue : it also acquired a yellowish tint in the middle. Up to this point I argued that I was seeing interference fringes between a spherical supplementary wave and the prolate wave from the mirror, and on this basis I expected that as the Z-disk was moved farther out, so that the centre became increasingly "low," high-order "low" fringes would begin to develop from the middle of its now yellowish-pink centre. But this was not what happened : the dark border separating the pink (low) centre from the blue (high) ring surrounding it split into two concentric dark borders, the outer one belonging to the blue ring and expanding with it, and the inner one belonging to the pink, which now began to *contract* ; and in the annular space between these dark borders higher-order fringes arose in pairs, expanding towards the expanding blue ring and contracting towards the contracting pink centre, as the Z-disk was moved farther out. Finally, when the blue ring had expanded to the edge of the mirror, the pink centre had contracted to 1 cm. diameter, and between it and the blue there were five concentric nondescript-coloured rings which only appeared really well defined when the Z-disk was very exactly centred, and lost visibility rapidly on decentring. On careful inspection one could see that the effect of decentring was to split these rings into two sets, one belonging to the blue, and moving with it and with the Z-disk, and the other belonging to the pink, moving with it and against the Z-disk. Both sets of rings at the same time split up into pairs of opposing crescents. Clearly one could no longer argue that the supplementary wave was spherical, and the final fringe system would hardly bear a more precise interpretation than that the focal length of the centre was shorter than that of the outer zone, and that the prolateness amounted to several fringes. I then knife-edge tested the mirror zonally : its prolateness with respect to the sphere of closest fit to the centre was 8×10^{-5} cm. : this agrees with the $2\frac{1}{2}$ fringes seen on the Zernike test if we assume these nondescript-coloured fringes to refer to $\lambda = 6{\cdot}4 \times 10^{-5}$ cm. – red light. The Zernike test, then, in spite of the use of too large a Z-disk, had shown roughly the right amount of prolate error. But a test with two knife-edges showed nearly one fringe of astigmatism, and this I had not seen with the Z-disk. Clearly that could only have been because the Z-disk was too large or not circular. I therefore repeated the Zernike test with many different Z-disks, with the following result : Every Z-disk that showed really brilliant colours when some distance inside focus gave a substantially circular fringe system

at mean focus, thus failing to detect the astigmatism. Every Z-disk which showed faint colours till it was within a few fringes of mean focus and correctly centred, gave a fringe system showing the right amount of astigmatism : when such a Z-disk was set just outside focus for the central zone of the mirror, so that the centre showed primary low colour, the high ring surrounding the centre had not circular symmetry, but was composed of two crescents, the tips of which just touched one another on the low astigmatic axis ; outside this high ring were nondescript-coloured (low) fringes, elliptical in shape, to the extent of just one fringe at the edge of the mirror.

I obtained a fringe system complementary to the above, showing a ring of primary low colour, surrounded internally and externally by several orders of high fringes, by testing a spherical mirror on a test null for a prolate ellipsoid. The star was placed slightly to the right of the far focus, and a pair of small perpendicular flats were placed so that their line of intersection passed through the near focus, thus returning the light to the mirror so as to form the final image slightly to the left of the far focus, doubling all the mirror errors save those antisymmetrical with respect to a plane through the focus perpendicular to both flats. (One can double *all* the errors by using not two perpendicular flats but three—the "optical cube"—with their corner at the near focus. Mr. B. K. Johnson has pointed out to me that it is essential to decentre the star in such a way that all the light traverses the three flats in the same order. This is possible, and when it is done no lines due to the junctions of the three flats will be seen on the mirror. Extreme accuracy in their perpendicularity is then not essential.) I noted in this experiment a fact apparently in conflict with current opinion : I have seen it stated that although prolate error ("turned-down edge") in a converging wave-front produces an image looking fuzzy inside and sharp with internal diffraction rings outside focus, the converse does not hold for a wave-front with oblate error ("turned-up edge"). Now my spherical mirror was producing oblate error in the final wave-front, and it gave an image looking fuzzy outside and sharp with internal diffraction rings inside focus.

§ 7. *Astigmatism.*—It was of the first importance to verify that, provided one resisted the temptation to use a large Z-disk on account of its attractive appearance when out of focus, astigmatism could and would always be detected. I therefore set up the 12·5 cm. speculum previously discussed, so that the image was displaced horizontally by 4·5 cm. from the star : this introduces $\frac{1}{2}$ fringe of astigmatism (in $\lambda = 5 \times 10^{-5}$ cm.). As focus was approached from inside, the Zernike fringes became increasingly elliptical, until at the vertical focal line the fringe system consisted of a horizontal blue band (high) bordered above and below by neutral tint shading to deep tawny yellow, which became rather lighter at the top and bottom of the mirror. Moving the Z-disk $\frac{1}{2}$ fringe farther out in focus brought it to the horizontal focal line, when the fringe system became a vertical band of deep tawny yellow, bordered on either side by neutral tint shading to blue, which became rather whiter towards the sides of the mirror. All Z-disks which satisfied the criterion of smallness—colours very faint when 3 fringes out of focus—showed the astigmatism in correspondingly contrasting colours.

I also had occasion to test a glass disk of 11 cm. diameter, 93 cm. radius of curvature, which showed a little more than $\frac{1}{2}$ fringe of astigmatism plus about $\frac{1}{4}$ fringe of oblate error: on displacing the image 1·8 cm. in the appropriate direction from the star—which cancels 0·6 fringe of astigmatism—I obtained a circular fringe system showing the oblate error alone. I am satisfied that the only circumstances under which astigmatism is liable to escape detection are when it is masked by a still larger spherical or zonal aberration, and, even then, only if an unnecessarily large Z-disk is used.

§ 8. *Irregular Errors.*—I have been trying to figure aspherical surfaces by strictly local working—the optical analogy of the engineer's process of scraping a flat—the point being that this is presumably the only method possible when the desired figure is very deeply aspherical (say by several mm.), and is not a figure of revolution. This process necessarily produces a highly irregular surface, "true to figure" in the same sense that a cobbled pavement can be said to be "flat," and the whole interest attaches to just what fraction of a wave-length it is practicable to reduce the "cobbles." If the testing is done with vertical and horizontal knife-edges used in succession, the interpretation of the test is very difficult indeed. Zonal measurement with both knife-edges and graphical integration along two co-ordinates is out of the question owing to cumulative errors, and the only procedure possible seems to be to look at both knife-edge shadows in succession, and consider them as views of the errors in bas-relief, lit from perpendicular directions, which, as is known, is not strictly permissible. Perhaps that is why one is liable to make mistakes in the process, which is extremely tedious and exhausting in practice.

On the other hand, with the Zernike test indicating the absolute errors, it seemed that highly localised figuring would form a practicable process, and to form some idea of its possibilities I figured a decentred ellipsoid in speculum metal, 12·5 cm. diameter, having the near focus 102 cm. and the far focus 395 cm. from its centre, the near focus being distant 12·5 cm. from the line joining the far focus to the centre of the disk, so that the axis of revolution passes clear of the disk by about 6 cm. The desired figure departs by some 20 fringes from the nearest sphere, half the asphericity being astigmatic and half comatic. I put in most of the astigmatism—at the cost of introducing a large irregular error at the outset—by fine grinding. When the mirror had been polished (with a 2·5 cm. polisher) I tested it with the star at the far focus and the Z-disk at the near focus. The errors were so large (of the order of 10 fringes) that it was not possible to see the Zernike fringes over more than a small portion of the mirror at a time. I therefore had to test with a rather large Z-disk, placed either inside or outside focus for all zones of the mirror, and move the Z-disk laterally, so as to roll the "hypothetical test-plate" over all parts of the mirror in turn (p. 389), noting where the fringe systems became smallest (with the Z-disk inside focus)—these places being the tops of the hills. Polishers were used of various sizes, slightly smaller than the areas on which it was desired to work. At the end of three days the Zernike fringes spread over the whole mirror, only two or three orders of interference being present. It took a further six

Fig. 1.

(*a*) Zernike photograph : light areas high ; dark areas low.
(*b*) Vertical knife-edge, coming in from the right.
(*c*) Horizontal knife-edge, coming upwards at mean focus.
(*d*) ,, ,, ,, ,, $\frac{1}{4}$ mm. outside mean focus. Image cone, F/8.

days, using sometimes a pitch polisher 1 cm. diameter and sometimes the finger-tip, to reduce the errors until only the two primary colours showed (except at the extreme edges)—indicating errors of the order of $\pm \frac{1}{4}$ fringe. The procedure was to set the Z-disk at the mean focus, and paint dots of rouge over all the areas showing primary high colour. (The dots of rouge, reflecting practically nothing, showed up in the same colour as the halo—practically the same colour as the star.) Figuring was then carried out over the rouged areas for periods of the order of 5 minutes, and the mirror was retested. I do not think the process would have taken so long had I realised at the outset the importance of choosing a Z-disk which only develops its colours strongly when very near mean focus. Not realising this, I failed to keep the mirror free from astigmatism, and in the final removal of the astigmatism I produced a fresh set of irregular errors.

I stopped figuring when, except at the extreme edge, only the primary colours showed, and tried to photograph the Zernike fringes. This proved extremely difficult, for 20 minutes' exposure was necessary, and the apparatus did not remain in adjustment for so long, which is hardly surprising, seeing that a movement of the Z-disk of ·01 mm. made the colours practically vanish. However, I succeeded in taking a photograph which gives a rough idea of the distribution of the errors : this is shown in fig. 1 (*a*), together with photographs with a vertical knife-edge coming in from the right at mean focus (*b*), and with a horizontal knife-edge coming upwards at mean focus (*c*), and also $\frac{1}{4}$ mm. outside focus (*d*). The primary inside focus colour (blue) has photographed as light, and the outside focus colour (yellow-brown) as dark. Thus the light areas in the Zernike photograph 1 (*a*) are high, and the dark low by about $\frac{1}{4}$ fringe. Inspection of the two knife-edge photographs, (*b*) and (*c*), will give some idea of the difficulty of deciding where to figure such a surface from knife-edge tests alone. But it should be remembered that in practice one cannot photograph the two knife-edge tests before each figuring operation, so that normally one cannot have the two knife-edge tests side by side, and glance rapidly from one to the other.

§ 9. "*Accidental*" *Z-disks.*—A clean microscope slide, exposed to the atmosphere, will soon accumulate on its surface particles of foreign matter which will work as Z-disks. Most of them are opaque, and so give a fringe system in the same colours inside and outside focus, but an appreciable number are transparent, and work as phase-retarding disks. In fact, it is possible to do quite a satisfactory Zernike test with an "accidental" Z-disk. One can also make Z-disks some of which work quite well by simply touching a clean microscope slide with the finger-tip, though only a small proportion of the natural-grease particles thus imprinted on the slide are sufficiently round. It is best to touch the slide very lightly for this purpose. I have also done Zernike tests with a drop of milk and water between a cover-glass and slide : the mixture should be so dilute as to be only faintly milky. Milk contains fat globules of all sizes from ·02 mm. to less than ·001 mm. diameter : those that one succeeds in finding with an F/8 image produce excellently coloured fringes. There are also Z-disks present in one's eye : most people, when making knife-edge tests, will have seen small circular patches,

sometimes brilliantly coloured, surrounded by rings, appearing on the mirror and moving when the eye is moved. Observers have recognised that it is possible to use the pupil of the eye as a knife-edge, and so to see the errors of a mirror by holding one's eye in the right place with respect to the image. It occurred to me that it should be possible to make a Zernike test, using one of the natural Z-disks present in the eye, and I tried this on the prolate spheroidal mirror previously discussed, using an obviously rather large Z-disk which for an hour at least was a persistent feature of my right eye. As might be expected, I found it extremely difficult to hold my head—supported on both hands—steady enough, but I was able to see the green "high" patch created by this Z-disk when inside focus expand into a crescent with its concave side towards the centre ; it moved rapidly round the centre as I endeavoured to centre it, which I could not do for long enough to catch more than a fleeting glimpse of a green "high" ring. However, from the crescent shape of the patch when the Z-disk was not central, it was obvious that the mirror was prolate.

§ 10. *Zernike Test using an Actual Star.*—By courtesy of Professor F. J. M. Stratton I was able to witness an attempt made by Dr. R. O. Redman to do a Zernike test on the 36-inch Newtonian telescope (by Dr. Common) of the Cambridge Solar Physics Observatory, using an actual star as source. The Zernike fringes were in continual rapid motion, owing to atmospheric irregularity, so that it was only possible to see them when the Z-disk was some distance out of focus, and we must undoubtedly have been using Z-disks far larger than should be used for testing this F/3·7 mirror at focus. The out-of-focus fringe systems were elliptical, with considerable eccentricity, the major axis of each fringe system changing direction by 90° when the Z-disk was so decentred as to carry the fringe system from one side of the mirror to the other: thus the mirror is astigmatic, and the astigmatism is not regular. This was known to be the case.

Very perfect seeing conditions would be necessary to detect errors of less than one fringe in this way.

§ 11. *The Limitations of Testing with a Z-disk.*—The Zernike test becomes more difficult to carry out when the focal ratio of the image is large (*i.e.* F number small) for two reasons : first, because the diameter of the Z-disk must decrease *pari passu* with that of the Airy disk, and it is difficult to make very small Z-disks of the thickness which shows nicely coloured fringes; and, second, because a corresponding decrease is necessary in the diameter of the geometrical image of the star, so that the intensity of the light leaving the mirror-surface is decreased. If the star is not sufficiently small, the delicacy of the test is reduced in one of two ways : if the star is so fed with light as to be in effect self-luminous (*i.e.* fed by a fully corrected very wide angle condensing system, focussed on the pinhole), then the fringes are blurred, because the fringe systems formed by the independently lit points of the star-surface do not coincide. If the star is fed with wave-fronts whose radii of curvature when they reach the pinhole are large compared with the diameter of the pinhole, then any individual wave-train will not spread with equal amplitude over the whole mirror, but will have appreciable

amplitude only over a restricted part of it, and will thus form an Airy disk of the same order of diameter as the pinhole. To obtain a sufficiently strong supplementary wave it will be necessary to use a correspondingly large Z-disk, and so the fringe-system formed on any part of the mirror will depend only on the figure of the mirror near to the part in question, so that long-period errors will not be shown up to their full extent : astigmatism will not be apparent, and absolute focal position will not be determinable with precision. The same difficulty arises with the knife-edge test : if the delicacy of the test (expressed in fringes) is to be maintained as the focal ratio is increased, the geometrical image of the star must be correspondingly reduced. With either test, if we use a star giving a geometrical image a given fraction of the width of the Airy disk, and look not directly at the mirror but at the image thereof in some optical system, the brilliance of the mirror's image depends only on its angular diameter and on the intrinsic brilliance of the star, and not on the focal ratio of the mirror itself. In fact, we can increase the apparent surface brightness of the mirror to any degree not exceeding the intrinsic brilliance of the star, if we are prepared to look at it through a reducing telescope minimifying it sufficiently ; and if the telescope objective is perfectly corrected, not as a telescope, but as a microscope objective, we may conveniently place the Z-disk not at the Airy disk formed by the mirror, but at the magnified image of the Airy disk which the telescope can be arranged to form, so that we can work with a larger and more easily made Z-disk. One would, however, always prefer—other things being equal—to avoid the reduction in angular diameter of the mirror's image, and also the necessity for a perfectly corrected microscope objective in the telescope.

I have tried a Zernike test without a reducing telescope on an unsilvered glass disk 11·25 cm. diameter, 31·5 cm. radius of curvature (imaging at F/2·8), using a star ·005 mm. diameter. I found plenty of Z-disks sufficiently small to show about the right number of fringes when set a few fringes inside or outside focus, but they nearly all showed "dark" and "light" as primary inside and outside focus colours : presumably all the really small Z-disks were too thin to develop colour-contrast. The largest "halo" that I was able to produce extended 2 cm. radially from the mirror : it was not quite regular. The fringe system at mean focus showed that the centre and edge of the mirror were about $\frac{1}{4}$ fringe low (which I confirmed with a knife-edge), and the system was astigmatic by about $\frac{3}{4}$ fringe. The astigmatic axes did not rotate when the mirror was rotated, so that this astigmatism must be ascribed to the decentring of the star from the optic axis, which I could not reduce below 2·5 mm. : the direction and sign of the astigmatism were correct for this. Now the astigmatism introduced by this amount of decentring is $\frac{5}{4}$ fringe (in $\lambda = 5 \times 10^{-5}$ cm.), so that although it is not clear to what wave-length the observed $\frac{3}{4}$ fringe of astigmatism should be referred, it would appear that I had failed to detect the whole of the astigmatism. The visibility of the fringes was only moderately good even at mean focus. However, it is gratifying to see that the method even with a star that is rather too large is still capable of moderate accuracy, at F/2·8.

I have used the method on an F/7 image, with a very good spherical mirror, and had no difficulty in finding Z-disks giving blue and yellow as primary colours in strong contrast when the Z-disk was set $\pm \frac{1}{4}$ fringe from focus.

I am not sure whether it would be possible to increase the intrinsic brilliance of the star sufficiently to test with a ·005 mm. star after two reflections from unsilvered glass, which are necessary in null-testing a paraboloid with the aid of a flat. I do not know how much I am losing in intensity, with the gas-filled lamp as source, by not correcting the condensing lens. Perhaps the gain in source-brilliancy of 10 or so, to be obtained by the use of an arc as source, together with the automatic removal, due to the increased size of the source, of loss due to aberrations in the condensing system, would be sufficient to permit testing with two reflections from unsilvered glass, without a reducing telescope, using a star small enough for a paraboloid such as that used at Meudon, of F/3. Paraboloids of the modest aperture of F/8 can certainly be Zernike-tested at the focus, using a star lit by a gas-filled lamp.

Professor Zernike has pointed out to me that one could increase the available light at least 100 times by using a slit instead of a pinhole, and a Z-strip instead of a Z-disk, and that the appearance of irregular error is very little altered by this change, which makes the test null for that part of the error which is not constant along a co-ordinate perpendicular to the strip. And indeed I find that when spherical aberration and astigmatism are absent, and the residual error is irregular, the substitution of a Z-strip for a Z-disk makes very little difference to the appearance at focus : it is quite difficult to tell, from the appearance of the fringe system (even though one has also seen it with a disk), in what direction the Z-strip lies. (I made at first the mistake of using too wide a strip (·03 mm.). It is difficult to make the resin fibres so narrow as not to exceed ·01 mm. after pressing, and I found it simpler to make strips by simply stroking the surface of a glass plate with a "cutanit" (molybdenum-titanium carbide) tool. If the pressure is not too great, no sign of fracture is visible under the microscope, the glass having either flowed or been planed away. These strips give "dark" and "light" as inside and outside focus colours.)

It may be, then, that a slit and a strip which can be rotated together through a right angle, for the detection of astigmatism, will be the form in which the Zernike test will be used in practice in the figuring of wide-aperture reflectors.

But I would always prefer, if enough light is available, to use a star and a Z-disk, so that the whole of the error can be seen at once; and I feel it is perhaps better to develop methods for null-testing big reflectors, not at the focus (for after all we can only test conic-sections null-fashion in that way, with the aid of a flat or spherical mirror, and the Ritchey-Chrétien curves, for example, do not belong to that class), but at the centre of apical curvature : it should not be impossible to devise systems of compensating mirrors of which neither the asphericity nor the diameter need be so great as that of the mirror under test, which will supply light having the correct asphericity

to stigmatise after one reflection from the unsilvered surface : the intensity would then be high enough to permit the use of a Z-disk.

To take an example, is it easier to make a six-inch compensating mirror having a prescribed asphericity of about 5 fringes, or a three-foot flat, in order to null-test a three-foot paraboloid of F/3·7? And would it not be worth while to figure, though it might have to be with zonal testing, a small compensating mirror, in order to be able to apply during the figuring of a large Ritchey-Chrétien reflector this very beautiful and sensitive null interference test which Professor Zernike has placed at our disposal?

Imperial College of Science
and Technology :
1934 *February* 24.

AN ANALYSIS OF THE RADCLIFFE PROPER MOTIONS IN THE SELECTED AREAS.

H. Knox-Shaw, M.A., D.Sc., Radcliffe Observer.

For the past twenty-five years the Radcliffe Observatory has been engaged on determining the proper motions of faint stars in the Selected Areas. The catalogue containing the results for more than 32,000 stars is now in the press.* After omitting (*a*) the stars brighter than 9·0, (*b*) the faintest stars in each area, since their proper motions have been determined with less weight, and (*c*) those with annual proper motions larger than 0″·1, there remain some 25,000 stars, which have been subjected to analysis with the object of testing whether they show the same tendencies to systematic motion as the brighter stars. A detailed description of this work will appear in the volume already referred to ; the present paper contains a brief account of the methods employed and some comments on the results obtained.

The material was divided into two parts, comprising the stars of magnitude 9·0 to 14·0 and those from 14·1 downwards, the magnitudes being on the international scale. These two groups, referred to hereafter as the brighter and fainter stars, contain 10,342 and 14,569 stars respectively, the mean limiting magnitude of the latter being 15·0. The areas have been grouped together, one area in declination +75° with two at +60°, two at +45° with two at +30°, and two at +15° with two on the equator, thus forming thirty regions symmetrically distributed over the northern hemisphere. The proper motions as given in the catalogue are relative to the mean of the comparison stars used for each area ; the number of these averaged 128, and their mean magnitude 13·7. They are thus sufficiently numerous and faint to form a base of reference that is unlikely to be sensibly affected by their peculiar motions, especially as no star with proper motion greater than about 0″·5 per annum has been used as a comparison star.

* *The Radcliffe Catalogue of Proper Motions in the Selected Areas* 1 *to* 115, 1934.

The relative proper motions were plotted in the usual way on squared paper for each area, the brighter and fainter groups being treated separately. A shift of the origin by an amount equal in magnitude but opposite in sign to the mean parallactic motion of the comparison stars then makes the motions absolute. For the calculation of the parallactic motions the secular parallax was obtained by adapting the figures in Table 8 of *Groningen Publications*, 45. The Solar Apex was assumed, in the first instance, to be at 273°, +44°, the position found by Smart from the Cambridge proper motions.* The number of proper motions in each ten degrees of position angle was then counted. These position angles were made to refer to the centres of the regions formed by the grouped areas, by turning the tracing-paper bearing the radial diagram through the necessary number of degrees in each case. We thus obtain for each area the number of proper motions in each ten degrees of position angle as projected on the tangent plane at the group centre. Sums of these were then taken for the constituent areas of a group and the results smoothed by taking as the number in any ten degrees the sum of the actual number and those of the two contiguous ten degrees.

Plots of these figures, numbers against position angles, showed unmistakably in the majority of groups the presence of star-streaming, but they were more irregular than is usually found to be the case for brighter stars. This was to be expected, as the proper motions of these faint stars are naturally small and the disturbing effect of accidental error thus relatively large. The average value of a proper motion for the brighter group of stars varies from about 0″·011 near the galaxy to 0″·024 in high latitudes; for the fainter stars the values are 0″·010 and 0″·020 respectively. The probable error of a proper motion for an area of mean weight is ± 0″·0037. Thus, especially in low galactic latitudes, the true directions of a considerable proportion of the motions must be masked by accidental scatter.

After considering for some time what procedure to adopt for the analysis of these figures, I came to the conclusion that a method of curve-fitting such as Eddington's would involve a strain on my powers of discretion beyond what they would bear, and I decided to employ an ingenious "automatic" method due to Schwarzschild.† Probably the greatest drawback to Schwarzschild's Ellipsoidal Hypothesis, and the main reason why it has been so little employed in investigations of this nature, is the assumption of fore and aft symmetry in the most favoured direction for the stellar motions, the number of stars moving in the one direction being taken to be the same as of those moving in the opposite direction. Eddington's Two Drift Theory does not suffer from this limitation, and in dealing by his method with the proper motions of the bright stars, found from meridian observations, the number of stars moving in Drift I has generally been found considerably larger than those in Drift II. This difference has, however, been found to decrease as fainter stars have been treated, and there seems no reason to suppose the existence of any inequality in the

* *M.N.*, 87, 137, 1926; *Cambridge Observations*, 26, 1928.
† *Göttingen Nachrichten*, p. 191, 1908.

case of stars of the order of magnitude that we are now dealing with. Thus a strong argument against the employment of the Ellipsoidal Hypothesis is removed in this case. An argument definitely in its favour is the following. Study of the plotted curves suggested the existence in several cases of the third drift, sometimes referred to as Drift O, formed by stars at rest relatively to the mass of the stars considered and thus showing only the solar motion. Owing to the small difference in many of the regions between the position angles of the Solar Apex and that of Drift I, it is not easy to be sure of this ; nor is it easy to differentiate it from the scattering effect due to accidental error, but the feeling that, if the curve-fitting method was used, the curves ought properly to be analysed into three drifts, was the final deterrent. So I decided rather to risk the dangers of an automatic method and to employ that of Schwarzschild, for in that method the existence of any "stationary" stars will not affect the direction found for the Vertex, but merely tend to equalise the values derived for the diameters of the velocity ellipsoid.

I will not in this note describe Schwarzschild's method. Those interested may refer to his paper already cited or to the forthcoming *Radcliffe Catalogue*. It gives not only θ_A, the direction of the Solar Apex, and θ_V, that of the Vertex, the direction of preferential motion freed from the effects of the solar motion, but also the quantities h/α, h/β, and their ratio β/α, where α, β are the major and minor semi-axes of the velocity ellipse, the projection of the velocity ellipsoid on the tangential plane at the centre of the region, and $h = u \sin \lambda_A$; u being the velocity of the Sun and λ_A the angular distance of the Solar Apex from the region. The directions θ_A and θ_V are found fairly simply ; most of the trouble experienced lies in evaluating the quantities h/α, h/β and β/α.

Each of the thirty regions (groups of areas) then furnishes a pair of equations of the following form for determining the Solar Apex :—

$$\begin{aligned} -X \sin \alpha \qquad + Y \cos \alpha \qquad\qquad &= h/\beta \sin \theta_A, \\ -X \cos \alpha \sin \delta - Y \sin \alpha \cos \delta + Z \cos \delta &= h/\beta \cos \theta_A, \end{aligned}$$

whence

$$\tan A = Y/X,$$

$$\tan D = Z/\sqrt{X^2 + Y^2},$$

$$u/B = \sqrt{X^2 + Y^2 + Z^2},$$

where α, δ are the right ascension and declination of the centre of the region, A, D those of the Solar Apex, and $B(=\beta)$ is the semi-minor axis of the velocity ellipsoid. Similar equations with θ_V substituted for θ_A and $\sqrt{\alpha^2/\beta^2 - 1}$ for h/β give the right ascension and declination of the Vertex and the quantity $\sqrt{A^2/B^2 - 1}$, from which the ratio of the axes of the velocity ellipsoid can be determined, A being the semi-major axis.

In the case of the brighter stars one of the regions, whose distance from the Solar Apex was 164°, failed to yield any value for θ_A, and consequently only twenty-nine regions enter into the solution for the Apex. The Vertex

has been derived from all thirty regions. For the fainter stars both Apex and Vertex have been derived from twenty-eight regions. The question of the rejection of regions from the solution has been given much thought. In an automatic method, such as that employed, apart from the rare cases which fail altogether to provide a value for θ_A or θ_V, one is liable to obtain some very discordant values, especially when the region is near the Apex or Vertex. But discordance in position angle alone is not the best index for rejection, and the general rule adopted has been to reject regions when the residual in position angle multiplied by the sine of the distance from the Apex (or Vertex) is greater than 30°. The equations were solved by least squares giving equal weight to each. Weights proportional to the number of stars in the region have been used by some investigators. Such a procedure seemed objectionable in this case, as the number of the brighter stars depended on the galactic latitude of the region, as it did also for the fainter stars apart from differences due to variation in the limiting magnitude. Thus in general the regions with the largest number of stars were those where the proper motions were the smallest, and where consequently the effect of accidental error was most serious. It therefore seemed the wisest course, as well as the simplest, to give each region the same weight. The results of the solutions are as follows :—

(Solar Apex assumed at 273°, +44°)

Solar Apex

Brighter Stars ($9^m.0 - 14^m.0$)	$272°.5 \pm 1°.4$	$+44°.3 \pm 1°.0$
Fainter Stars ($14^m.1 - 15^m.0$)	$271°.1 \pm 2°.0$	$+41°.4 \pm 1°.5$

Vertex

Brighter Stars	$89°.9 \pm 1°.3$	$+22°.4 \pm 1°.2$
Fainter Stars	$84°.4 \pm 1°.8$	$+22°.2 \pm 1°.6$

It will be noticed that the position found for the Apex from the brighter stars is identical with that assumed for the purpose of converting from relative to absolute proper motion, while the fainter stars put the Apex only a few degrees away. It had from the beginning appeared doubtful as to how far the Apex found would be independent of that assumed, and this close agreement accentuated these doubts. It was therefore decided to repeat the calculations with a different assumption as to the position of the Apex. It was now taken to be at 270°, +34°, a position more in accordance with that generally derived from bright stars, and after making the consequent small alterations in the parallactic motion of the comparison stars, never exceeding 0″.001 per annum in right ascension and only occasionally reaching 0″.002 in declination, the whole process was repeated. Retaining exactly the same regions as before in each of the four solutions the results now found are :

(Solar Apex assumed at 270°, +34°)

Solar Apex

Brighter Stars	268°·6 ± 1°·3	+33°·0 ± 1°·1
Fainter Stars	268°·5 ± 1°·8	+29°·5 ± 1°·5

Vertex

Brighter Stars	88°·6 ± 1°·3	+23°·0 ± 1°·2
Fainter Stars	84°·7 ± 1°·9	+23°·9 ± 1°·7

As far as the Solar Apex is concerned the solutions again reproduce the assumed position with considerable accuracy, the fainter stars as before putting it 3° farther south than the brighter. It is clear that the analysis has failed to make a contribution of any assured value to our existing knowledge of the position of this point. The case of the Vertex is different. Here there was no reason to suppose that the position found would depend on the assumption made as to the Solar Apex, and the two sets of values in fact agree as well as their probable errors would lead us to expect. Further consideration will be given to the Vertex later on.

Of the two standard methods of reducing photographic proper motions from relative to absolute, the first, in which use is made of the meridian proper motions of the bright stars in the field, apart from its having the grave disadvantage of introducing the systematic errors of the meridian proper motions, is rarely applicable when dealing with faint stars and restricted areas, owing to the large size of the photographic images and the paucity of the meridian stars. There is really no choice but to make use of the parallactic motion of some group of stars. The ideal is of course for these stars to be so faint that their parallactic motions are negligibly small. Measurable images of such stars are not in general available, as it would mean going down to something like the 18th magnitude, but it is clearly an advantage to refer the proper motions to a body of as faint stars as possible, apart from the danger of systematic magnitude error, which would naturally become more serious the greater the difference in magnitude between the stars whose proper motions are under discussion and those to which they are referred.

It was consequently decided to try the effect of using as the base of reference groups of the faintest stars for which reliable proper motions were available instead of the comparison stars. The mean magnitude of these faint stars was 14·8, as compared with 13·7 for the comparison stars. This change of only a magnitude produced, however, an appreciable reduction in the differences between the corrections for parallactic motion on the two assumptions as to the position of the Apex. The comparison stars coincide roughly with the group of brighter stars ($9^{m}\cdot0$ to $14^{m}\cdot0$), though they extend somewhat into the fainter group. The faint reference stars lie wholly in the latter group except in a very few areas, and thus the brighter stars are referred to them as to an entirely independent body of stars. Great care

had been taken to determine and eliminate systematic magnitude error, and the effect of any remaining in the proper motions is not thought likely to be serious.* The group of brighter stars only was treated in this way, and the results on the two assumptions as to the Apex are given below. For the Apex the position angles found were much more discordant than in the former determinations, and five regions were rejected from the solutions on this account. In the case of the Vertex no values of θ_V were given in two regions, and thus the solutions depend on twenty-eight regions.

FAINT REFERENCE STARS

(Solar Apex assumed at 273°, +44°)

	Solar Apex	
Brighter Stars	$271°.4 \pm 2°.6$	$+43°.6 \pm 1°.9$
	Vertex	
Brighter Stars	$94°.7 \pm 1°.3$	$+21°.7 \pm 1°.3$

(Solar Apex assumed at 270°, +34°)

	Solar Apex	
Brighter Stars	$273°.2 \pm 2°.6$	$+38°.6 \pm 2°.0$
	Vertex	
Brighter Stars	$93°.9 \pm 1°.2$	$+22°.7 \pm 1°.2$

The first solution for the Solar Apex again reproduces the assumed position, and while the second puts the declination half-way between the two assumed values the larger probable error makes it doubtful whether this has any significance as evidence for the more northerly position.

This reduction has indeed made me very dubious as to the independence of the determinations of the Solar Apex in similar investigations of faint stars whose proper motions are in the mean not more than a few times larger than the parallactic motion which it has been necessary to apply in the reduction to absolute. It is clear that if the relative proper motions are distributed in an entirely fortuitous manner, the only systematic feature of the absolute motions will be the effect of the solar motion that has been impressed upon them in making them absolute, and their analysis necessarily reproduces the Apex assumed. And it follows that however free the proper motions may be from accidental error the assumed Apex will have a preponderating effect in determining that given by the analysis, if the proper motions are small compared with the parallactic motions applied. The measure of independence of the final result will be conditioned by both the relative freedom from accidental error of the proper motions and the

* For a note on the discovery of the magnitude error, see *M.N.*, **87**, 439, 1927. Full details will appear in the *Radcliffe Catalogue*.

extent to which they exceed in magnitude the parallactic motions applied to them. And in these respects the present investigation seems to be at least as favourably situated as other work of this kind. It is true that the original assumption as to the Apex has not always been reproduced. Smart's investigation already cited is a case in point. His stars were brighter than those considered here and consequently his proper motions were larger, but so also were the parallactic motions he applied, as they were those of the B.D. stars in his fields. The ratio of probable error to mean proper motion is not much different in the two cases, though in this the advantage may lie slightly with the Cambridge figures. But the conditions are sufficiently similar to make it difficult to account for the fact that Smart found the declination of the Apex to be $+44°$ when he had assumed the value of $+34°$. Possibly his proper motions were not free from magnitude error in declination; it need be only very small to produce an effect of this kind, especially when the regions that enter into the solution are not very widely spread. I venture to suggest this as a possible explanation because Smart had not the opportunity of determining this error by an independent method such as has been used for the Radcliffe proper motions.

The present investigation cannot be said to provide any evidence for an Apex progressively farther north as fainter stars are dealt with, an hypothesis still favoured, I believe, by some workers in this field. Indeed for what it is worth, the evidence is against such a shift, as the fainter group of stars, those fainter than the 14th magnitude, gives an Apex 3° farther south than the brighter group.

The accordance of the various determinations of the position of the Vertex can be considered as satisfactory. In declination the agreement is extremely good; in right ascension the fainter stars give values about 5° less than the brighter group; and the latter when referred to the faint stars as a basis give the right ascension larger by 5° than when referred to the comparison stars. A combination of the solutions places the Vertex at $90°$, $+22°{\cdot}5$, the right ascension being less certain than the declination and having a tendency to be greater than 90° for the brighter group of stars and less for the fainter. The results of some other investigations on faint stars are given here for comparison, all as reduced by Smart:

Cambridge P.M.'s	$92° + 20°$,
Groningen P.M.'s	$91° + 15°$,
Nechvile's P.M.'s	$90° + 21°$.

The values found for the axes of the velocity ellipsoid have not been considered in this paper, as they seem to be relatively more affected by the accidental errors of the proper motions than do the positions found for the Solar Apex and Vertex. The quantities h/β and $\sqrt{\alpha^2/\beta^2 - 1}$ determined for each region should be proportional to the sines of the distances of the region from the Apex and Vertex respectively. As this was often far from being the case, and it was thought that in consequence the value of the higher accuracy of the position angles was being lost, further solutions were made by substituting for $\sqrt{\alpha^2/\beta^2 - 1}$ the values of $\sin \lambda$ computed with

reference to the Vertex already found from the first solution. The effect of this substitution was to make no material difference to the position found for the Vertex, but to reduce the probable errors by nearly one half.

Summary

The analysis of the proper motions of 25,000 stars in the Selected Areas by a method of Schwarzschild's leads to no conclusion as to the position of the Solar Apex, the resulting value being found to depend upon that assumed for the purpose of the reduction of the relative proper motions to absolute. Doubt is expressed as to how far positions of the Apex found from similar investigations can be regarded as independent of the initial assumption.

A good determination is, however, obtained of the position of the Vertex of preferential motion, viz. 90°, +22°·5, which is very near the positions found by Smart from the Cambridge and Nechvile's proper motions. The stars were divided into two groups, those brighter and those fainter than the 14th magnitude, and there is no difference that can be regarded as certainly significant between the results given by the two groups.

THE VELOCITY DISTRIBUTION OF THE TYPE A STARS WITH KNOWN PROPER MOTIONS AND RADIAL VELOCITIES.

R. A. Robb, M.Sc., F.R.S.E.

In dealing with the observed proper motions and radial velocities of stars it is desirable, if numbers permit, to study only those stars for each of which the proper motion and radial velocity is known. Such a study has been made by Gyllenberg and Malmquist * for the first order moments, and this paper extends this study to the second order moments, although a survey of the former moments will also be given. 843 stars of Types B8–A5, brighter than the sixth magnitude, will be considered.

For simplification of calculations the stars are allocated to Professor Charlier's 48 "galactic squares." These squares are symmetrical with respect to the galactic plane, the galactic north pole being that given by $\alpha = 190°$, $\delta = +28°$. Further particulars regarding these squares will be given later.

Two systems of co-ordinates are required in the first place. The system K_2 is the usual galactic system, the galactic longitude and latitude of a star being denoted by l and b respectively; co-ordinates and linear velocities will be denoted by $(X'', Y'', Z'', U'', V'', W'')$. The other system, K_3, has its Z-axis directed towards the centre of co-ordinates of any one of the 48 squares; its positive X and Y- axes are directed towards increasing galactic longitude and latitude respectively. Co-ordinates and linear velocities in this system K_3 are denoted by (X, Y, Z, U, V, W).

* *Lund Meddelanden*, I, 108, 1925.

If u, v are the observed proper motion components of a star in galactic longitude and latitude, w its observed radial velocity, and r its distance, then

$$u = \frac{U}{r}, \qquad v = \frac{V}{r}, \qquad w = W.$$

Also considering the stars of any one square, and denoting the mean value of $x_1, x_2, x_3, \ldots, x_n$ by $M(x)$, we have

$$M(u) = M(U)M\left(\frac{1}{r}\right), \qquad M(v) = M(V)M\left(\frac{1}{r}\right), \qquad M(w) = M(W).$$

This assumes no correlation between U, V with $\frac{1}{r}$. In the usual moment notation, denoting moments about the origin with a dash, we then have

$$\nu'_{100} = \theta_1 N'^{(3)}_{100}, \qquad \nu'_{010} = \theta_1 N'^{(3)}_{010}, \qquad \nu'_{001} = N'^{(3)}_{001}, \qquad \theta_1 = M\left(\frac{1}{r}\right).$$

These first order moments are used to find the components of the stream velocity, N'_{100}, N'_{010}, N'_{001}, along the three axes of the system K_2; N'_{100} is directed towards $l = 360°$, $b = 0°$, N'_{010} towards $l = 90°$, $b = 0°$, and N'_{001} towards the north galactic pole. As the proper motions and radial velocities are known, a value of θ_1 is also obtained. The components along the axes of system K_3 are then calculated, and the stars' motions are then freed from their stream velocity by subtracting the corresponding stream velocity components, which can be expressed in arc by multiplying them by θ_1.

If u', v' and w' denote these resultant velocities, the second order moments, for any one square,

$$\nu_{200} = \frac{\Sigma u'^2}{n}, \quad \nu_{020} = \frac{\Sigma v'^2}{n}, \quad \nu_{002} = \frac{\Sigma w'^2}{n}, \quad \nu_{110} = \frac{\Sigma u'v'}{n}, \quad \nu_{101} = \frac{\Sigma u'w'}{n}, \quad \nu_{011} = \frac{\Sigma v'w'}{n},$$

in the system K_3 can then be found, n being the number of stars in the square. These second order moments are then expressed in terms of the second order moments N_{ijk}, where $i+j+k=2$, of the galactic system K_2. These latter moments are defined by

$$N_{200} = \frac{\Sigma U''^2}{N} - N'^2_{100} = N'_{200} - N'^2_{100},$$

$$N_{020} = \frac{\Sigma V''^2}{N} - N'^2_{010} = N'_{020} - N'^2_{010},$$

$$N_{110} = \frac{\Sigma U''V''}{N} - N'_{100} \cdot N'_{010} = N'_{110} - N'_{100} \cdot N'_{010},$$

and so on, N being the total number of stars under consideration. The transformation formulæ are given by

$$\nu_{200} + \bar{u}_0^2 = \gamma_{11}^2\theta_2 N'_{200} + \gamma_{21}^2\theta_2 N'_{020} + \gamma_{31}^2\theta_2 N'_{002} + 2\gamma_{21}\gamma_{31}\theta_2 N'_{011} + 2\gamma_{31}\gamma_{11}\theta_2 N'_{101} + 2\gamma_{11}\gamma_{21}\theta_2 N'_{110},$$

$$\nu_{020} + \bar{v}_0^2 = \gamma_{12}^2\theta_2 N'_{200} + \gamma_{22}^2\theta_2 N'_{020} + \gamma_{32}^2\theta_2 N'_{002} + 2\gamma_{22}\gamma_{32}\theta_2 N'_{011} + 2\gamma_{32}\gamma_{12}\theta_2 N'_{101} + 2\gamma_{12}\gamma_{22}\theta_2 N'_{110},$$

$$\nu_{002}+\bar{w}_0^2=\gamma_{13}^2N'_{200}+\gamma_{23}^2N'_{020}+\gamma_{33}^2N'_{002}+2\gamma_{23}\gamma_{33}N'_{011}+2\gamma_{33}\gamma_{13}N'_{101}+2\gamma_{13}\gamma_{23}N'_{110},$$

$$\nu_{110}+\bar{u}_0\bar{v}_0=\gamma_{11}\gamma_{12}\theta_2N'_{200}+\gamma_{21}\gamma_{22}\theta_2N'_{020}+\gamma_{31}\gamma_{32}\theta_2N'_{002}+(\gamma_{31}\gamma_{22}+\gamma_{21}\gamma_{32})\theta_2N'_{011}+(\gamma_{31}\gamma_{12}+\gamma_{11}\gamma_{32})\theta_2N'_{101}+(\gamma_{11}\gamma_{22}+\gamma_{21}\gamma_{12})\theta_2N'_{110},$$

$$\nu_{101}+\bar{u}_0\bar{w}_0=\gamma_{11}\gamma_{13}\theta_1N'_{200}+\gamma_{21}\gamma_{23}\theta_1N'_{020}+\gamma_{31}\gamma_{33}\theta_2N'_{002}+(\gamma_{31}\gamma_{23}+\gamma_{21}\gamma_{33})\theta_1N'_{011}+(\gamma_{31}\gamma_{13}+\gamma_{11}\gamma_{33})\theta_1N'_{101}+(\gamma_{11}\gamma_{23}+\gamma_{21}\gamma_{13})\theta_1N'_{110},$$

$$\nu_{011}+\bar{v}_0\bar{w}_0=\gamma_{12}\gamma_{13}\theta_1N'_{200}+\gamma_{22}\gamma_{23}\theta_1N'_{020}+\gamma_{32}\gamma_{33}\theta_1N'_{002}+(\gamma_{32}\gamma_{23}+\gamma_{22}\gamma_{33})\theta_1N'_{011}+(\gamma_{32}\gamma_{13}+\gamma_{12}\gamma_{33})\theta_1N'_{101}+(\gamma_{12}\gamma_{23}+\gamma_{22}\gamma_{13})\theta_1N'_{110},$$

where

$$\begin{aligned}\bar{u}_0&=\theta_1(\gamma_{11}N'_{100}+\gamma_{21}N'_{010}+\gamma_{31}N'_{001}),\\ \bar{v}_0&=\theta_1(\gamma_{12}N'_{100}+\gamma_{22}N'_{010}+\gamma_{32}N'_{001}),\\ \bar{w}_0&=\quad\gamma_{13}N'_{100}+\gamma_{23}N'_{010}+\gamma_{33}N'_{001},\end{aligned}$$

$$\gamma_{11}=-\sin l,\qquad \gamma_{21}=+\cos l,\qquad \gamma_{31}=0,\qquad \gamma_{12}=-\sin b\cos l,$$
$$\gamma_{22}=-\sin b\sin l,\qquad \gamma_{32}=+\cos b\qquad \gamma_{13}=+\cos b\cos l,$$
$$\gamma_{23}=+\cos b\sin l,\qquad \gamma_{33}=+\sin b,\qquad \theta_2=M\left(\frac{1}{r^2}\right).$$

These six equations are then solved simultaneously by the method of least squares by the following method. Assuming, as before, $1/r$ to be independent of the velocities, the equations are first transformed by taking approximate values of N'_{200}, N'_{020}, . . . and θ_2. Each equation yields 7 normal equations, which could be solved for the 7 unknowns. In order to obtain one set of solutions, however, and to reduce calculations, corresponding normal equations are added together, the normal equations from the product moments being first multiplied by 2. The normal equations can then be shown to be as follows, weights being assigned according to the number of stars in each square.

$$\begin{aligned}x'+l_1\theta_{20}s&=0,\\ y'+l_2\theta_{20}s&=0,\\ z'+l_3\theta_{20}s&=0,\\ u'+m_1\theta_{20}s&=0,\\ v'+m_2\theta_{20}s&=0,\\ w'+m_3\theta_{20}s&=0,\end{aligned}$$

$$\theta_{20}s(n_2-l_1^2-l_2^2-l_3^2-2m_1^2-2m_2^2-2m_3^2)=n_1-n_2.$$

In these equations x', y', z', u', v', w', $\theta_{20}s$ are the corrections to be applied to the approximate values x_0, y_0, z_0, u_0, v_0, w_0, θ_{20} of N'_{200}, N'_{020}, N'_{002}, N'_{011}, N'_{101}, N'_{110} and θ_2 respectively. If N is the total number of stars, and square brackets indicate summation over all squares,

$$l_1=\frac{1}{N}[(1-\gamma_{13}^2)^2x_0+\gamma_{13}^2\gamma_{23}^2y_0+\gamma_{13}^2\gamma_{33}^2z_0+2\gamma_{13}^2\gamma_{33}\gamma_{23}u_0-2(1-\gamma_{13}^2)\gamma_{13}\gamma_{33}v_0-2(1-\gamma_{13}^2)\gamma_{13}\gamma_{23}w_0],$$

$$l_2=\frac{1}{N}[\gamma_{13}^2\gamma_{23}^2x_0+(1-\gamma_{23}^2)^2y_0+\gamma_{23}^2\gamma_{33}^2z_0-2(1-\gamma_{23}^2)\gamma_{33}\gamma_{23}u_0+2\gamma_{23}^2\gamma_{13}\gamma_{33}v_0-2(1-\gamma_{23}^2)\gamma_{13}\gamma_{23}w_0],$$

$$l_3 = \frac{1}{N}[\gamma_{13}^2\gamma_{33}^2 x_0 + \gamma_{23}^2\gamma_{33}^2 y_0 + (1-\gamma_{33}^2)^2 z_0 - 2(1-\gamma_{33}^2)\gamma_{23}\gamma_{33}u_0 - 2(1-\gamma_{33}^2)\gamma_{13}\gamma_{33}v_0 + 2\gamma_{33}^2\gamma_{13}\gamma_{23}w_0],$$

$$m_1 = \frac{1}{N}[\gamma_{13}^2\gamma_{23}\gamma_{33}x_0 - (1-\gamma_{23}^2)\gamma_{23}\gamma_{33}y_0 - (1-\gamma_{33}^2)\gamma_{23}\gamma_{33}z_0 + (\gamma_{13}^2 + 2\gamma_{23}^2\gamma_{33}^2)u_0 + (2\gamma_{33}^2 - 1)\gamma_{13}\gamma_{33}v_0 + (2\gamma_{23}^2 - 1)\gamma_{33}\gamma_{13}w_0],$$

$$m_2 = \frac{1}{N}[-(1-\gamma_{13}^2)\gamma_{13}\gamma_{33}x_0 + \gamma_{23}^2\gamma_{33}\gamma_{13}y_0 - (1-\gamma_{33}^2)\gamma_{33}\gamma_{13}z_0 - (1-2\gamma_{33}^2)\gamma_{13}\gamma_{23}u_0 + (\gamma_{23}^2 + 2\gamma_{33}^2\gamma_{13}^2)v_0 - (1-2\gamma_{13}^2)\gamma_{33}\gamma_{23}w_0],$$

$$m_3 = \frac{1}{N}[-(1-\gamma_{13}^2)\gamma_{13}\gamma_{23}x_0 - (1-\gamma_{23}^2)\gamma_{13}\gamma_{23}y_0 + \gamma_{33}^2\gamma_{13}\gamma_{23}z_0 - (1-2\gamma_{23}^2)\gamma_{33}\gamma_{13}u_0 - (1-2\gamma_{13}^2)\gamma_{33}\gamma_{23}v_0 + (\gamma_{33}^2 + 2\gamma_{13}^2\gamma_{23}^2)w_0],$$

$$A = \gamma_{11}^2 x_0 + \gamma_{21}^2 y_0 + \gamma_{31}^2 z_0 + 2\gamma_{21}\gamma_{31}u_0 + 2\gamma_{31}\gamma_{11}v_0 + 2\gamma_{11}\gamma_{21}w_0,$$
$$B = \gamma_{12}^2 x_0 + \gamma_{22}^2 y_0 + \gamma_{32}^2 z_0 + 2\gamma_{22}\gamma_{32}u_0 + 2\gamma_{32}\gamma_{12}v_0 + 2\gamma_{12}\gamma_{22}w_0,$$
$$D = \gamma_{11}\gamma_{12}x_0 + \gamma_{21}\gamma_{22}y_0 + \gamma_{31}\gamma_{32}z_0 + (\gamma_{31}\gamma_{22} + \gamma_{21}\gamma_{32})u_0 + (\gamma_{31}\gamma_{12} + \gamma_{11}\gamma_{32})v_0 + (\gamma_{11}\gamma_{22} + \gamma_{21}\gamma_{12})w_0,$$

$$n_1 = \frac{1}{N\theta_{20}}\left[A(\nu_{200} + \bar{u}_0^2) + B(\nu_{020} + \bar{v}_0^2) + 2D(\nu_{110} + \bar{u}_0\bar{v}_0)\right],$$

$$n_2 = l_1x_0 + l_2y_0 + l_3z_0 + 2m_1u_0 + 2m_2v_0 + 2m_3w_0,$$

where

$$Nx_0 = \left[\gamma_{11}^2\frac{\nu_{200}+\bar{u}_0^2}{\theta_{20}} + \gamma_{12}^2\frac{\nu_{020}+\bar{v}_0^2}{\theta_{20}} + \gamma_{13}^2(\nu_{002}+\bar{w}_0^2) + 2\gamma_{11}\gamma_{12}\frac{\nu_{110}+\bar{u}_0\bar{v}_0}{\theta_{20}} + 2\gamma_{11}\gamma_{13}\frac{\nu_{101}+\bar{u}_0\bar{w}_0}{\theta_1} + 2\gamma_{12}\gamma_{13}\frac{\nu_{011}+\bar{v}_0\bar{w}_0}{\theta_1}\right],$$

$$Ny_0 = \left[\gamma_{21}^2\frac{\nu_{200}+\bar{u}_0^2}{\theta_{20}} + \gamma_{22}^2\frac{\nu_{020}+\bar{v}_0^2}{\theta_{20}} + \gamma_{23}^2(\nu_{002}+\bar{w}_0^2) + 2\gamma_{21}\gamma_{22}\frac{\nu_{110}+\bar{u}_0\bar{v}_0}{\theta_{20}} + 2\gamma_{21}\gamma_{23}\frac{\nu_{101}+\bar{u}_0\bar{w}_0}{\theta_1} + 2\gamma_{22}\gamma_{23}\frac{\nu_{011}+\bar{v}_0\bar{w}_0}{\theta_1}\right],$$

$$Nz_0 = \left[\gamma_{32}^2\frac{\nu_{020}+\bar{v}_0^2}{\theta_{20}} + \gamma_{33}^2(\nu_{002}+\bar{w}_0^2) + 2\gamma_{32}\gamma_{33}\frac{\nu_0{}^{11}+\bar{v}_0\bar{w}_0}{\theta_1}\right],$$

$$Nu_0 = \left[\gamma_{22}\gamma_{32}\frac{\nu_{020}+\bar{v}_0^2}{\theta_{20}} + \gamma_{23}\gamma_{33}(\nu_{002}+\bar{w}_0^2) + \gamma_{21}\gamma_{32}\frac{\nu_{110}+\bar{u}_0\bar{v}_0}{\theta_{20}} + \gamma_{21}\gamma_{33}\frac{\nu_{101}+\bar{u}_0\bar{w}_0}{\theta_1} + (\gamma_{32}\gamma_{23}+\gamma_{22}\gamma_{33})\frac{\nu_{011}+\bar{v}_0\bar{w}_0}{\theta_1}\right],$$

$$Nv_0 = \left[\gamma_{32}\gamma_{12}\frac{\nu_{020}+\bar{v}_0^2}{\theta_{20}} + \gamma_{33}\gamma_{13}(\nu_{002}+\bar{w}_0^2) + \gamma_{11}\gamma_{32}\frac{\nu_{110}+\bar{u}_0\bar{v}_0}{\theta_{20}} + \gamma_{11}\gamma_{33}\frac{\nu_{101}+\bar{u}_0\bar{w}_0}{\theta_1} + (\gamma_{32}\gamma_{13}+\gamma_{12}\gamma_{33})\frac{\nu_{011}+\bar{v}_0\bar{w}_0}{\theta_1}\right],$$

$$Nw_0 = \left[\gamma_{11}\gamma_{21}\frac{\nu_{200}+\bar{u}_0^2}{\theta_{20}} + \gamma_{12}\gamma_{22}\frac{\nu_{020}+\bar{v}_0^2}{\theta_{20}} + \gamma_{13}\gamma_{23}(\nu_{002}+\bar{w}_0^2) + (\gamma_{11}\gamma_{22}+\gamma_{21}\gamma_{12})\frac{\nu_{110}+\bar{u}_0\bar{v}_0}{\theta_{20}} + (\gamma_{11}\gamma_{23}+\gamma_{21}\gamma_{13})\frac{\nu_{101}+\bar{u}_0\bar{w}_0}{\theta_1} + (\gamma_{12}\gamma_{23}+\gamma_{22}\gamma_{13})\frac{\nu_{011}+\bar{v}_0\bar{w}_0}{\theta_1}\right].$$

If equal weights are assigned to each of the 48 squares we find that

$$\begin{aligned}
48l_1 &= +25{\cdot}3096x_0 + 3{\cdot}2576y_0 + 3{\cdot}2032z_0,\\
48l_2 &= +3{\cdot}2576x_0 + 25{\cdot}0680y_0 + 3{\cdot}3208z_0,\\
48l_3 &= +3{\cdot}2032x_0 + 3{\cdot}3208y_0 + 26{\cdot}0632z_0,\\
48m_1 &= +22{\cdot}8740u_0,\\
48m_2 &= +22{\cdot}7616v_0,\\
48m_3 &= +21{\cdot}9284w_0.
\end{aligned}$$

The lengths and directions of the principal axes of the velocity ellipsoid are then found in the usual manner by solving Jacobi's equation. The mean errors in the length of the semi-axes are taken to be the same as those in the three main directions in the galactic system of co-ordinates. This is justified on account of the fact that the three main directions in the galactic system of co-ordinates differ by very small angles from the directions of the principal axes of the ellipsoid.

The material used in this paper consists of stars brighter than the sixth magnitude belonging to the spectral classes B8–A5, whose proper motions and radial velocities are known. The proper motions are taken from Boss's *Preliminary General Catalogue* (*P.G.C.*), and the radial velocities from the catalogue compiled by Schlesinger,* who has reduced them to the Lick system. A total of 843 stars was obtained. No stars were rejected on account of the fact that they were members of the Taurus or Ursa Majoris streams, and only one star was rejected owing to its very large (probable) absolute velocity. The proper motion components were calculated for increasing galactic longitude and latitude (in the system K_3 given above), and were further expressed in reduced measure by multiplying by the factor $10^{0{\cdot}2m}$, where m is the apparent magnitude of the star.

From a study of the radial velocities of the stars of spectral types B8–A5, Professor Lindblad † has concluded that there is a definite galactic rotation and K effect for the B8–B9 stars. Corrections for these effects have accordingly been made to the radial velocities of the B8–B9 stars. There are large probable errors associated with these effects for the stars of types A0–A5, and no corrections have been made to the radial velocities of these stars. No corrections have been made to the reduced proper motions owing to irregularities that have not yet been explained.‡

The stars under consideration have been divided into two groups, the first containing those stars that lie within the squares C1–C12, D1–D12, and the second those stars that lie within the squares A1, A2, B1–B10, E1–E10, F1, F2. The first group contains those stars that lie in the zone between the galactic equator and the parallels of latitude $\pm 30°$; the second group of stars lies between the parallels of latitude $\pm 30°$ and the galactic poles. It may be recalled here that the zone between the equator and the

* *Catalogue of Bright Stars*, 1930.
† *M.N.*, **90**, 511, 1930.
‡ Dyson, *M.N.*, **90**, 233, 1929.

parallel of latitude $b = +30°$ is divided into 12 squares C1–C12, C1 containing those stars whose galactic longitude (l) lies between 0° and 30°, C2 those with l between 30° and 60°, and so on. The zone between $b = +30°$ and $b = +66°\ 26'{\cdot}6$ is divided into 10 squares B1–B10, and the calotte round the north galactic pole into two squares A1 and A2. The southern hemisphere is divided in a similar fashion, viz. D1–D12 for b between 0° and $-30°$, E1–E10 for b between $-30°$ and $-66°\ 26'{\cdot}6$, and F1, F2 for the region round the south galactic pole. The first group of stars, mentioned above, will in future be denoted as the galactic group, the second as the non-galactic group. As the radial velocities have been corrected for the K effect, the squares have been combined diametrically, thus confining the computations to the northern hemisphere. The weight assigned to any one compound square has been taken as the number of stars in that square.

Table I gives the results obtained from the first order moments.

TABLE I

Group	Number of Stars	N'_{100} km./sec.	N'_{010} km./sec.	N'_{001} km./sec.	S km./sec.	Co-ordinates of Apex				θ_1
						L	B	A	D	
						° °	° °	°	°	″
Galactic	506	−17·12	−5·54	−6·69	19·2 ± 1·1	17·9 ± 2·8	+20·4 ± 3·0	269·1	+24·7	0·116
Non-Galactic	337	−10·70	−3·79	−6·09	12·9 ± 1·4	19·5 ± 5·3	+28·2 ± 4·8	261·4	+28·8	0·164

In Table I the following symbols have been used :—

S, the velocity of the Sun.
L, B, the galactic longitude and latitude of the apex.
A, D, the right ascension and declination of the apex.

The striking feature of Table I is the difference between N'_{100} for the two groups of stars. For the galactic group $N'_{100} = -17{\cdot}12 \pm 1{\cdot}13$, and for the non-galactic group $N'_{100} = -10{\cdot}70 \pm 1{\cdot}54$, and it may be shown that this difference is significant. The other moments show no such significant differences. With regard to θ_1 the galactic group gives $\theta_1 = 0''{\cdot}116 \pm 0''{\cdot}009$, and the non-galactic group gives $\theta_1 = 0''{\cdot}164 \pm 0''{\cdot}022$. The two values of θ_1 are also significantly different from one another.

In the determination of the solar constants of Table I the squares were combined diametrically, and Table II shows the differences obtained between the observed and calculated velocity components for the different squares of the northern hemisphere. These differences are denoted by ϵ_{100}, ϵ_{010} and ϵ_{001}, referring respectively to the differences in longitude, latitude and line of sight. It will be noted that the residuals in the ϵ_{010} component are much larger for the non-galactic than for the galactic group.

TABLE II

Squares Combined Diametrically

Square	l	b	No.	ϵ_{100}	ϵ_{010}	ϵ_{001} km./sec.
	° °	° °		″	″	
A1	0–180	66–90	23	+0·288	−0·128	−0·58
A2	180–360	,,	27	+ ·144	+ ·066	+0·43
B1	0– 36	30–66	26	− ·067	− ·082	−2·46
B2	36– 72	,,	33	+ ·008	− ·102	+1·86
B3	72–108	,,	34	+ ·017	+ ·039	+1·06
B4	108–144	,,	23	+ ·056	− ·120	+2·87
B5	144–180	,,	37	+ ·082	+ ·045	+0·11
B6	180–216	,,	27	+ ·029	+ ·170	−2·74
B7	216–252	,,	23	+ ·168	+ ·024	−1·85
B8	252–288	,,	22	− ·039	− ·025	+4·10
B9	288–324	,,	28	− ·104	− ·053	−1·59
B10	324–360	,,	34	+ ·017	− ·046	−1·26
C1	0– 30	0–30	46	− ·011	− ·027	+2·00
C2	30– 60	,,	50	+ ·015	+ ·016	−5·01
C3	60– 90	,,	39	− ·097	− ·068	+1·43
C4	90–120	,,	37	+ ·067	− ·004	+2·16
C5	120–150	,,	39	− ·108	+ ·016	−2·77
C6	150–180	,,	35	− ·013	− ·004	+0·11
C7	180–210	,,	37	− ·098	+ ·043	+0·52
C8	210–240	,,	30	+ ·032	+ ·026	−4·21
C9	240–270	,,	44	+ ·107	− ·073	−1·48
C10	270–300	,,	47	− ·065	+ ·012	+0·87
C11	300–330	,,	50	− ·143	+ ·051	−3·28
C12	330–360	,,	52	− ·021	+ ·048	+0·76

In the previous calculations the use of reduced proper motions places the stars at a distance R where they have the apparent magnitude zero. The absolute magnitudes of the sub-classes of spectral Type A have, however, been given by Dr. Trumpler * as follows :—

Type	B8	B9	A0	A2	A3	A5
M	−0·2	−0·3	+0·9	+1·7	+2·0	+2·3

where M is the absolute magnitude. Thus for stars of the same apparent magnitude in the various sub-classes there will be considerable differences of distance. If, therefore, the various sub-classes are to be grouped together it would appear advisable to correct the apparent magnitudes of the stars in such a way that all the sub-classes are reduced to a fixed absolute magnitude. The absolute magnitude chosen is that for Type A0. Thus, for example, to the apparent magnitudes of the stars of Type B8 must be added the difference +1·1 between Types A0 and B8 so that the stars are made fainter by this amount. The reduced proper motions for any star being defined by

$$u' = u \,.\, 10^{0\cdot 2m},$$
$$v' = v \,.\, 10^{0\cdot 2m},$$

* *L.O.B.*, No. 420, 1930.

where u, v are the observed proper motions and m the apparent magnitude, it will be seen that the reduced proper motions must be corrected by multiplying by the following factors :—

Type	B8	B9	A0	A2	A3	A5
Factor	1·1070	1·0570	1·0000	0·9294	0·9033	0·8787

Table III gives the Sun's velocity and the co-ordinates of the apex for the two groups of stars, and a comparison of this table with Table I shows that the results are practically identical.

TABLE III

Group	Number of Stars	N'_{100} km./sec.	N'_{010} km./sec.	N'_{001} km./sec.	S km./sec.	Co-ordinates of Apex				θ_1
						L	B	A	D	
						°	°	°	°	″
Galactic	506	−17·10	−5·60	−6·74	19·21	18·1	+20·5	269	+25	0·113
Non-Galactic	337	−10·73	−3·80	−6·07	12·90	19·5	+28·1	261	+29	0·159

The stream velocity components were next calculated for each square, the values of θ_1, found above, being used to convert the proper motions to linear velocities. In Table IV are given the stream velocities for each of the compound squares, B1 E1, B2 E2, . . . , C1 D1, C2 D2, . . . , together with the directions of the motions in the apex direction. The combined squares C3 D3 and C10 D10 give the smallest and largest values respectively of the stream velocity, and in the non-galactic group the squares B2 E2 and B9 E9 give the similar effect. The direction of the motion for the C3 D3 squares is also quite different from that of the other squares.

TABLE IV

Squares	S km./sec.	Co-ordinates of Apex	
		L	B
		°	°
B–E	12·88	19·5	+28·2
B1, E1	13·13	26·3	+29·7
B2, E2	9·79	21·6	+55·7
B3, E3	11·23	20·5	+25·4
B4, E4	15·17	16·3	+30·9
B5, E5	12·54	25·2	+26·7
B6, E6	10·60	28·0	+24·9
B7, E7	14·01	19·3	+21·7
B8, E8	17·56	28·4	+11·4
B9, E9	17·54	12·0	+23·7
B10, E10	13·93	24·5	+30·5

Squares	S km./sec.	Co-ordinates of Apex	
		L	B
C–D	19·20	17·9	+20·4
C1, D1	17·79	9·0	+15·4
C2, D2	16·96	16·7	+17·2
C3, D3	14·71	44·0	+37·9
C4, D4	16·03	9·4	+12·0
C5, D5	19·45	15·1	+11·2
C6, D6	19·35	19·4	+17·9
C7, D7	18·44	19·6	+26·7
C8, D8	25·56	23·5	+22·8
C9, D9	19·85	8·8	+30·1
C10, D10	29·98	21·5	+20·0
C11, D11	23·39	22·3	+28·0
C12, D12	18·13	17·9	+15·2

The second order moments will now be considered. As has been shown above, the diametrical grouping of the squares frees the velocities of the stars to a large extent from the galactic rotation effect, and hence only the stream velocity components (in arc) have been subtracted from the proper motions. The radial velocities of the B8–B9 stars, as already noted, have been corrected for the rotation effect. In forming the second order moments about the mean, the mean deviation I was first found and the standard deviation was then assumed to be given by $\sigma = 1{\cdot}253$ I. Table V gives the principal results, the stars being again taken in two groups. In this table σ_1, σ_2 and σ_3 are the lengths of the semi-axes of the velocity ellipsoid, and their directions are given in galactic co-ordinates (L, B) and equatorial co-ordinates (A, D). With regard to the mean errors in σ_1, σ_2 and σ_3 the number of equations of condition is $k = 72$, but it was decided to take $k = 36$ in view of the different amounts contributed by these equations to the mean errors. As will be seen from this table there are no significant differences between the lengths of the respective semi-axes of the two groups, and in both cases the smallest axis points to the galactic pole. The longitude of the vertex also agrees well for the two groups.

TABLE V

	Galactic Stars	Non-Galactic Stars
N	506	337
σ_1	18·28 ± 0·87 km./sec.	15·87 ± 1·21 km./sec.
L_1	349°·3	354°·9
B_1	− 9°·3	− 7°·6
A_1	283°	284°
D_1	− 14°	− 8°

	Galactic Stars	Non-Galactic Stars
σ_2	7·15 ± 1·67 km./sec.	7·93 ± 1·48 km./sec.
L_2	330°·0	50°·5
B_2	+ 80°·4	+ 76°·8
A_2	199°	200°
D_2	+ 23°	+ 38°
σ_3	10·68 ± 1·18 km./sec.	9·05 ± 1·37 km./sec.
L_3	78°·7	86°·3
B_3	+ 3°·3	− 9°·1
A_3	345°	4°
D_3	+ 63°	+ 53°
θ_2	·0166 ± ·0014	·0319 ± ·0034

If the vertex direction is assumed to lie in the galactic plane—that is, $N_{101} = N_{011} = 0$—then the position of the vertex and the lengths of the semi-axes of the velocity ellipsoids are shown in Table VI. The mean errors will be slightly less than those given in Table V, as there are now only 5 variables to consider.

TABLE VI

Galactic Stars	Non-Galactic Stars
σ_1 18·2 km./sec.	16·2 km./sec.
L_1 349°·6	355°·2
A_1 275°·1	277°·7
D_1 − 9°·2	− 4°·2
σ_2 7·8 km./sec.	8·3 km./sec.
σ_3 10·8 km./sec.	9·1 km./sec.
θ_2 0·0163	0·0311

Table VII gives, for each square, the observed second order moments ν_{200}, ν_{020}, ν_{002} (in system K_3), together with the moments calculated from a modified form of the equations given in the introduction. These latter moments have been designated by ${}_c\nu_{200}$, ${}_c\nu_{020}$ and ${}_c\nu_{002}$. The differences $\epsilon_{200} = \nu_{200} - {}_c\nu_{200}$, $\epsilon_{020} = \nu_{020} - {}_c\nu_{020}$, $\epsilon_{002} = \nu_{002} - {}_c\nu_{002}$ have been examined in order to ascertain if any of them differ significantly from zero, and the following table shows these squares in which the differences are significant :—

ϵ_{200}	ϵ_{020}	ϵ_{002}
A1	D5	E7
D3	D10	C3
D10	...	F1
A1, F1	C5, D5	C3, D3

[TABLE

TABLE VII

l	b	Square	Observed			Calculated		
			v_{200}	v_{020}	v_{002}	$_cv_{200}$	$_cv_{020}$	$_cv_{002}$
° °								
0–180	+66° to +90°	A1	1·0136	0·1591	57·12	0·3757	0·1189	66·82
180–360	,,	A2	·7273	·0731	126·68	·3757	·1211	67·70
° °								
0–36	+30° to +66°	B1	·0581	·1061	143·52	·1526	·2428	120·39
36–72	,,	B2	·3769	·1856	87·20	·2999	·1596	80·14
72–108	,,	B3	·5388	·0824	106·30	·3757	·1086	73·42
108–144	,,	B4	·2839	·2375	179·83	·2751	·1472	123·77
144–180	,,	B5	·1761	·1452	278·59	·1372	·2104	176·46
180–216	,,	B6	·0372	·3145	176·62	·1526	·2046	168·26
216–252	,,	B7	·1319	·0733	90·67	·2999	·1399	111·54
252–288	,,	B8	·1373	·0776	130·78	·3757	·1149	76·00
288–324	,,	B9	·2483	·1112	41·85	·2751	·1771	96·77
324–360	,,	B10	·1442	·2634	83·30	·1372	·2524	130·17
° °								
0–36	−30° to −66°	E1	·0947	·1679	251·92	·1526	·2046	168·26
36–72	,,	E2	·2421	·1191	149·40	·2999	·1399	111·54
72–108	,,	E3	·5129	·0734	97·46	·3757	·1149	76·00
108–144	,,	E4	·2885	·1442	111·53	·2751	·1771	96·77
144–180	,,	E5	·0471	·1696	81·32	·1372	·2524	130·17
180–216	,,	E6	·0761	·3745	146·22	·1526	·2428	120·39
216–252	,,	E7	·1565	·1554	221·59	·2999	·1596	80·14
252–288	,,	E8	·2790	·1220	64·35	·3757	·1086	73·42
288–324	,,	E9	·1458	·0839	56·46	·2751	·1472	123·77
324–360	,,	E10	·0863	·1203	158·43	·1372	·2104	174·46
° °								
0–180	−66° to −90°	F1	·3342	·2315	158·89	·3757	·1211	67·70
180–360	,,	F2	·1478	·0452	74·15	·3757	·1189	66·82
° °								
0–30	0° to +30°	C1	·1324	·0815	152·03	·1137	·0679	254·52
30–60	,,	C2	·1939	·0467	144·00	·2008	·0576	163·60
60–90	,,	C3	·1596	·0573	348·57	·2727	·0480	111·70
90–120	,,	C4	·2455	·0430	209·38	·2575	·0451	158·53
120–150	,,	C5	·1461	·0381	281·57	·1704	·0490	265·08
150–180	,,	C6	·0376	·0554	171·09	·0985	·0545	330·48
180–210	,,	C7	·0322	·0432	270·60	·1137	·0570	291·42
210–240	,,	C8	·3604	·0382	96·83	·2008	·0565	184·81
240–270	,,	C9	·2033	·0791	139·24	·2727	·0570	111·54
270–300	,,	C10	·1806	·0283	224·70	·2575	·0618	137·04
300–330	,,	C11	·0904	·0782	105·88	·1704	·0689	228·01
330–360	,,	C12	·0725	·0631	289·34	·0985	·0723	287·79
° °								
0–30	0° to −30°	D1	0·0964	·0548	228·61	·1137	·0570	291·42
30–60	,,	D2	·1768	·0325	166·93	·2008	·0565	184·81
60–90	,,	D3	·4973	·0922	198·53	·2727	·0570	111·54
90–120	,,	D4	·2893	·0410	128·37	·2575	·0618	137·04
120–150	,,	D5	·1829	·1318	272·25	·1704	·0689	228·01
150–180	,,	D6	·0989	·0758	264·06	·0985	·0723	287·79
180–210	,,	D7	·0579	·0449	339·30	·1137	·0679	254·52
210–240	,,	D8	·3143	·0294	155·75	·2008	·0576	163·60
240–270	,,	D9	·1147	·0370	176·89	·2727	·0480	111·70
270–300	,,	D10	·6042	·1676	233·78	·2575	·0451	158·53
300–330	,,	D11	·1045	·0835	134·33	·1704	·0490	265·08
330–360	,,	D12	·0805	·1098	376·36	·0985	·0545	330·48

The differences in squares A1 and F1 are probably due to wrong values of θ_1 and θ_2, since it has been shown that there is a decided dependence of these quantities on galactic latitude, and in the calculations the squares round the poles were grouped with the squares in the intermediate zone between the equator and the poles. With regard to square D5 it has to be noted that the Taurus stream is situated in this square, and this fact will probably account for the deviation noticed. The squares D3 and D10 have already, in the discussion of the first order moments, been denoted as irregular, the stream velocity components differing significantly from the mean components obtained from all squares. Allowing for this difference in stream velocity the errors ϵ_{200} are, for these squares, found to be no longer significantly different from zero. It seems most probable, therefore, that the irregularities which occur in squares D3 and D10 are due to an actual difference in stream velocity.

Professor Schlesinger * has listed the parallaxes, from all sources, of 580 of the stars that have been used in the previous calculations, and the stream velocity and lengths of the semi-axes of the velocity ellipsoid, calculated from these stars, were compared with the results of Tables I and V. Tables VIII and IX give these constants calculated from 577 parallax stars, the following 3 stars being excluded :—

Boss, *P.G.C.* 1515 in square C5.	$U'' = -107{\cdot}6$ km./sec. $V'' = -73{\cdot}6$,, $W'' = -27{\cdot}8$,, $\pi = 0''{\cdot}002$
Boss, *P.G.C.* 4511 in square C2.	$U'' = -103{\cdot}0$ km./sec. $V'' = +13{\cdot}4$,, $W'' = +20{\cdot}6$,, $\pi = +0''{\cdot}011$
Boss, *P.G.C.* 2647 in square B6.	$U'' = -115{\cdot}9$ km./sec. $V'' = +43{\cdot}9$,, $W'' = +38{\cdot}9$,, $\pi = +0''{\cdot}011$

TABLE VIII

Group	N	N'_{100} km./sec.	N'_{010} km./sec.	N'_{001} km./sec.
Galactic	324	−14·41	−3·99	−4·86
Non-Galactic	253	−10·14	−4·00	−6·81

TABLE IX

Group	σ_1 km./sec.	σ_2 km./sec.	σ_3 km./sec.
Galactic	17·51	6·45	9·94
Non-Galactic	17·39	8·34	9·85

* *Catalogue of Bright Stars*, 1930.

Comparing the above two tables with Tables I and V it is seen that the agreement is satisfactory, the two groups of stars showing a difference in stream velocity and a similarity in the lengths of the axes of the velocity ellipsoids.

In conclusion I must thank Dr. Gyllenberg for helpful advice and criticism.

The University,
Glasgow.

A METHOD OF ANALYSING STELLAR VARIABILITY.

E. A. Milne, F.R.S.

1. The main object of the following paper is to propose a simple method of studying the behaviour of pulsating variable stars. The method is applicable to all classes of variables for which simultaneous measures of brightness and radial velocity are available, though it takes its most convenient form when the measures can be reduced to values of the energy output (apart from a here irrelevant multiplying factor), and the measures of radial velocity reduced to the actual surface-velocity in the pulsation. The method suggested itself in connection with certain theoretical considerations concerning the nature of Cepheid and other variation, and will be so presented in the first instance, but it will be seen that the applicability and utility of the method are independent of theoretical considerations. The method results in the construction, for each star observed, of a characteristic curve, which for cyclic pulsations is a closed curve. The properties of these curves give considerable insight into the phase relations in Cepheid variation and the relation of the course of the cycle to the corresponding steady-state configuration about which oscillations are occurring. Further, they bring out in a striking way certain features of the pulsation, and suggest most interesting general questions. Their further study, for all observable variables, holds out promise of increasing our understanding of the nature and origin of stellar variation. Essentially the method consists in the construction of a Hertzsprung-Russell diagram for the life-history of each variable star, with radius replacing effective temperature.

2. *The* (r, L) *Diagram for a Variable Star.*—In my work on steady-state configurations of stellar masses * I frequently emphasized the importance of constructing, for any given chemical composition and any given relative source-distribution, curves of radius r against luminosity L for constant mass M. Such curves give explicit recognition to the fact that, as far as steady-state considerations are concerned (*i.e.* as far as we can get simply from taking into account mechanical equilibrium and the constancy of thermal state), a given mass M can be associated in the steady state with any luminosity L (less than some limit), each mass M for an assigned

* E.g. *Zeits. für Astrophys.*, **4**, 75, 1932 ; *M.N.*, **92**, 610, 1932.

arbitrary L possessing one or more configurations each of definite radius. (There are, it is not hard to show, in general at least two possible configurations for any given pair (M, L).) The family of curves (r, L) for constant M afford a mesh or background on which any observed pair (M, L) may be plotted, and the test of the accuracy of a theory of stellar constitution lies in comparing the observed radius, obtained in some manner, with the theoretical radius associated with the plotted point in the diagram. A genuine mass-luminosity law—that is, an actual correlation of L with M for any class of observed stars—will be represented by a locus in the diagram defining L as a function of M; a statistical correlation of luminosity with mass will be represented by a band. Such correlations are to be distinguished in a marked way from the $r = f(L, M)$ relation from which the mesh of curves has been constructed, obedience to such a relation being shown by any set of points lying on the curves, whether confined to certain regions of the diagram or not. The general form of such curves, which I hope to discuss in a later paper, is immaterial to the considerations which follow relating to variable stars. What is essential is the recognition that a star in a steady state, of given mass M, has two other observable characteristics describing its configuration, namely, L and r.

What is the corresponding state of affairs for a star not in a steady state? During any disturbances which it may undergo its mass M may be supposed to remain constant, but L and r will vary in some way. The simplest way of exhibiting the history of such a variation is accordingly to use the same type of diagram as was described above for steady states, and to plot either r or $\log r$ against either L or $\log L$ during the variation. For a variable star observed both spectroscopically and radiometrically * $\log_{10} L$ is given apart from an additive constant simply from the radiometric magnitudes, whilst the change in r, i.e. $r - r_0$, is given by integrating the observed radial velocities with respect to the time t, after making allowance for the differing velocities of approach of the different regions of the stellar disc.† Thus in these cases direct observation gives, apart from additive constants, the values of $\log_{10} L$ and r; these are therefore probably the most convenient to plot in practice. Actually the arguments which follow take a somewhat simpler form if $\log_{10} r$ as y is plotted against $\log_{10} L$ as x; the conversion of the results of the velocity integration, namely, values of $r - r_0$, into values of $\log_{10} r$ requires an estimate of the mean radius of the star, but the shape of the plotted curve will not be expected to be very sensitive to errors in this estimate.

Suppose then for simplicity that from actual observations $\log_{10} r$ has been plotted against $\log_{10} L$, and that against each plotted point the epoch has been written in. A curve will result which will be characteristic of the changes undergone by this particular star, and a mere glance at the curve

* *Cf.* Pettit and Nicholson's recent important paper in *Ap. J.*, **78**, 320, 1933.

† The observed radial velocities must, of course, first be averaged with respect to the time to give the velocity of centre of gravity of the star, which must then be subtracted from the observed velocities to give the mean velocity of approach of the surface. The correcting factor for reducing the average disc-velocity to the velocity of pulsation is very closely 24/17, taking disc-darkening into account as well.

together with the time-markings on it will tell the whole history of the variation.

3. *Form of the Characteristic Curves.*—What is the form to be expected for such curves? We will see how far *a priori* considerations carry us before constructing an actual example. Let us consider the case of a regular variable with a definite period, definite light-curve and definite velocity-curve. Then the characteristic curve will necessarily be *closed*, and will be described once in each period; the time-markings in such a case, instead of being written in Julian days, can conveniently be written as a phase, reckoned in hours or days, measured from some suitable zero. A particular limiting case will occur when the closed curve reduces to an arc described in a to-and-fro motion, the area enclosed being then zero. But the most general possible characteristic curve for a regular variable will be a closed curve of non-zero area. The circumstance that the curve will in general enclose an area and not simply consist of an arc, traced and retraced, is the important feature disclosed by the present method of analysis. It follows simply from recognition of the fact that two variables L and r are necessary to describe the momentary state of a star of mass M, and that accordingly the most general periodic (r, L) locus is a closed curve. The most general cyclic changes capable of being undergone by a star are analogous to the motion of a spherical pendulum and not an ordinary pendulum.*

4. *Tangency Properties.*—Let us carry the argument a little further. During the cycle of changes undergone by the star it will possess a maximum and minimum bolometric luminosity, $L_{\max}$ and $L_{\min}$. The characteristic curve will therefore touch the vertical straight lines $x = \log_{10} L_{\max}$ and $x = \log_{10} L_{\min}$. Secondly, it will possess a maximum and minimum radius, $r_{\max}$ and $r_{\min}$. The curve will therefore touch the horizontal straight lines $y = \log_{10} r_{\max}$ and $y = \log_{10} r_{\min}$. Thirdly, it will possess a maximum and minimum effective temperature T_e, defined by $4\pi r^2 \sigma T_e^4 = L$. The curve will therefore touch the pair of parallel straight lines

$$y = \tfrac{1}{2}x - \tfrac{1}{2}\log_{10}(4\pi\sigma T_{e\,\max}^4)$$
$$y = \tfrac{1}{2}x - \tfrac{1}{2}\log_{10}(4\pi\sigma T_{e\,\min}^4).$$

Of these the higher in the diagram corresponds to $T_{e\,\min}$, the lower to $T_{e\,\max}$. The curve will therefore touch three pairs of parallel straight lines. The simplest such curve is an ellipse, by Pascal's hexagon theorem. This is the curve of lowest degree in x and y satisfying the conditions. Without in any way implying that the characteristic curve of an actual periodic variable will be an ellipse, we may expect that it will be of general elliptic appearance. Such an ellipse† is shown in fig. 1, the points of contact being A, A'; B, B'; H, H'.

5. *Coincidence of Maximum and Minimum Luminosities with Large Surface*

* Actually there is no strict mechanical analogue.

† Actual characteristic curves for δ Cephei and η Aquilæ have their major axes much more nearly horizontal than is shown in fig. 1. The curves for δ Cephei and η Aquilæ have been constructed by Mr. I. A. Getting, working under the direction of Prof. H. H. Plaskett at the University Observatory, Oxford.

Velocities.—One property of such curves follows by inspection: if the representative point P describes the curve with anything approaching uniform velocity, the greatest value of dr/dt will occur at A and A', *i.e.* at L_{max} and L_{min}. We cannot, however, decide whether the velocity at L_{max} is one of approach or one of recession. If the rate of description of the curve is non-uniform, the value of $d(\log r)/dt$, which is the resolved velocity of P in the y-direction, will still have a tendency to reach its maximum numerical value at A and A'. There is indeed one limiting case, in which the lines

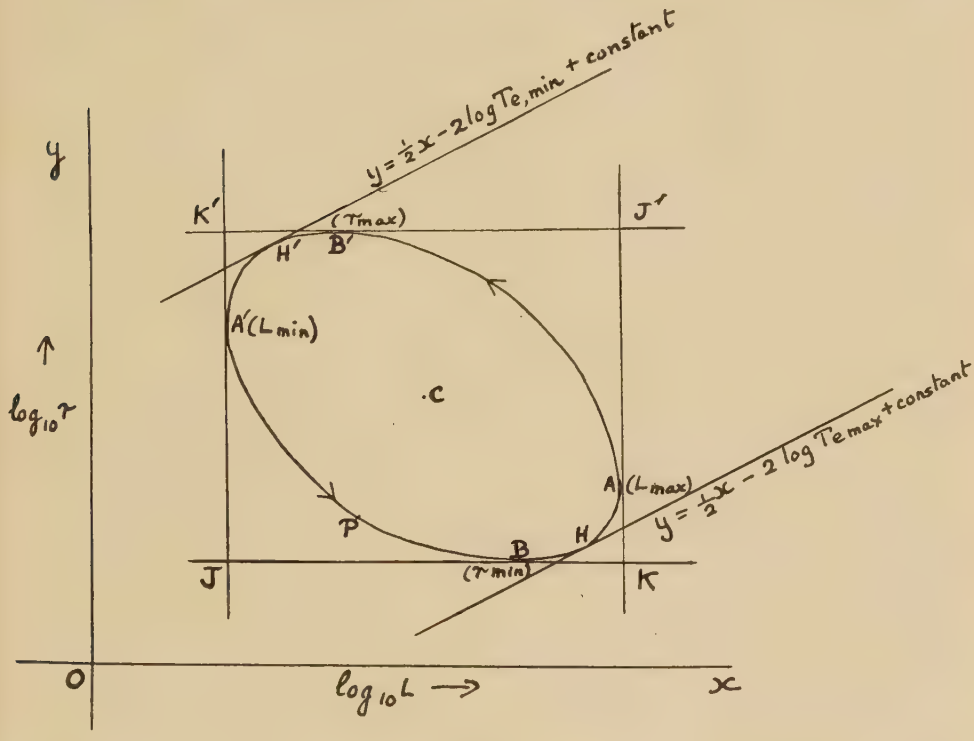

Fig. 1.

defining $T_{e(max)}$ and $T_{e(min)}$ intersect the corners K, K' of the rectangle $JKJ'K'$, the ellipse reduces to the diagonal KK', described twice in a cycle, and the representative point must come to *rest* at K and K'; hence in this case the stellar surface comes to rest at L_{max} and L_{min}. This is the case described in Eddington's researches on adiabatic stellar pulsations, in which L_{max} and $T_{e(max)}$ coincide with r_{min}, L_{min} and $T_{e(min)}$ with r_{max}. We see that Eddington's analysis by no means describes the most general type of oscillation.

We thus see that we have gained insight into that most characteristic feature of Cepheid variation, the general coincidence of the greatest surface velocity with the epochs of L_{max} and L_{min}.

6. *Sense of Description of the Characteristic Curve.*—In an actual Cepheid maximum luminosity coincides with maximum velocity of *approach*. This

defines the sense of description of the characteristic curve as being $BAB'A'$ and not $BA'B'A$; for at A, *i.e.* at L_{max}, the star is expanding and the motion of P is parallel to the direction of r increasing. Moreover, the fact that the relation of coincidence of maximum velocity of approach with maximum luminosity holds for all Cepheids shows that the sense of description of the characteristic curve is also a characteristic of the phenomenon; the arrows always point counter-clockwise. For Cepheid variables the characteristic curve is therefore irreversible, for in nature it is described in one direction only. Any theory of Cepheids must explain this irreversibility.

We must be careful not to suggest that all variables will show the same sense of description of their characteristic curves as Cepheids. It is well known * that the long-period variables show the opposite phase-relation-maximum velocity of *recession* corresponding to maximum luminosity. Nevertheless it is tempting to examine what conclusions may be drawn from the observed sense of description for Cepheids.

7. *Energy Relations.*†—Until the source of stellar energy is more definitely known it is impossible to say how the rate of liberation of energy in the interior varies during the cycle of the pulsation. All we can say is that the time-average of the rate of liberation of energy in the interior during a cycle must equal the time-average of the rate of output at the surface—that is, the time-average of the bolometric luminosity. In general, at an arbitrary phase of the cycle, the total output of energy at the surface, reckoned from some convenient zero, will not be equal to the total liberation in the interior reckoned from a corresponding zero. The amount of energy of all kinds located in the material of the star—gravitational, thermal, radiant and kinetic—will therefore not be a constant. This differentiates a pulsating star markedly from the ordinary vibrating systems of dynamics, for which the energy is conserved. Instead of a fixed amount of energy passing alternately from kinetic to potential form and back again, we have a periodically variable amount of energy located in the system.

If Ω (a function of t) is the amount of energy in the system at time t, L the instantaneous luminosity, E the rate of liberation of energy, then we have the relation

$$\frac{d\Omega}{dt} = E - L. \qquad (1)$$

A whole variety of pulsation problems arise (as investigated by Rosseland) ‡ depending on the form of E, the general problem being to determine $L(t)$, given the physical laws controlling E.

A particular case of great interest is when E is constant. This is the

* Russell, Dugan and Stewart, *Astronomy*, **2**, 773.

† Energy relations are considered more fully in my paper "The Energetics of Non-steady States, with an Application to Cepheid Variation," *Quart. Journ. Math. (Oxford)*, 1933 December, where it is shown that under certain circumstances a criterion for the existence of undamped oscillations in luminosity may be found, and that then the maxima in the light-curve will be more pronounced than the minima.

‡ *Oslo Obs. Pub.*, No. 1, **1**, 1931.

case dealt with in the first instance in Eddington's pulsation analysis, for there not only E but also ϵ, the rate of liberation per unit mass, is constant; Rosseland has called this the "radio-active" model. Again, if the pulsations were chiefly a surface phenomenon, not extending deep into the interior, E would be constant. Again, a slow response of rate of liberation to changing conditions will leave E unaltered. The case $E = \text{const.}$ is, in fact, a fundamental case, and only when this has been fully examined shall we be in a position to judge what effect the pulsations have, if any, on the rate of liberation.

Let us consider then $E = \text{const.}$ Then by integrating over a cycle of period T we have

$$E = \frac{1}{T}\oint L dt. \tag{2}$$

Accordingly E is equal to the time-average of the output of energy at the surface, say L_0. By (1) we have now

$$\frac{d\Omega}{dt} = -(L - L_0) \tag{3}$$

whence

$$\Omega - \Omega_0 = -\int_0^t (L - L_0) dt, \tag{4}$$

where Ω_0 is the total energy at some epoch $t = 0$. The graphs of $L - L_0$ and Ω, plotted against t, are shown below (fig. 2) for a typical case. We see that Ω_{max} occurs at the epoch at which $L = L_0(1)$, $L_0(1)$ denoting the mean luminosity where it occurs on the ascending branch of the luminosity curve; and that Ω_{min} occurs at the epoch at which $L = L_0(2)$, $L_0(2)$ denoting the mean luminosity where it occurs on the descending branch of the luminosity curve. Further, in a cycle beginning with $L_0(1)$, the temporal sequence is

$$\Omega_{max}, L_{max}, \Omega_{min}, L_{min}, \Omega_{max}. \tag{5}$$

By inspection of fig. 1 we see that $L_0(1)$ occurs for a Cepheid in the vicinity of r_{min}, and $L_0(2)$ in the vicinity of r_{max}. Hence Ω_{max} occurs in the vicinity of r_{min}, Ω_{min} in the vicinity of r_{max}. Now at r_{max} or r_{min} the star has come to rest, the kinetic energy is zero, and the energy is gravitational, thermal and radiant. In a conservative oscillating system, the behaviour following r_{max} or r_{min} would be such that the energy becomes partly transformed into kinetic energy at the expense of other forms of energy. In our case it is tempting to conjecture that the re-expansion following r_{min}, occurring as it does in the vicinity of Ω_{max}, is partly helped by the excess of energy over the average. Similarly the contraction following r_{max}, occurring as it does in the vicinity of Ω_{min}, may be partly helped by the deficiency of energy below the average. For an excess energy will tend to cause expansion; a deficiency of energy, contraction. It would, in fact, be paradoxical if Ω_{max} coincided with r_{max}, for the tendency of Ω_{max} to cause expansion would be incompatible with the existence of a maximum value for r.

If we could actually be sure on dynamical grounds that Ω_{max} must occur at r_{min} and Ω_{min} at r_{max}—and we have seen that it is only a question of which of Ω_{max} and Ω_{min} is to be associated with which of r_{max} and r_{min}—the temporal sequence (5), which we have established, would imply the temporal sequence

$$r_{min},\ L_{max},\ r_{max},\ L_{min},\ r_{min}. \qquad (6)$$

This would fix the sense of description of the characteristic curve in agreement with the observed sense for Cepheids. Actually all we have proved

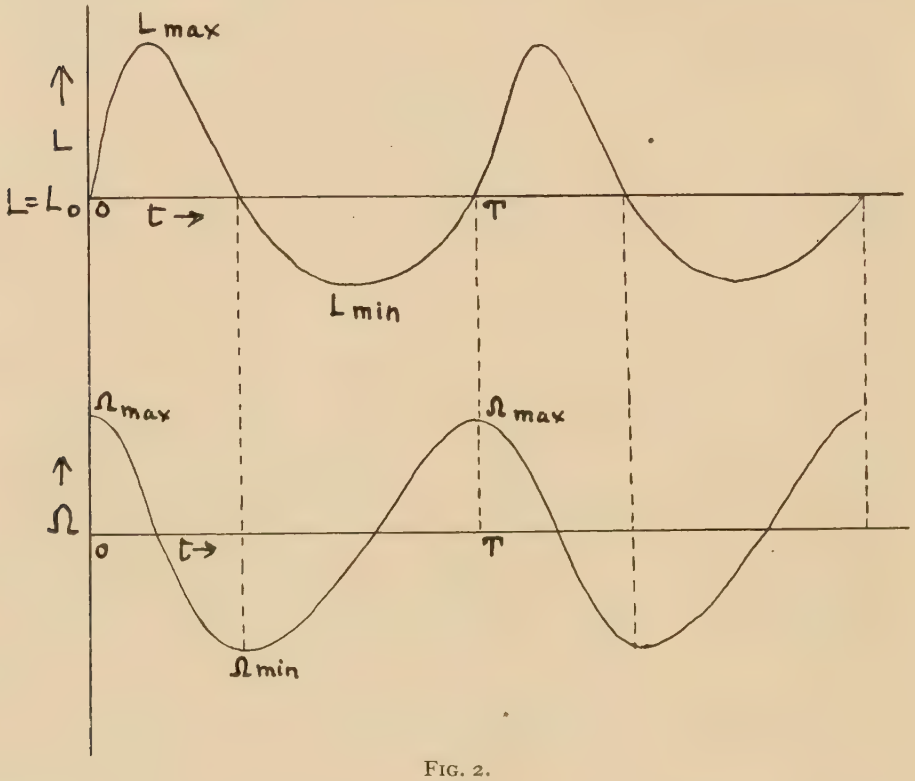

FIG. 2.

a priori is that the order is either r_{min}, L_{max}, r_{max}, L_{min}, r_{min} or r_{max}, L_{max}, r_{min}, L_{min}, r_{max}, save in the exceptional case when the characteristic curve reduces to an arc, when L_{max} coincides with r_{min}, L_{min} with r_{max}.* Observation pronounces in favour of the first alternative.

It is only when $E(t)$ is independent of t that Ω_{max} will occur precisely at L_0 (1), Ω_{min} at L_0 (2). When E responds in some way to the course of the cycle, Ω_{max} will not occur precisely at L_0 (1). If, for example, r_{min} follows L_0 (1), and if Ω_{max} actually coincides with r_{min}, as suggested, then Ω would be increasing at L_0 (1), and so, at L_0 (1), $E(t)$ would slightly exceed L_0.

* In this discussion I have benefited by a conversation with Sir Arthur Eddington, to whom I described an earlier sketch of these ideas in the summer of 1933. Eddington is in no way responsible for the correctness or otherwise of the present form of the argument.

If Ω_{max} coincides with r_{min}, Ω_{min} with r_{max}, then it is clear that at the two points in a complete cycle at which the radius r takes a given value, the two values of Ω will be approximately equal; for the chords joining points of equal energy, being horizontal (tangents) at r_{max} and r_{min}, cannot depart far from horizontality anywhere. Hence, very closely, the radius r will be a *single-valued* function of Ω during the cycle, although both Ω and r pass twice through each value lying between their maxima and minima. This justifies an assumption made in my paper "The Energetics of Non-steady States . . ." (*loc. cit.*). It was there assumed that a certain time-lag, denoted by T, was a single-valued function of Ω. Now T will depend chiefly on the radius r, which we have seen to be a single-valued function of Ω. Hence the assumption is justified.

8. *Long-period Variables.*—For the long-period variables the opposite sense of description is observed. Possibly for these stars, for which the period is long enough for the rate of liberation in the interior to respond to the cycle, $E(t)$ is not approximately constant. Again, if the long-period variables are really continuous with the Cepheids and are another form of the same physical phenomenon, we should have to suppose that in the general (r, L) diagram, as we pass from Cepheids to M-type variables, the characteristic curve gradually closes up to an arc enclosing zero area and then opens out again with reversed sense of description. For a retraced arc enclosing zero area the two senses of description are indistinguishable.

9. In the meantime we may be content with having gained some insight into the meaning of the observed phase-relations in Cepheids. Every student of the subject must have reflected that the observed coincidence of maximum luminosity with maximum velocity of approach is unlikely to be a mere accident due to the accumulation of small phase differences between luminosity and state of expansion resulting in an exact phase-difference of $\pi/2$. The present train of thought gives the phase difference immediately as about $\pm \pi/2$, this being the inevitable consequence of the fact that the most general cyclic path in the (r, L) diagram is a closed curve, not a retraced arc. This in turn is just the expression of the circumstance that an initial disturbance is specified by arbitrary values of two observable variables * δL and δr.

10. *Area of a Characteristic Curve.*—Various questions suggest themselves with regard to characteristic curves. I mention first the physical meaning of the area of such a curve. In the (r, L) diagram, the area of the curve is equal to

$$\oint (L - L_0) dr$$

which may be written

$$\oint (L - L_0) \frac{dr}{dt} dt.$$

* More strictly, the initial boundary circumstances must involve the specification of *three* variables, δL, δr and $d(\delta r)/dt$. These must be equivalent to defining the initial position of P in the (r, L) diagram and the slope of the tangent at P to the path.

Let $L - L_0$ and dr/dt be expanded in Fourier series in the time. Then every term in the expansion of dr/dt in phase with the term of the same order in the expansion of $L - L_0$ gives a non-zero contribution to the integral of the product, and so the area of the curve is a measure of the agreement in phase between luminosity and velocity.

We can see at a glance that for a Cepheid the characteristic curve encloses an area and is not simply a retraced arc. For if we plot the observed light-curve above the corresponding velocity-curve (fig. 3), we see that a given luminosity L', represented by the line VW, is attained at the two epochs represented by the abscissæ G, F of the velocity-curve. The area

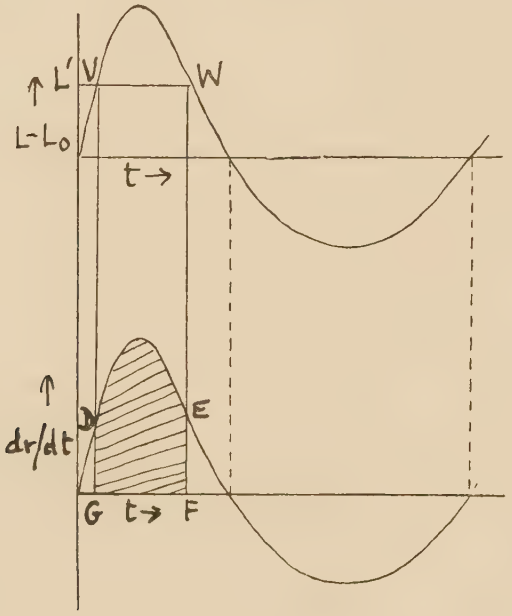

Fig. 3.

$DEFG$ represents the difference in stellar radius at the two epochs G and F. This is in general not zero. Hence the same luminosity is attained at two different radii. Hence in the (r, L) or $(\log_{10} r, \log_{10} L)$ diagram a given ordinate $L = L'$ meets the characteristic curve in two distinct points; these points only coincide at $L = L_{\max}$ or $L = L_{\min}$. Hence the characteristic curve consists of two distinct branches which coalesce at $L_{\max}$ and $L_{\min}$ and together enclose an area.

11. *Equilibrium Configuration.*—A second question of interest is: what is the point in the (r, L) diagram which represents the steady-state configuration about which the star is oscillating? Presumably it is a point in the interior of the characteristic curve of abscissa $L_0 = \frac{1}{T}\oint L dt$. But we are not entitled to assume that the radius of the equilibrium configuration is the time-mean of the radius during the cycle. If, as is likely, the equilibrium configuration is represented by a point such as C in fig. 1, then we have

the interesting result that the star never passes through its equilibrium configuration during its cycle.*

12. *Relation to Equilibrium Locus.*—A third question is: what is the relation of the ellipse-like characteristic curve to the locus of equilibrium configurations of the same mass in the (r, L) diagram? This curve enumerates all the pairs (r, L) possible for the mass M, for given relative source-distribution and given ultimate chemical composition. In fig. 4 let the steady-state locus through C meet the characteristic curve in R, R', the tangent at $B(r_{\min})$ in I and the tangent at $B'(r_{\max})$ in I'. At B and B' the

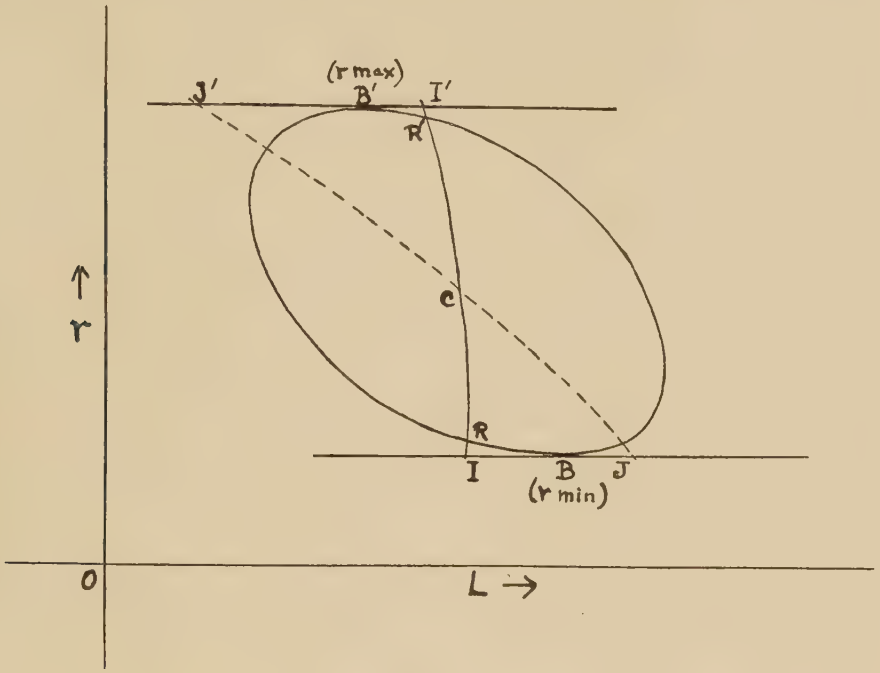

FIG. 4.

star has come momentarily to rest. At B it has the same radius, and also the same mass, as the steady-state configuration represented by I. If it were placed at I, *i.e.* given also the right luminosity, it would remain in equilibrium, and oscillations would not start. Actually at B it has too large a luminosity if I is to the left of B, as shown in fig. 4. Accordingly, at B it is at rest and provided with too large a luminosity for equilibrium, and therefore must expand. This is consistent with B being $r_{\min}$. Similarly at B' it is also at rest, but has too small a luminosity compared with the equilibrium configuration I' of the same radius. It must therefore contract, which is consistent with B' being $r_{\max}$. If, on the other hand, the equilibrium curve were like $\mathcal{J}\mathcal{J}'$ (fig. 4), at B the star would have too small a luminosity for equilibrium and would contract, contradicting the fact that B is at $r_{\min}$; a similar contradiction would occur over B'. It appears then that a necessary condition for cyclic pulsations is that the points I and I' in

* This does not seem to have been previously noticed.

which the equilibrium curve meets the horizontal tangents to the characteristic curve must be such that I is to the left of $r_{\min}$ and I' to the right of $r_{\max}$. In the limiting case in which I coincides with B, the star just reaches an equilibrium configuration with zero kinetic energy and will therefore remain there in equilibrium. Oscillations cannot therefore be occurring, which is a contradiction. Similarly if I' coincides with B'. Thus II' cannot coincide with BB'. The slope of the equilibrium curve in the neighbourhood of C must be reached from BB' by a clockwise rotation.

We have seen that the star never passes through its mean or equilibrium configuration, C. On the other hand, it passes through two other distinct equilibrium configurations, namely, the points R and R', where the characteristic curve intersects the locus of steady-state configurations of the same mass. It passes through these configurations (which have the correct r and L for equilibrium) with non-zero kinetic energy, and so does not remain in them. We see again that R and R' cannot coincide with $r_{\min}$ and $r_{\max}$, or oscillations would not occur.

13. *General Paths in the* (r, L) *Diagram.*—If a star is started in a non-equilibrium configuration represented by an arbitrary point P of the (r, L) diagram, and given at the same time an arbitrary surface velocity, the representative point P will move in a variety of possible ways, depending on the initial state of internal distribution of density, temperature and velocity, all of which are concealed from observation. If the neighbouring equilibrium configurations are stable, P will either (i) oscillate through some point C, to and fro ; or (ii) describe or pass asymptotically into a recurrent orbit ; or (iii) spiral round and into some point C. The third case would mean that oscillations die down, and Cepheid pulsations would not occur ; the second case is the Cepheid case already discussed ; * as for the first case, which is the one described in Eddington's theory, it is not known whether it occurs in nature. A full mathematical discussion of these possibilities would need to pay careful attention to boundary conditions from the outset, for r and L are boundary variables. Eddington's theory seems to me unsatisfactory on various grounds. It does not show why all stars are not Cepheids. Again, strictly adiabatic oscillations imply conservation of energy, but a vibrating star is, as we have seen, not a conservative system. Again, the

* In this (Cepheid) case, not only must the associated equilibrium configuration be stable, but also the periodic orbit itself must be stable. This shows at once why all stars are not Cepheids. Stability alone does not ensure the possibility of Cepheid pulsation—a further condition is required. For one form of this condition, see my paper, "The Energetics of Non-steady States, etc.," *loc. cit.* It is this condition which is responsible for the existence of a *period-luminosity law.* Since two independent variables L, M fix a *steady state*, the condition that this steady state is also associated with a form of stable (undamped) periodic motion may be put in the form $\phi(L, M) = 0$. The period P will also be given by a relation of the form $P = f(L, M)$. Elimination of M between these gives $F(P, L) = 0$, a period-luminosity law. In the paper cited I deduced the relation $\phi(L, M) = 0$ by proving that a certain "damping" parameter, itself a function of the two variables L, M, must take a definite numerical value, namely unity, for undamped oscillations to be possible. Other existing treatments of the Cepheid pulsation problem have not yet introduced these considerations.

theory of adiabatic oscillations requires in effect that each element of material be adiabatically sealed off from its neighbours, but then consistently with this assumption there would be no support by light-pressure, for the mechanical effect of light-pressure depends essentially on the radiation escaping and being absorbed by the surroundings. In fact, strictly adiabatic sealing-off would inhibit all flow of radiation. Eddington's theory only applies strictly when there is no leak, *i.e.* when the luminosity of the star is zero, and a small leak is not sufficient—it must be sufficiently large to give the observed luminosity. It is probable that the equation for the flow of energy in a non-steady state, as developed by Jeans, Vogt, Rosseland, Woltjer and the writer in various forms, applied not only in the interior but right up to the boundary, would lead to other (r, L) paths beyond the retraced arc of Eddington's theory, and a criterion for the existence of stable periodic (r, L) orbits.

14. *Conclusion.*—Further questions which might be studied in connection with characteristic curves are (1) the spacing of the time-markings round the curve, (2) the extent to which the actual curves are ellipses, (3) the variation of their shape and size over the (r, L) diagram, *i.e.* from spectral type to type, (4) whether "kinks" in the light-curves and velocity-curves disappear on plotting, appearing simply as irregularities in disposition of time-markings. Again, a grid of parallel straight lines representing loci of constant effective temperature T_e in the $(\log_{10} L, \log_{10} r)$ diagram can be drawn, and their intersections with the characteristic curve compared with observed colour-temperature T_c. A prediction of the theory, given by inspection from fig. 1, is that $T_{e(\max)}$ and $T_{e(\min)}$ should occur in the temporal sequence

$$r_{\min},\ T_{e(\max)},\ L_{\max},\ r_{\max},\ T_{e(\min)},\ L_{\min},\ r_{\min}.$$

This could be tested by observation, but the observed values of T_c will not necessarily coincide with the predicted values of T_e. The grid of temperature parallels can be applied in a simple way to determine bolometric magnitude corrections without recourse to colour observations.

Evidently simultaneous observations of spectroscopic radial velocity and radiometric magnitude would be well worth while for any variable star. Irregularity of period is of no consequence in this method—the plot will show immediately whether the star retraces its successive configurations (periodic case), spirals inwardly to a steady state or spirals outwardly. Thus damped motion, either periodic or aperiodic, can be investigated in just as simple a manner as undamped cyclic motion, provided the observations are sufficient to determine the mean radial velocity.

The method provides a rational basis for the classification of all variable stars showing change of radius, according to the shapes, sizes and senses of description of their characteristic curves. It adds great force to the case for observing all variables for radial velocity—for example, the RV Tauri variables,* which would be highly interesting as being intermediate between the Cepheids and the long-period variables.

* *Cf.* R. F. Sanford, *Ap. J.*, **79**, 77, 1934. Dr. Sanford's paper appeared after the above had been written.

It is the method which I wish to emphasize rather than the theoretical considerations which led to it or the preliminary deductions made from its application. The insight it gives into phase-relations and the period-luminosity law seems a sufficient justification of its utility. Both objective study of the curves themselves and further theoretical investigations of the dynamical and thermodynamical conditions under which they can be described are much to be desired.

The present investigation was completed before any actual curves had been constructed from observations. Professor H. H. Plaskett has since constructed the characteristic curve of δ Cephei; it proves to be a slightly pointed oval, with axis at a small negative slope in the ($\log_{10} r$, $\log_{10} L$) diagram, and the sharper end near $L_{\max}$; the time-markings are non-uniformly distributed around it. It will be published later. The construction of the characteristic curves of other variables is being undertaken by Mr. I. A. Getting at the University Observatory, Oxford. I am much indebted to Professor Plaskett for his helpful discussion over many points in this paper.

Wadham College, Oxford:
1934 *January* 1.

RADIATIVE EQUILIBRIUM OF THE EXTENDED PHOTOSPHERE.

N. A. Kosirev.

(Communicated by the Secretaries)

1. The explanation of the anomalous colour-temperatures of the early-type stars may be looked for either in selective light absorption in interstellar space, or in the peculiarities of the physical structure of the atmospheres and photospheres of these stars. The present existing observational data can be brought into agreement with both points of view. However, it seems to us that according to some of the observational data the explanation involving the peculiarities of the star itself is the more natural. We have in view the statistical correlation (as found by Gerasimovič) between the anomalous temperatures of early-type stars and their absolute magnitudes; next, a certain tendency of the B-type stars with emission lines (Be) towards greater colour-indices; and, finally, a considerable difference between temperatures (pointed out by V. Ambarzumian) determined by Zanstra's method from the lines of hydrogen and from ionised helium in the Wolf-Rayet stars. The last item, namely, the excess of temperature determined from *He* II over that determined from hydrogen lines, can hardly be explained by the incomplete absorption of hydrogen, and rather indicates a deviation of the Wolf-Rayet stars' radiation from Planck's curve in the far ultra-violet part of the spectrum.

Connecting the anomalous colour-temperatures of the B-type stars with the peculiarities of their physical structures, we should look for the cause of this anomaly in the deviation of the energy-distribution curve from Planck's formula. The theory of the radiative equilibrium of photospheric layers, which well explains the spectra of normal stars, gives Planck's distribution law, on the assumption of a coefficient of absorption independent of wave-length. It seems unlikely that the absorption coefficient as a function of wave-length can differ sensibly from star to star. Should we even give up the hypothesis of grey absorption when dealing with certain stars, it would still seem more natural to suppose an increase of absorption in the ultra-violet part of the spectrum. In that case, as is easily seen, we have not an excess of radiation, but on the contrary a deficiency. Retaining the hypothesis of grey absorption, we may obtain an ultra-violet excess by the assumption that the temperature in the outer layers of the star increased as a function of optical depth much more rapidly than follows from the usual treatment of the radiative equilibrium of photospheric layers. One might think that the temperature distribution in some stars is being established not by the condition of radiative equilibrium, but by some other condition such as convective equilibrium. However, the transfer of radiation in stars plays so essential a part, that even at those enormous velocities of material flow which are observed in the Wolf-Rayet stars, the convective transfer of heat cannot essentially alter the temperature distribution determined by the condition of radiative equilibrium.* On the other hand, computations have shown that the temperature gradient in adiabatic equilibrium cannot sufficiently explain the spectrum of such an anomalous star as, *e.g.*, P Cygni.

From all the above considerations it follows that when explaining the anomalies of colour-temperatures of the early-type stars, it is most rational to retain the condition of radiative equilibrium with the hypothesis of grey absorption. For the photospheric layers of normal stars the theory of radiative equilibrium gives the following dependence of black-body radiation B upon optical depth τ:—

$$B = B_0(1 + \tfrac{3}{2}\tau). \qquad (1)$$

This formula holds on the assumption that the radius of curvature of the photospheric layers is infinite. Supposing, however, the outer layers to be extremely extended, *i.e.* that the radius r varies considerably with τ, $B(\tau)$ will no longer be represented by formula (1). In that case the temperature gradient will be much greater than follows from formula (1), and we shall be able to obtain an anomalous distribution of energy in the spectrum. The circumstance that some early-type stars can possess an exceedingly extended photosphere appears to be quite natural. In stars of the Wolf-Rayet and P Cygni types the material outflow can begin at very large optical

* N. A. Kosirev, *Poulk. Obs. Circ.*, No. 6, 1932. For lack of sufficient data on physical conditions in the outer layers of Wolf-Rayet stars, it was mentioned in that article that these stars might be regarded as an exception to the conclusion obtained. However, basing on the results of § 7 of the present paper, it is easily seen that temperature conditions for the Wolf-Rayet stars are determined by radiative equilibrium.

depths; and since, at the ejection, density grows very slowly with depth, the change of optical depth will be accompanied by a considerable change in radius. Perhaps some stars of the Be type present analogous examples. Finally, stars of the B type with absorption spectra and anomalous colour-temperatures may possibly be objects with exceedingly extended photospheres owing to some peculiar conditions of their equilibrium. The above-mentioned effects of absolute magnitude may possibly be related to this consideration.

2. Examine now the problem of radiative equilibrium of the outer layers, assuming these layers to be spherical, and their radius sensibly changing with the change of optical depth. The equation of transfer of the radiative energy,

$$\frac{dI}{ds} = \kappa\rho B - \kappa\rho I,$$

can be rewritten in this case in the form

$$\cos\theta\frac{\partial I}{\partial r} - \frac{\sin\theta}{r}\frac{\partial I}{\partial\theta} = \kappa\rho B - \kappa\rho I. \tag{2}$$

In these formulæ I is the intensity of radiation proceeding in the direction of the element ds, κ is the absorption coefficient, ρ the density and θ the angle between the direction of the ray and the normal to the layer at the given point. The condition of radiative equilibrium gives

$$B = \frac{1}{4\pi}\int I d\omega. \tag{3}$$

Regarding κ and ρ as known functions of r, we can obtain the relation between B and r from equations (2) and (3). An exact solution of this problem being rather complicated, we shall recur to a certain approximation corresponding to that of Eddington. Introduce the following notation :—

$$\mathcal{J} = \frac{1}{4\pi}\int I d\omega, \qquad H = \frac{1}{4\pi}\int I\cos\theta d\omega, \qquad L = \frac{1}{4\pi}\int I\cos^2\theta d\omega.$$

Integrating equation (2) over all solid angles and bearing in mind condition (3), we easily obtain

$$\frac{dH}{dr} + \frac{2}{r}H = 0.$$

From this

$$H = \frac{a}{r^2} \tag{4}$$

—an obvious result—namely, that for the sphere the flow of radiation on the assumption of radiative equilibrium is inversely proportional to the square of radius (a in this formula is a certain constant). Multiplying both parts of equation (2) by $\cos\theta$ and integrating this equation with respect to $d\omega$, we find

$$\frac{dL}{dr} + \frac{1}{r}\mathcal{J} - \frac{3}{r}L = -\kappa\rho H. \tag{5}$$

Using equations (4), (5) and the condition of radiative equilibrium,

$$B = \mathcal{J}, \tag{6}$$

we can now obtain the approximate solution of our problem. For the given point in the star, denote by I_1 the mean intensity of radiation proceeding outward relatively to the tangent plane drawn through this point toward the spherical layer, and by I_2 the mean intensity of radiation proceeding inward. Then, following Eddington, we may write the approximate equations

$$\mathcal{J} = \tfrac{1}{2}[I_1 + I_2], \qquad H = \tfrac{1}{4}[I_1 - I_2], \qquad L = \tfrac{1}{3}\mathcal{J}. \tag{7}$$

We obtain in this case from equation (5)

$$\mathcal{J} = -3\int H\kappa\rho dr.$$

Write

$$d\tau = -\kappa\rho dr.$$

Then

$$\mathcal{J} = 3\int_0^\tau H d\tau + C.$$

The constant C is determined by the condition that when $\tau = 0$, $\mathcal{J} = 2H_{\tau=0} = 2H_0$. Hence, using formulæ (6) and (4) we find

$$B = \frac{2a}{R^2} + 3a\int_0^\tau \frac{d\tau}{r^2}, \tag{8}$$

where R is the radius at $\tau = 0$. For small variations in r this formula is equivalent to formula (1). Formula (8) is an approximate solution of our problem.

Let us assume, for example, that in the outer layers of a star r and τ are connected by a relation of the type

$$\frac{1}{r^2} \propto \tau^n. \tag{9}$$

In this case $\tau = 0$ at infinite r, i.e. $R = \infty$, and the first term in the right-hand part of the formula (8) vanishes. Therefore in the case of the proportionality (9) we have the following relation between temperature T and optical depth :—

$$T = T_1\tau^{\frac{n+1}{4}}. \tag{10}$$

Here T_1 is the temperature of the photosphere at $\tau = 1$.

3. In order to obtain the dependence of r on τ we must know the circumstances of formation of the extended photosphere. We shall examine here only a very simple case, namely, the origin of formation of the extended photosphere being the outflow of matter from the star. Assuming a photosphere of that kind to be dynamically stable, we can easily see that in this case $r(\tau)$ will be approximately expressed by formula (9). Indeed, at large velocities we may consider the velocity of the outflow of matter to be

practically constant within a considerable interval of τ. Then from the condition of continuity we have

$$\rho \propto \frac{1}{r^2}. \tag{11}$$

In this case $\tau = 0$ only at $r = R = \infty$. From the formula (8) we see that then also $B = 0$. Adopt for the absorption coefficient the following dependence on temperature and density :—

$$k \propto \frac{\rho}{T^4} \propto \frac{\rho}{B}. \tag{12}$$

Then

$$d\tau \propto \frac{1}{Br^4} dr.$$

From formula (8) we have

$$\frac{dB}{dr} \propto \frac{1}{r^2}\frac{d\tau}{dr} \propto \frac{1}{r^6 B}.$$

Therefore

$$B \propto r^{-\frac{5}{2}}.$$

By means of this expression and the expression for τ,

$$\tau = \int_r^\infty \kappa\rho dr,$$

we find that the optical depth must depend upon r, according to the law :

$$\tau^4 \propto \frac{1}{r^2}. \tag{13}$$

Thus, in the case under examination the index n in formula (9) is equal to 4. Consequently, for photospheric layers that have arisen owing to the outflow of matter,

$$T = T_1 \tau^{\frac{5}{4}}. \tag{14}$$

4. We shall determine now for the case of the temperature distribution (14) the distribution of energy in the spectrum. Examine the ray proceeding from the star, whose direction passes by at a linear distance a from the centre of the star. Integrating equation (2), and noting that

$$\cos\theta = \sqrt{1 - \left(\frac{a}{r}\right)^2},$$

we find the following expression for the intensity $I(\lambda, a)$ of this radiation :—

$$I(\lambda, a) = \int_a^\infty e^{-\int_r^\infty \frac{\kappa\rho}{\sqrt{1-\left(\frac{a}{r}\right)^2}} dr} B(\lambda, T) \frac{\kappa\rho}{\sqrt{1-\left(\frac{a}{r}\right)^2}} dr$$
$$+ \int_a^\infty e^{-\left[\int_a^\infty \frac{\kappa\rho}{\sqrt{1-\left(\frac{a}{r}\right)^2}} dr + \int_a^r \frac{\kappa\rho}{\sqrt{1-\left(\frac{a}{r}\right)^2}} dr\right]} B(\lambda, T) \frac{\kappa\rho dr}{\sqrt{1-\left(\frac{a}{r}\right)^2}}. \tag{15}$$

Here function $B(\lambda, T)$ is determined by Planck's formula :

$$B(\lambda, T) = C\lambda^{-5}\left[e^{\frac{c_2}{\lambda T}} - 1\right]^{-1}. \tag{16}$$

In the given formula for $I(\lambda, a)$ the first integral corresponds to radiation, issuing from the hemisphere facing us, while the second integral corresponds to radiation, issuing from the reverted hemisphere. The complete intensity of the star radiation $I(\lambda)$ will be obtained when integrating $I(\lambda, a)$ by a :

$$I(\lambda) = 2\pi\int_0^\infty I(\lambda, a)ada. \tag{17}$$

Using the formula (13) and the expression for τ, we can evaluate the following expression entering into formula (15) :—

$$\frac{\kappa\rho}{\sqrt{1-\left(\frac{a}{r}\right)^2}} = \frac{c}{\sqrt{r(r^2-a^2)}}, \tag{18}$$

where c is a certain constant. Introduce instead of r the variable θ—the angle between the direction from the centre of the star to the observer, and the radius drawn to the given point in the star (a is supposed constant). Then the expression (15) is considerably simplified. As a result of a few simple transformations we have

$$I(\lambda, a) = \frac{c}{\sqrt{a}}\int_0^\pi \sqrt{\operatorname{cosec}\theta}\, e^{-\frac{2c}{\sqrt{a}}\psi(\theta)} B(\lambda, T)d\theta, \tag{15a}$$

where

$$\psi(\theta) = \tfrac{1}{2}\int_0^\theta \sqrt{\operatorname{cosec} x}\, dx. \tag{19}$$

From equation (17) it follows that

$$I(\lambda) = 2\pi c\int_0^\infty\int_0^\pi \sqrt{a\operatorname{cosec}\theta}\, e^{-\frac{2c}{\sqrt{a}}\psi(\theta)} B(\lambda, T)d\theta da. \tag{17a}$$

We shall introduce in this expression instead of a the optical depth τ as a new variable. From the relation (18) it follows that

$$\tau = \frac{2c}{\sqrt{r}}. \tag{20}$$

As $\sin\theta = \frac{a}{r}$,

$$\tau = \frac{2c}{\sqrt{a\operatorname{cosec}\theta}}. \tag{21}$$

We shall transform the variables in the double integral of formula (17a), using the relation (21) and leaving θ unaltered. Then

$$I(\lambda) = 32\pi c^4\int_0^\infty B(\lambda, T)\frac{d\tau}{\tau^4}\int_0^\pi e^{-\tau\sqrt{\operatorname{cosec}\theta}\psi(\theta)}\sin\theta d\theta.$$

From formula (20) we see that the constant c entering into the expression for $I(\lambda)$ can be substituted by R_1—radius of the star at $\tau = 1$. With the

aid of formulæ (16) and (14) we find this final expression for the distribution of energy in the spectrum of anomalous stars under consideration:

$$I(\lambda) = \pi R_1^2 C \lambda^{-5} E(\lambda, T_1), \tag{22}$$

where

$$E(\lambda, T_1) = \int_0^\infty \left[e^{\frac{c_2}{\lambda T_1 \tau^{\frac{5}{4}}}} - 1 \right]^{-1} \Phi(\tau) \frac{d\tau}{\tau^4} \tag{23}$$

and

$$\Phi(\tau) = 2 \int_0^\pi e^{-\tau \sqrt{\operatorname{cosec} \theta}} \psi(\theta) \sin \theta d\theta. \tag{24}$$

These formulæ possess quite an obvious physical interpretation. The function $\Phi(\tau)$ replaces the usual exponential factor of absorption, while the denominator τ^4 (as seen from formula (20)) is inversely proportional to the area of the radiating discs.

We shall now deduce the expression for the density of radiation $\rho(\lambda)$ in the outer layers of the star, *i.e.* at $\tau < 1$. These layers may be termed the atmosphere of the star, in so far as spectral lines have their origin here. Neglect radiation emitted by the atmosphere of the star. This is quite admissible, especially when computing $\rho(\lambda)$ for short wave-lengths. In order to compute $\rho(\lambda)$ we shall introduce into the expression

$$\rho(\lambda) = \frac{1}{c} \int I(\lambda) d\omega = \frac{2\pi}{c} \int I(\lambda) \sin \theta_0 d\theta_0,$$

the value $I(\lambda)$ being given by (15*a*). Here θ_0 is the angle between the direction of the ray and that of the normal in the point under investigation, and c is the light-velocity. At a considerably large R—the distance of the point in the atmosphere of the star from its centre—we obtain ultimately for $\rho(\lambda)$,

$$\rho(\lambda) = \delta \frac{4\pi}{c} C \lambda^{-5} E(\lambda, T_1), \tag{25}$$

where δ is the usual dilution factor:

$$\delta = \tfrac{1}{4} \left(\frac{R_1}{R} \right)^2. \tag{26}$$

We see that the constant R_1 plays the part of a radius of normal stars for the objects under examination. The other constant T_1, which is equal to the temperature of the star at distance R_1 from the centre, is a substitute for the boundary temperature. T_1 can be computed from a comparison of formula (22) with the observed distribution of energy in the spectrum of the star.

5. We shall now proceed to make concrete computations of the distribution of energy in the spectrum, using formulæ (22), (23) and (24). First of all we must observe that formula (24) contains the function $\psi(\theta)$ determined from equation (19). The table of this function, formed by numerical integration, is given below.

$\theta°$	θ_R	$\psi(\theta)$	$\theta°$	θ_R	$\psi(\theta)$
0°	0·000	0·000	90°	1·571	1·311
8° 36′	0·150	0·387	105°	1·833	1·443
15°	0·262	0·512	120°	2·094	1·579
30°	0·524	0·727	135°	2·356	1·726
45°	0·785	0·896	150°	2·618	1·895
60°	1·047	1·044	165°	2·880	2·110
75°	1·309	1·180	180°	3·142	2·623

With the aid of this table it is possible to tabulate also the function $\Phi(\tau)$ defined by equation (24):

τ	$\Phi(\tau)$	τ	$\Phi(\tau)$	τ	$\Phi(\tau)$
0·0	4·00	1·8	$3·54.10^{-1}$	9·0	$9·84.10^{-5}$
0·2	2·92	2·0	2·77	10·0	3·42
0·4	2·22	2·5	1·52	12·0	$3·98.10^{-6}$
0·6	1·67	3·0	$8·34.10^{-2}$	14·0	$4·87.10^{-7}$
0·8	1·28	4·0	2·76	16·0	$5·67.10^{-8}$
1·0	$9·76.10^{-1}$	5·0	$8·28.10^{-3}$	18·0	$7·26.10^{-9}$
1·2	7·51	6·0	2·68	20·0	$8·24.10^{-10}$
1·4	5·82	7·0	$9·06.10^{-4}$		
1·6	4·50	8·0	2·94		

In both these tables the last figure of the values of the functions may not be quite reliable. With the help of the table of the function $\Phi(\tau)$ it is not difficult to compute from formulæ (23) and (22) the distribution of energy in the spectrum for definite values of T_1. We shall perform these computations for several definite objects.

P Cygni.—The spectrum of this star of type B1 is characterised by bright emission lines *H* and *He* I. The contours of these lines and the shift of absorption lines show that the outflow of matter from this star proceeds with velocities of the order of 150 km. per sec. A large number of immediate spectrophotometric measurements of the distribution of energy in the spectrum give the value of temperature as within 6000°–7000° for the portion of the spectrum from 400 $\mu\mu$ to 600 $\mu\mu$. According to Dufay * there is also observed a certain tendency for the temperature to increase with the decrease of wave-length. The spectrum of the star being of the B1 type, the ionisation temperature must be about 18,000°. In other words, the distribution of energy in the spectrum of this star must be such as to have the temperature value of about 18,000° for small wave-lengths of the order of 500–1000 A. Beals's measurements of the total intensities of the hydrogen and helium lines, combined with an application of Zanstra's method to the atmosphere of this star, yield temperatures of the above-mentioned order.† The comparison of formula (23) with the observational data shows that a good agreement between theoretical and measured temperatures can be obtained if $T_1 = 5560°$. We shall adopt this value of T_1. We give below the values $E(\lambda, T_1)$ computed for different wave-lengths.

* *Publ. L'Obs. Lyon*, **1**, 1, 1933.
† *M.N.*, **92**, 684, 1932.

λ	$E(\lambda, T_1)$	T
$\lambda_1 =$ 500 A.	$4{\cdot}18.10^{-8}$	$T(\lambda_1, \lambda_4) = 21{,}300°$
$\lambda_2 = 1{,}000$	$3{\cdot}61.10^{-6}$	$T(\lambda_2, \lambda_4) = 15{,}100°$
$\lambda_3 = 4{,}000$	$2{\cdot}76.10^{-3}$	$T(\lambda_3, \lambda_4) = 7{,}500°$
$\lambda_4 = 5{,}000$	$7{\cdot}14.10^{-3}$	
$\lambda_5 = 5{,}875$	$1{\cdot}38.10^{-2}$	
$\lambda_6 = 6{,}563$	$2{\cdot}01.10^{-2}$	$T(\lambda_3, \lambda_6) = 7{,}050°$
$\lambda_7 = 8{,}000$	$4{\cdot}3\ .10^{-2}$	$T(\lambda_4, \lambda_7) = 6{,}000°$

The values of $T(\lambda_i, \lambda_\kappa)$ contained in the third column of this table are those computed from two $E(\lambda_i, T_1)$ and $E(\lambda_\kappa, T_1)$ by means of Planck's formula. Thus, these are the values which the observer must estimate when studying the distribution of energy in the spectrum. We see that the calculated distribution agrees well with that actually observed. In order to make this comparison more complete, we must also consider the temperatures which must be obtained when applying Zanstra's method to this star. We shall next have to compare our results of computation with Beals's data.

Zanstra's method gives on the assumption of black-body radiation the following equation for the determination of T:—

$$\int_{x_0}^{\infty} \frac{x^2}{e^x - 1} dx = \sum \frac{x^3}{e^x - 1} A_\nu. \tag{27}$$

Here $x = \frac{h\nu}{\kappa T} = \frac{c_2}{\lambda T}$, x_0 is the value of x at $\nu = \nu_0$, ν_0 is the frequency of ionisation of the given element, and A_ν represents a total relative intensity of the emission line of the given element divided by the wave-length of the line. It is clear that in our case of the distribution of energy in the spectrum equation (27) must be replaced by the relation

$$\int_0^{\infty} \frac{\Phi(\tau)}{\tau^{\frac{1}{4}}} \int_{\frac{x_0}{\tau^{\frac{5}{4}}}}^{\infty} \frac{y^2 dy}{e^y - 1} d\tau = \sum x^3 E(\lambda, T_1) A_\nu. \tag{28}$$

This relation can be obtained from formula (27), considering the fact that in our case the expression $(e^x - 1)^{-1}$ must be replaced by the function $E(\lambda, T_1)$. In formula (28) x stands for the expression $x = \frac{h\nu}{\kappa T_1}$. On the right-hand part of this formula we shall leave only a single term, corresponding to the most intense line of the element in the visible part of the spectrum. Then, if I_1 is given, we can evaluate the value of A_ν corresponding to this spectral line. Computations are greatly simplified, $\int_x^{\infty} \frac{y^2}{e^y - 1} dy$ having already been tabulated in papers on Zanstra's method. For hydrogen with the adopted value of T_1, x_0 equals 32·6. We shall regard all the absorbed ultra-violet radiation beyond the limit of the Lyman series as giving $H\alpha$ (6563 A.). Then $A_\nu = 0{\cdot}0115$, as seen from computations. For *He* I, $x_0 = 51{\cdot}27$. Restricting ourselves to a most intense line 5875 A. we get $A_\nu = 0{\cdot}00111$. Making use of these values for A_ν, we shall be able to determine T from (27). This T will be obtained by the observer using Zanstra's

method. Below is given a final summary, comparing observations (given by Beals for *H* and *He* I) and the theoretical calculation.

	Obs.	Theor.
$T_{He\,I}$	25,000°	23,000°
T_H	18,000	16,650
$T_{sp.\,ph.}$	6,000	7,050

The Wolf-Rayet Stars.—These are objects with exceedingly high surface temperatures from which matter is ejected. Therefore it seems of great interest to elucidate the question as to how far their continuous spectrum can be described from the point of view of our scheme. The following data may be considered most typical for the Wolf-Rayet stars. The temperature determined by Zanstra's method from the line 4686 *He* II is 70,000°.* The hydrogen lines in these stars are relatively weak, and we may adopt for the temperature, resulting from Zanstra's method by *Hα*, a value of the order of 30,000°.† This decrease of temperature for hydrogen corresponds to the difference between the temperatures determined by the method of Zanstra for the nuclei of the planetary nebulæ from the *He* II and *H* lines. Immediate spectrophotometric measurements of the distribution of energy in spectrum are hampered by the presence of a large number of emission bands. Still, observations of this kind give an average temperature of the order of 17,000°.‡

Adopt $T_1 = 50{,}000°$ for the typical case of the Wolf-Rayet star. For such a great value of T_1 we may considerably simplify the right-hand part of formula (28). From the expression (23) for $E(\lambda, T_1)$ it follows that the largest values of the sub-integral function in this formulæ will be obtained at small τ. For these τ we may simply put down $\Phi(\tau) = 4$. Then substituting $\frac{x}{\tau^{\frac{5}{4}}}$ by y, we find

$$\underset{\text{at } x << 1}{x^3 E(\lambda, T_1)} = 3{\cdot}2x^{\frac{3}{5}}\int_0^\infty \frac{y^{\frac{7}{5}}}{e^y - 1}\,dy = 5{\cdot}51x^{\frac{3}{5}}. \qquad (29)$$

Making use of formulæ (28) and (29) we can compute the values of A_ν with the adopted value of T_1. For *He* II we obtain from computations $A_\nu = 0{\cdot}0330$, assuming that all the ultra-violet radiation beyond ionisation frequency ($x_0 = 12{\cdot}55$) result in the one line 4686. For *H*, restricting ourselves to *Hα*, we find $A_\nu = 0{\cdot}394 (x_0 = 3{\cdot}140)$. From these data we can compute the values of T, estimated by the observer :

	Obs.	Theor.
$T_{He\,II}$	70,000°	67,000°
T_H	(30,000)	28,000
$T_{sp.\,ph.}$	(17,000)	14,000

The figures in brackets are those obtained from rough averagings. The spectrophotometric temperature given in this table has been computed in

* Beals, *loc. cit.*

† The author is indebted for this information to Dr. V. A. Ambarzumian.

‡ Gerasimovič, *H.C.*, 339, 1929.

the following way. It results from formulæ (22) and (29) that at high temperatures the distribution of energy in spectrum must be represented by the proportionality

$$I(\lambda) \sim \lambda^{-\frac{13}{5}} T^{\frac{12}{5}}, \tag{30}$$

and not by the Rayleigh-Jeans law of the inverse proportionality of intensity of radiation to the fourth power of the wave-length. From formula (30) we see that we shall obtain not an infinite value of T, but a certain definite value T depending on the adopted λ when examining the distribution of energy in the spectrum of hot anomalous stars. The number given in the above table has been obtained for $\lambda_1 = 600\,\mu\mu$ and $\lambda_2 = 400\,\mu\mu$. It is quite possible experimentally to distinguish the law (30) from the Rayleigh-Jeans formula. Observations to this end should be of great interest.

From the two cases examined we see that the theory treated in this paper is in good agreement with observations, in spite of the rather rough assumptions (the constancy of the outflow velocity and the law (12) for the absorption coefficient).

6. We have seen that it is possible to determine the constant T_1 from the distribution of energy in the spectrum or from the relative intensities of emission lines. The following will show us how to determine the effective temperature T_{eff} of the star, provided T_1 is known. We shall as usual define T_{eff} by the formula

$$I = \pi R_1^2 \sigma T_{\text{eff}}^4, \tag{31}$$

where I is the integrated radiation of the star and σ is Stefan's constant. On the other hand, integrating the expression $I(\lambda)$ (*cf.* formula (22)) with respect to λ, we easily find

$$I = \pi R_1^2 \sigma T_1^4 \cdot 2\int_0^{\pi} \left[\frac{\sin\theta}{\psi(\theta)}\right]^2 d\theta.$$

Comparing this formula with formula (31), we have

$$T_{\text{eff}} = \sqrt[4]{A}\, T_1, \tag{32}$$

where

$$A = 2\int_0^{\pi} \left[\frac{\sin\theta}{\psi(\theta)}\right]^2 d\theta = 2{\cdot}231. \tag{33}$$

Thus the factor $\sqrt[4]{A}$, with whose aid T_1 can be transformed into T_{eff}, differs but little from the corresponding factor $\sqrt[4]{2}$ of the usual theory of the radiative equilibrium connecting the boundary temperature with T_{eff}. For instance, for P Cygni we obtain $T_{\text{eff}} = 6800°$.

With the aid of formula (31), T_{eff} being known, we can determine the constant R_1, which may be regarded as the radius of the star. To this end we must know I, *i.e.* the absolute bolometric magnitude of the star. We shall now see in what way, provided the visual brightness of the star be known, one can obtain the bolometric magnitude. It becomes necessary to determine the bolometric correction Δm:

$$\Delta m = m_{\text{vis}} - m_{\text{bol}}.$$

Evidently $$\Delta m = -\tfrac{5}{2} lg_{10} P(T_1),$$

where $$P(T_1) = \frac{\int_0^\infty V(\lambda) I(\lambda, T_1) d\lambda}{\int_0^\infty I(\lambda, T_1) d\lambda}. \tag{34}$$

In this last formula $V(\lambda)$ means the eye-sensitiveness curve, and $I(\lambda, T_1)$ is determined by the expression (22). As a result of several transformations we have

$$P(T_1) = \frac{1}{A} \int_0^\infty P_b(T_1 \cdot \tau^{\frac{5}{4}}) \tau \Phi(\tau) d\tau. \tag{35}$$

Here $P_b(T_1 \cdot \tau^{\frac{5}{4}})$ is a function corresponding to Planck's distribution of radiation. The values of this function can be obtained from the bolometric-corrections tables drawn up for normal stars. Such tables have been formed by Eddington * for low temperatures and by Pike † for high temperatures. The following table Δm is formed with the aid of these tables by means of numerical integration by formula (35):—

T_1	Δm	T_1	Δm
4,000°	+0·74	20,000°	+1·51
5,000	0·80	40,000	2·28
6,000	0·80	60,000	2·80
7,000	0·84	80,000	3·16
8,000	0·91	100,000	3·49
10,000	1·04		

Comparing the data in this table with the usual bolometric corrections, we notice for our case a characteristic relatively small change of Δm, and their more irregular variations with temperature. From the above table we get, for instance, for P Cygni, $\Delta m = +0{\cdot}80$, and for the typical Wolf-Rayet star, $\Delta m = +2{\cdot}54$.

7. Adopt for the Wolf-Rayet stars an absolute visual magnitude equalling $-3{\cdot}3$.‡ Then, from formula (31) and an analogous formula for the Sun, we have $R_1 = R_\odot$. If R_1 is known, it is possible to determine also the density of the photospheric layers of the star at $\tau = 1$. Indeed, from formulæ (18) and (20)

$$\kappa_1 \rho_1 = 1/2R_1. \tag{36}$$

Here κ_1 and ρ_1 are the values of the absorption coefficient and the density at $\tau = 1$. For a numerical estimation of κ we shall avail ourselves of Chandrasekhar's formula, differing in some way from the approximate formula (12) adopted by us:

$$\kappa = \frac{5{\cdot}62 \cdot 10^{19} \chi^2 P x}{T^{\frac{11}{2}} a}. \tag{37}$$

* Eddington, *The Internal Constitution of the Stars*, p. 138, 1926.

† Pike, *M.N.*, **89**, 538, 1929.

‡ Payne, *The Stars of High Luminosity*, p. 85, 1930.

In this formula P is electron pressure, χ is ionisation potential in volts, a is atomic weight and x is the percentage of ionisation. Assume the outer layers of the Wolf-Rayet stars to consist chiefly of helium. Then at conditions existing in the outer layers of these stars, gas must essentially consist of atoms *He* II and electrons. Take the following data: $\chi = 25\ V$, $a = 4$, $x = 1$ and P being half of the gas-pressure. Then from formulæ (36) and (37) we find

$$\rho_1 = \frac{6 \cdot 10^{-5}}{\sqrt{R_1}} \cong 2 \cdot 10^{-10}.$$

Thus we obtain a density of the order of the density of the photospheric layers of the Sun. Adopting the velocity of the outflow of matter $v = 1000$ km. per sec., we can calculate $\frac{dM}{dt}$, the annual loss of mass of the star:

$$\frac{dM}{dt} = -4\pi R_1^2 \rho_1 v \,.\, 3 \cdot 10^7 \cong -10^{-5} \frac{M_\odot}{\text{year}}.$$

If we can apply the mass-luminosity law to the Wolf-Rayet stars their masses will be of the order of $10 M_\odot$. Therefore we may infer that their annual loss of mass is 10^{-6} of their masses. Thus the upper limit of the duration of the Wolf-Rayet stage is about 10^6 years. The relative number of the Wolf-Rayet stars is exceedingly small, one star of that type falling to approximately 10^5 stars. The general number of the Wolf-Rayet stars known to us is but a little more than 100. The result obtained by us showing an exclusively short stage of this star does not, consequently, stand in opposition to statistical data. It is only necessary to assume that the Wolf-Rayet phenomenon is nothing exceptional, but that, on the contrary, many stars have to go through this stage in their evolution.

Compute now the density and the quantity of the matter ejected from P Cygni. Assume its absolute magnitude equal to -5. Then $R_1 \cong 100 R_\odot$. To estimate numerically the absorption-coefficient we shall adopt the hypothesis that hydrogen plays the main part in absorption, and shall take the ionisation temperature of the order of 15,000°. In this case one obtains $\rho_1 = 2 \cdot 10^{-12}$. Thus the density of the photospheric layers of P Cygni is considerably smaller than the corresponding density of the Wolf-Rayet stars. Adopting $v = 150$ km. per sec., we get for $\frac{dM}{dt}$ a value of the order $4 \cdot 10^{-4} M_\odot$. This latter estimation depends to a great extent upon R_1, *i.e.* upon the absolute magnitude of the star. Therefore the result obtained merely suggests the fact that the annual loss of mass of P Cygni is somewhat larger than that of the Wolf-Rayet stars.

8. We shall see now whether any emission lines can arise in the spectrum of the star in the case of the adopted law of continuous outflow of matter. According to Rosseland, for an atom in the atmosphere of the star ($\tau < 1$), we should compare two cycles of transitions, $1 \to 2 \to 3 \to 1$ (probability W_{23})

and $1 \to 3 \to 2 \to 1$ (probability W_{32}). We shall neglect the stimulated radiation. Then from formula (25) for the density of radiation we have

$$\frac{W_{23}}{W_{32}} = \delta \frac{E_{12} \cdot E_{23}}{E_{13}}. \tag{38}$$

Here $E_{i\kappa}$ represents the function E (formula (23)) for the frequency $\nu_{i\kappa}$. It is easy to see without recurring to any mathematical argument that the factor accompanying δ in this formula is, generally speaking, less than unity. As we have actually seen above, the decrease of intensity with the increase of ν, in the spectrum of the objects considered, proceeds more slowly than that required by Wien's law. Consequently, if we take, for instance, $\delta = \frac{1}{400}$, the number of transitions giving the emission will exceed by more than 400 times the number of absorptions. This happens at $R = 10R_1$. From formula (20) it follows that for this R, $\tau = 0{\cdot}3$. The absorption coefficient beyond the limit of the ultimate series must by far exceed κ, the mean value of the absorption coefficient. Therefore, in that part of the atmosphere of the star where emission lines can possibly arise, there remains a number of atoms quite sufficient for total absorption of light beyond the series limit of the atoms. For a Wolf-Rayet star using the value ρ_1 obtained above, we find that the number of atoms falling to one sq. cm. of the surface of the sphere of the radius $R = 10R_1$ equals 10^{24}. The absorption coefficient for one atom for the ultimate series of hydrogen is 10^{-17}. Consequently, $\tau_H \cong 10^7(1 - x)$. It can be seen that the mean percentage of normal atoms of hydrogen in the atmosphere of the Wolf-Rayet stars is not less than 10^{-7}. Thus we see that it is quite possible to apply Zanstra's method to the hydrogen lines of the Wolf-Rayet stars.

In § 1 an assumption was mentioned that the spectrum of anomalous B-type stars with absorption lines can be explained from the point of view of an extended photosphere, like the spectrum with emission lines. A spectrum of that kind can evidently arise in stars with extended photospheres but with a rapid decrease of density towards their limbs. Perhaps under certain circumstances this type of an equilibrium configuration of a star may occur.

Summary.—In the present paper a suggestion is expressed that some stars (supergiants) may have very extended photospheres. The examination of the problem of the radiative equilibrium in the outer layers of such stars leads to a dependence of the temperature upon the optical depth, which differs from this dependence in a normal photosphere. The application of this theory to the question of the distribution of the energy in the spectrum may possibly explain the anomalous colour-temperatures of the early-type stars. As an example, the case of the extended photospheres originated by the outflow of the matter from certain stars (Wolf-Rayet and P Cygni-type stars) is examined in detail. Some conclusions are obtained about the physical conditions in the outer layers of these stars.

Poulkovo Observatory:
1933 *September.*

THE RADIATIVE EQUILIBRIUM OF EXTENDED STELLAR ATMOSPHERES.

S. Chandrasekhar, Ph.D.

§ 1. The problems of radiative equilibrium which arise in the theory of stellar atmospheres have all been solved by idealising the outer layers of a star to be stratified in parallel planes. This last idealisation is of course a very justifiable one in all the commoner problems of the stellar atmospheres, but the recent work of Menzel, Miss Payne, Beals and others on the Wolf-Rayet stars and Novæ appear to show that we are here dealing with cases where the curvature of the outer layers must enter the abstract formulation of the respective problems in a very fundamental way. It is therefore convenient to have the solutions of the standard problems in the theory of radiative equilibrium with the curvature of the outer layers taken properly into account, and this paper, which is of a preliminary character, is a first step in that direction.

The plan of the paper is as follows: Section I, where the first integral of the equation of transfer is obtained, deals with the methods of approximation. Section II is devoted to the Schuster-Schwarzschild problems, and Section III to the formation of absorption lines. Lastly, Section IV treats the radiative equilibrium of a planetary nebula.

I. *The Fundamental Equations and the Methods of Approximation*

§ 2. *The Flux-Integral.*—Let I be the specific intensity of the radiation at a point P and at a distance r from the origin O and in a direction making an angle θ with OP in the positive direction of the radius vector. Let ρ and T be the density and temperature at any point and κ the coefficient of mass-absorption supposed independent of wave-length. Lastly, let B (a function of r only) be the intensity of the black body radiation corresponding to the temperature of the matter at any point r. The equation of transfer in polar co-ordinates is

$$\cos\theta\frac{\partial I}{\partial r}-\frac{\sin\theta}{r}\frac{\partial I}{\partial\theta}=\kappa\rho(B-I). \tag{1}$$

The equation of radiative equilibrium is, as usual,

$$2B=\int_0^\pi I\sin\theta d\theta. \tag{2}$$

Multiplying (1) by $\sin\theta d\theta$ and integrating between 0 and π we get after some transformations that

$$\frac{d}{dr}r^2\int_0^\pi I\cos\theta\sin\theta d\theta=0. \tag{3}$$

If we write

$$F = 2\int_0^\pi I \sin\theta \cos\theta d\theta, \tag{4}$$

then πF is merely the net flux of radiation at the point r. Hence by (3) the *first integral* of the equation of transfer is

$$Fr^2 = \text{constant} = F_0 \text{ (say)}. \tag{5}$$

§ 3. *The Methods of Approximation.*—The problem is to obtain the solution of (1) subject to (2) or its equivalent (5). Even in the case where the material is regarded as being stratified in parallel planes it has not been possible to integrate the equation of transfer exactly, and the two main methods of approximation that have been used in the "plane case" are the following :—

(*a*) The Schuster-Schwarzschild method of approximation in which we simply integrate the equation of transfer between $0 \leqslant \theta < \frac{1}{2}\pi$ and $\frac{1}{2}\pi \leqslant \theta \leqslant \pi$ and replace I in the two respective hemispheres by their average values I_1 and I_2.

(*b*) A second type of approximation which is due to Milne * is to seek a solution of the equation of transfer consistent with the flux integral. The approximations obtained by this method are much more accurate than those obtained by the method (*a*). A less rigorous but a much more rapid method of obtaining solutions (identical with those obtained by Milne's method) is the Eddington † type of approximation, which consists in the following two steps. If

$$\mathcal{J} = \tfrac{1}{2}\int_0^\pi I \sin\theta d\theta, \tag{6}$$

and

$$K = \tfrac{1}{2}\int_0^\pi I \cos^2\theta \sin\theta d\theta, \tag{7}$$

then we put

$$K = \tfrac{1}{3}\mathcal{J}, \tag{8}$$

suggested by the mean value of $\cos^2\theta$ over the sphere. Secondly, one uses the boundary condition that at the boundary

$$F(0) = 2\mathcal{J}(0). \tag{9}$$

§ 4. In treating the problems of radiative equilibrium in polar co-ordinates it is however not clear that one could use the same methods of approximation. Indeed, as McCrea ‡ first showed, the Schuster-Schwarzschild method of approximation applied to our case without any modification leads to inconsistencies. But, as will be shown subsequently, if one uses the Milne-Eddington type of approximation without any modification then one is not led to such inconsistencies. This, however, does not mean that this method of approximation is the proper one to work with when treating the problem in polar co-ordinates.

* E. A. Milne, *M.N.*, **81**, 382, 1921, which is the standard paper on the subject.
† A. S. Eddington, *Internal Constitution of Stars* (Cambridge), p. 322.
‡ W. H. McCrea, *M.N.*, **88**, 729, 1928.

Actually the type of approximation one finally adopts in a special case has, of course, to be chosen from physical considerations. If, for instance, we are considering the radiative equilibrium of a tenuous atmosphere (like the chromosphere) enveloping a parent star, then, as was first pointed out by McCrea, a consistent method of approximation is always to average over $0 < \theta < \sin^{-1}(a/r)$ and $\sin^{-1}(a/r) \leqslant \theta \leqslant \pi$ (instead of $0 < \theta < \pi/2$ and $\pi/2 \leqslant \theta < \pi$), where a is the radius of the parent star. On this basis McCrea indicated the method of approximation which should replace the usual Schuster-Schwarzchild method of approximation. Here we shall also develop methods for an approximation which should replace the usual Milne-Eddington type of approximation. Of course, this method of averaging is suitable only when one has an unambiguous "a" occurring in the problem. If we are considering extended photospheres, for instance, then this method of averaging can no longer be valid. We shall then use the Milne-Eddington type of approximation which, as we have already pointed out, does not lead us to any inconsistency.

II. *The Schuster-Schwarzschild Problems*

§ 5. We shall first consider the case where the McCrea type of averaging has to be adopted.

At a point r we define θ_r to be $\sin^{-1}(a/r)$. Now, multiply the equation of transfer by $\frac{1}{2}\sin\theta d\theta$ and integrate from 0 to θ_r. On the left-hand side we have

$$\tfrac{1}{2}\int_0^{\theta_r}\left\{\cos\theta\sin\theta\frac{\partial I}{\partial r}-\frac{\sin^2\theta}{r}\frac{\partial I}{\partial\theta}\right\}d\theta,$$

which, after partially integrating the second term, transforms into

$$\tfrac{1}{2}\int_0^{\theta_r}\frac{\cos\theta\sin\theta}{r^2}\frac{\partial}{\partial r}(r^2I)d\theta-\frac{a^2}{r^3}I(r,\theta_r),$$

which, after another partial integration, yields

$$\frac{1}{2r^2}\frac{\partial}{\partial r}r^2\int_0^{\theta_r}I\cos\theta\sin\theta d\theta-\tfrac{1}{2}I(r,\theta_r)\left[\cos\theta_r\frac{\partial\theta_r}{\partial r}\right]_r\sin\theta_r-\frac{a^2}{2r^3}I(r,\theta_r). \quad (10)$$

But

$$\sin\theta_r=a/r\,;\qquad \cos\theta_r\frac{\partial\theta_r}{\partial r}=-\frac{a}{r^2}. \quad (10')$$

The last two terms in (10) cancel and we are left with

$$\frac{1}{2r^2}\frac{d}{dr}r^2\int_0^{\theta_r}I\cos\theta\sin\theta d\theta. \quad (11)$$

Defining

$$F_1=2\int_0^{\theta_r}I\sin\theta\cos\theta d\theta\,;\qquad F_2=2\int_{\theta_r}^{\pi}I\sin\theta\cos\theta d\theta, \quad (12)$$

$$\mathcal{J}_1=\tfrac{1}{2}\int_0^{\theta_r}I\sin\theta d\theta\,;\qquad \mathcal{J}_2=\tfrac{1}{2}\int_{\theta_r}^{\pi}I\sin\theta d\theta, \quad (13)$$

we have finally
$$\frac{1}{4r^2}\frac{d}{dr}r^2F_1=\tfrac{1}{2}\kappa\rho[(1-\cos\theta_r)B-2\mathfrak{J}_1]. \tag{14}$$

Similarly
$$\frac{1}{4r^2}\frac{d}{dr}r^2F_2=\tfrac{1}{2}\kappa\rho[(1+\cos\theta_r)B-2\mathfrak{J}_2]. \tag{15}$$

The equation of radiative equilibrium now takes the form
$$B=\mathfrak{J}_1+\mathfrak{J}_2=\mathfrak{J}\text{ (say)}. \tag{16}$$

§ 6. *A First Approximation.*—Equations (14), (15) and (16) are exact. Now replace I in the ranges $(0, \theta_r)$ and (θ_r, π) by their average values I_1 and I_2. We then have
$$F_1=2\int_0^{\theta_r} I\sin\theta\cos\theta d\theta=I_1\frac{a^2}{r^2}, \tag{17}$$
$$F_2=2\int_{\theta_r}^{\pi} I\sin\theta\cos\theta d\theta=-I_2\frac{a^2}{r^2}. \tag{17'}$$
Also
$$\mathfrak{J}_1=\tfrac{1}{2}I_1(1-\cos\theta_r);\quad \mathfrak{J}_2=\tfrac{1}{2}I_2(1+\cos\theta_r). \tag{18}$$

By (17) and (17') we have
$$F=F_1+F_2=(I_1-I_2)\frac{a^2}{r^2}. \tag{19}$$

From the flux-integral (5) we easily deduce from the above that,
$$(I_1-I_2)=F_a, \tag{20}$$
where F_a is the flux of radiation at $r=a$. The equation of radiative equilibrium now takes the form
$$B=\tfrac{1}{2}I_1(1-\cos\theta_r)+\tfrac{1}{2}I_2(1+\cos\theta_r). \tag{21}$$

Solving (20) and (21) for I_1 and I_2 we have
$$I_1=B+\tfrac{1}{2}F_a(1+\cos\theta_r), \tag{22}$$
$$I_2=B-\tfrac{1}{2}F_a(1-\cos\theta_r). \tag{22'}$$

Equations (14) and (15) in their averaged form are
$$\frac{a^2}{4r^2}\frac{dI_1}{dr}=\tfrac{1}{2}\kappa\rho(B-I_1)(1-\cos\theta_r), \tag{23}$$
$$\frac{a^2}{4r^2}\frac{dI_2}{dr}=\tfrac{1}{2}\kappa\rho(I_2-B)(1+\cos\theta_r). \tag{23'}$$

Substituting (22) and introducing the new variable τ defined by
$$d\tau=-\kappa\rho dr, \tag{24}$$
we find that
$$\frac{dI_1}{d\tau}=\frac{dI_2}{d\tau}=F_a, \tag{25}$$

or

$$I_1 = \tfrac{1}{2}F_a + B_0 + F_a\tau, \tag{26}$$

$$I_2 = -\tfrac{1}{2}F_a + B_0 + F_a\tau, \tag{26'}$$

where B_0 is a constant of integration. Let $\tau = 0$ occur at $r = R$. Then to determine B_0 we use the boundary condition that at $r = R$, $\tau = 0$ (*cf.* equation (9)),

$$B(R, 0) = \tfrac{1}{2}F(R) = \tfrac{1}{2}F_a \cdot \frac{a^2}{R^2}. \tag{27}$$

This determines B_0. We find

$$B_0 = \tfrac{1}{2}F_a\,(\cos\theta_R + \sin^2\theta_R). \tag{28}$$

From (26) and (21) we then have

$$I_1 = \tfrac{1}{2}F_a(1 + \cos\theta_R + \sin^2\theta_R + 2\tau), \tag{29}$$

$$I_2 = \tfrac{1}{2}F_a(\cos\theta_R + \sin^2\theta_R - 1 + 2\tau), \tag{29'}$$

$$B = \tfrac{1}{2}F_a\{\sin^2\theta_R + (\cos\theta_R - \cos\theta_r) + 2\tau\}. \tag{29''}$$

(29″) now corresponds to Schwarzschild's solution

$$B = \tfrac{1}{2}F(1 + 2\tau), \tag{30}$$

where F now is the *constant* net flux. If T_0 is the boundary temperature at $r = R$, then (29″) relates T_0 to the effective temperature T_e (defined by $\pi F_a = \sigma T_e^4$) by the equation

$$T_0 = \sqrt[4]{\frac{a^2}{2R^2}}\,T_e. \tag{31}$$

We may finally notice that if R is very large compared with a then we have

$$I_1 = F_a(1 + \tau)\,; \quad I_2 = F_a\tau, \tag{32}$$

$$B = \tfrac{1}{2}F_a\{(1 - \cos\theta_r) + 2\tau\}. \tag{32'}$$

(32) is identical with the corresponding solution when the curvature is neglected.

§ 7. *A Second Approximation.*—We first define the two quantities K_1 and K_2 as follows :—

$$K_1 = \tfrac{1}{2}\int_0^{\theta_r} I\sin\theta\cos^2\theta d\theta\,; \qquad K_2 = \tfrac{1}{2}\int_{\theta_r}^{\pi} I\sin\theta\cos^2\theta d\theta. \tag{33}$$

Multiply the equation of transfer by $\frac{1}{2}\sin\theta\cos\theta d\theta$ and integrate from 0 to θ_r. On the L.H.S. we have, after partially integrating the second term,

$$\tfrac{1}{2}\int_0^{\theta_r}\frac{\sin\theta\cos^2\theta}{r^2}\frac{\partial}{\partial r}(r^2 I)d\theta - \frac{1}{2r}\int_0^{\theta_r} I\sin\theta(1 - \cos^2\theta)d\theta - \frac{a^2}{2r^3}\cos\theta_r I(r, \theta_r). \tag{34}$$

Again, partially integrating the first integral and using (10′), (13) and noting (33) the above reduces to

$$\frac{1}{r^2}\frac{d}{dr}r^2K_1 + \frac{1}{r}(K_1 - \mathcal{J}_1) = \frac{dK_1}{dr} + \frac{1}{r}(3K_1 - \mathcal{J}_1), \tag{35}$$

we have finally

$$\frac{dK_1}{dr}+\frac{1}{r}(3K_1-\mathfrak{J}_1)=\frac{\kappa\rho}{4}\left(\frac{Ba^2}{r^2}-F_1\right). \tag{36}$$

Similarly

$$\frac{dK_2}{dr}+\frac{1}{r}(3K_2-\mathfrak{J}_2)=\frac{\kappa\rho}{4}\left(-\frac{Ba^2}{r^2}-F_2\right). \tag{37}$$

Adding (36) and (37) and using the flux integral we have

$$\frac{d(K_1+K_2)}{dr}+\frac{1}{r}\{3(K_1+K_2)-(\mathfrak{J}_1+\mathfrak{J}_2)\}=-\frac{\kappa\rho}{4}F_a\cdot\frac{a^2}{r^2}. \tag{38}$$

§ 8. As before, let I_1 and I_2 be the mean intensities in the two ranges. Then we have

$$K_1=\tfrac{1}{6}I_1(1-\cos^3\theta_r)\,; \qquad K_2=\tfrac{1}{6}I_2(1+\cos^3\theta_r). \tag{39}$$

From (39), (18) and (19) we deduce that

$$3(K_1+K_2)-(\mathfrak{J}_1+\mathfrak{J}_2)=\frac{1}{2}\frac{a^2}{r^2}\cos\theta_r\,.\,(I_1-I_2),$$

$$=\frac{1}{2}\frac{a^2}{r^2}\cos\theta_r\,.\,F_a. \tag{40}$$

Substituting (40) in (38) we have

$$\frac{d(K_1+K_2)}{dr}=-F_a\cdot\frac{a^2}{2r^3}\cos\theta_r-F_a\cdot\frac{a^2\kappa\rho}{4r^2}. \tag{41}$$

On integration this yields

$$K_1+K_2=-\tfrac{1}{6}F_a\cos^3\theta_r+\frac{F_a}{4}\int_0^\tau\sin^2\theta_r d\tau+\tfrac{1}{3}K_0, \tag{42}$$

where K_0 is the constant of integration and $d\tau$ is defined as in (24). Hence by (16) and (40) we have

$$B=-\tfrac{1}{2}F_a\cos\theta_r+\tfrac{3}{4}F_a\int_0^\tau\sin^2\theta_r d\tau+K_0. \tag{43}$$

The constant K_0 is determined as before. We find

$$B=\tfrac{1}{2}F_a\left\{\sin^2\theta_R+(\cos\theta_R-\cos\theta_r)+\tfrac{3}{4}\int_0^\tau\sin^2\theta_r d\tau\right\}, \tag{44}$$

where at $r=R$, $\tau=0$. The above solution is analogous to the solution in the "plane problem" in the form first obtained by Milne. If R is very large compared with a, we have

$$B=\tfrac{1}{2}F_a\left\{(1-\cos\theta_r)+\tfrac{3}{4}\int_0^\tau\sin^2\theta_r\,.\,d\tau\right\}. \tag{45}$$

Relation (31) continues to be true in this order of approximation.

§ 9. We now consider the case where the type of averaging we have

used in the preceding sections is not valid. As has been pointed out we now use the unmodified Milne-Eddington type of approximation. Writing

$$\mathcal{J}=\mathcal{J}_1+\mathcal{J}_2\,; \qquad F=F_0/r^2\,; \qquad K=K_1+K_2, \tag{46}$$

we now have setting $3K=\mathcal{J}$ (*cf.* equation (38))

$$\frac{dK}{d\tau}=\frac{1}{4}\frac{F_0}{r^2}, \tag{47}$$

or

$$K=\tfrac{1}{4}F_0\int_0^\tau\frac{d\tau}{r^2}+\tfrac{1}{3}K_0, \tag{48}$$

where K_0 is a constant of integration. Let $\tau=0$ occur at $r=R$. Using the usual boundary condition we derive that

$$B=\tfrac{1}{2}F_0\left\{\frac{1}{R^2}+\tfrac{3}{2}\int_0^\tau\frac{d\tau}{r^2}\right\}, \tag{49}$$

or more simply in terms of the flux πF_R at $r=R$

$$B=\tfrac{1}{2}F_R\left\{1+\tfrac{3}{2}\int_0^\tau\frac{R^2}{r^2}d\tau\right\}. \tag{50}$$

If R is very large we have the simpler formula

$$B=\tfrac{3}{4}F_0\int_0^\tau\frac{d\tau}{r^2}. \tag{51}$$

§ 10. *Variation of Intensity.*—So far we have not attempted to determine I as a function r and θ. Having now determined B as a function of r we have to introduce this in the equation of transfer and solve it for I. The formal solution can be easily written down. If $I(\theta, p)$ refers to the intensity at a point P in a direction OA which is at a perpendicular distance p from the centre, then one easily verifies that

$$I(\theta,p)=e^{p\int_0^\theta\kappa\rho\,\mathrm{cosec}^2\,\theta d\theta}\int_\theta^\pi e^{-p\int_0^\theta\kappa\rho\,\mathrm{cosec}^2\,\theta d\theta}B(\theta)p\kappa\rho\,\mathrm{cosec}^2\,\theta d\theta. \tag{52}$$

We already know B as a function of r, and by means of the substitution $r=p\,\mathrm{cosec}\,\theta$ we can transform it into a function of θ. Thus (52) formally represents the solution to the problem. In practice, however, to perform the integrations we need to know the variation of $\kappa\rho$ with r, and for this reason it does not seem worth while to go into details over this, but we shall illustrate the general trend of the calculations corresponding to the solution (51) for B and when $\kappa\rho$ varies as some inverse power of r.

Let us then suppose that

$$\kappa\rho=cr^{-n}=cp^{-n}\sin^n\theta. \tag{53}$$

By (51) we now have

$$B=\frac{3F_0c}{4(n+1)p^{n+1}}\sin^{n+1}\theta. \tag{54}$$

Introducing this in (52) we have

$$I(\theta, p)=\frac{3F_0c^2}{4(n+1)p^{2n}}e^{cp^{-(n-1)}\int_0^\theta \sin^{n-2}\theta d\theta}\int_\theta^\pi e^{-cp^{-(n-1)}\int_0^\theta \sin^{n-2}\theta d\theta}\sin^{2n-1}\theta d\theta. \quad (55)$$

Writing

$$\alpha = cp^{-n+1} \quad (56)$$

we have

$$I(\theta, p)=\frac{3F_0\alpha}{4(n+1)p^2}e^{\alpha\int_0^\theta \sin^{n-2}\theta d\theta}\int_\theta^\pi e^{-\alpha\int_0^\theta \sin^{n-2}\theta d\theta}\alpha\sin^{2n-1}\theta d\theta. \quad (57)$$

We are interested only in the "emergent radiation," *i.e.* when $\theta=0$. Then we have

$$I(p)=\frac{3F_0\alpha}{4(n+1)p^2}\int_0^\pi e^{-\alpha\int_0^\theta \sin^{n-2}\theta d\theta}\alpha\sin^{2n-1}\theta d\theta. \quad (58)$$

§ 11. We will consider two special cases of (58).

Case I ($n=3$).—Now $\alpha=cp^{-2}$, and (58) simplifies to

$$I(p)=\frac{3F_0\alpha^2}{16c}\int_0^\pi e^{-\alpha(1-\cos\theta)}(1-\cos^2\theta)^2\alpha\sin\theta d\theta. \quad (59)$$

Introducing the new variable $\alpha\cos\theta=x$ we have

$$I(p)=\frac{3F_0\alpha^2e^{-\alpha}}{16c}\int_{-\alpha}^{\alpha}e^x\left(1-\frac{x^2}{\alpha^2}\right)^2dx. \quad (60)$$

On performing the integration we find that

$$I(p)=\frac{3F_0e^{-\alpha}}{\alpha^2c}[(\alpha^2+3)\sinh\alpha-3\alpha\cosh\alpha], \quad (61)$$

where $\alpha=c/p^2$.

The following limiting forms may be noted

$$I(p)\sim\frac{F_0c^2}{5p^6}\text{ for }p\text{ large}, \quad (62)$$

and

$$I(p)\sim\frac{3F_0}{2c}\left(1-\frac{3p^2}{c}\right)\text{ for }p\text{ small}. \quad (63)$$

Case II ($n=2$).—Now $\alpha=c/p$, and (58) simplifies to

$$I(p)=\frac{F_0\alpha^4}{4c^2}\int_0^\pi e^{-\alpha\theta}\sin^3\theta d\theta,$$

$$=\frac{3F_0}{2c^2}\frac{\alpha^4(e^{-\alpha\pi}+1)}{(\alpha^2+9)(\alpha^2+1)}. \quad (64)$$

We now have

$$I(p)\sim\frac{F_0c^2}{3p^4}\text{ for }p\text{ large}, \quad (65)$$

and

$$I(p) \sim \frac{3F_0}{2c^2} \text{ for } p \text{ small.} \tag{66}$$

Comparing (65) with (62) we notice that the more rapidly $\kappa\rho$ falls off with distance the more rapidly does $I(p)$ fall off with p. This is quite a physically understandable result.

§ 12. *A Purely Scattering Atmosphere.*—When we are dealing with a purely scattering atmosphere there is no interchange of energy between the different frequencies, and we shall therefore consider each frequency separately. Let s_ν be the coefficient of scattering, σ_ν the optical thickness $\int_\infty^r s_\nu \rho dr$. Assuming the scattered radiation to be equal in all directions the equation of transfer is

$$\cos\theta \frac{\partial I_r}{\partial r} - \frac{\sin\theta}{r}\frac{\partial I_r}{\partial r} = s_\nu\rho(I_\nu - \tfrac{1}{2}\int_0^\pi I_\nu \sin\theta d\theta). \tag{67}$$

We see that formally equation (67) is identical in form with the equations (1) and (2) taken together. Hence the analysis of the preceding sections apply to this case provided we replace τ and κ wherever they occur by σ_ν and s_ν respectively, and also add a suffix ν to all the symbols.

§ 13. *The Schuster Problem.*—The problem which is specifically associated with the name of Schuster is the following * : "A layer of gas scattering monochromatic radiation of frequency ν is placed in front of a bright background radiating with a given flux πG_ν. Given the optical thickness σ_ν of the scattering material, to determine the emergent flux." In our case we have to reformulate the problem in the following terms :—

"Enveloping a bright spherical surface radiating monochromatic radiation of frequency ν with a mean intensity i_ν, is an atmosphere of gas scattering monochromatic radiation of frequency ν. Given the radial optical thickness σ_ν of the surrounding atmosphere and given also that the bright spherical surface is of radius a and that the atmosphere extends to $r = R$, to determine the mean intensity $I_\nu(0)$ of the radiation emergent through a tangent cone drawn from a point $r = R$ to the sphere $r = a$."

It is clear from this formulation that we have now to adopt the type of averaging we have used in §§ 5–8. We shall use the results of the first approximation. From (29) we now have

$$I_1 = \tfrac{1}{2}F_\nu(a)(1 + \cos\theta_R + \sin^2\theta_R + 2\sigma_\nu). \tag{68}$$

At $r = a$, $I = i_\nu$ and we have

$$i_\nu = \tfrac{1}{2}F_\nu(a)(1 + \cos\theta_R + \sin^2\theta_R + 2\sigma_\nu). \tag{69}$$

While at $r = R$, $I_1 = I_\nu(0)$ and by (68)

$$I_\nu(0) = \tfrac{1}{2}F_\nu(a)(1 + \cos\theta_R + \sin^2\theta_R). \tag{70}$$

Hence we have the following solution for the "Schuster's problem" :—

$$r_\nu = \frac{I_\nu(0)}{i_\nu} = \frac{1 + \cos\theta_R + \sin^2\theta_R}{1 + \cos\theta_R + \sin^2\theta_R + 2\sigma_\nu}. \tag{71}$$

* *Cf.* E. A. Milne, *Phil. Trans. Roy. Soc.* (A), **228**, 421, 1929.

(71) replaces the usual Schuster's formula for r_ν, namely :—

$$r_\nu = \frac{1}{1+\sigma_\nu}. \tag{72}$$

As was to be expected, the value of r_ν depends not only on the optical thickness σ_ν, but also on the extent to which the scattering material is spread out. But this dependence is not very pronounced. Thus for a given σ_ν, r_ν is a *minimum* when $(1+\cos\theta_R+\sin^2\theta_R)$ is a maximum which it attains when $\theta_R = 60°$. When $\theta_R = 60°$, (71) takes the form

$$r_\nu = \frac{1}{1+(8/9)\sigma_\nu}. \tag{73}$$

$\theta_R = 60°$ corresponds to the scattering material being spread out to a distance $2/\sqrt{3}$ $(=1{\cdot}1547)$ times the radius of the original "photospheric surface."

Now it is known that in the more exact form of the Schuster's formula we have in the denominator of (72), $3/4\,.\,\sigma_\nu$ instead of simply σ_ν. For us to obtain the corresponding second approximation we really need to evaluate the integral (52) with B given by (44), for which we require the exact variation of $s_\nu\rho$ with r. As this is a rather complicated matter we shall not go into it here.

III. *The Formation of Absorption Lines* *

§ 14. In considering the formation of absorption lines it is not quite clear as to the method of approximation that has to be adopted. For the sake of simplicity we shall treat the problem on the un-modified Eddington type of approximation. The other type of averaging leads to far too complicated equations.

Let

κ_ν be the coefficient of continuous absorption applicable to both inside and immediately outside the absorption line,

s_ν (a function of ν) the coefficient of line absorption,

$I_\nu'(r, \theta)$ the intensity of the radiation in the frequency range ν to $\nu+d\nu$ within the line at a point distant r from the centre and in a direction making an angle θ with the positive direction of the radius vector and $I(r, \theta)$ the corresponding intensity if there had been no scattering (*i.e.*) outside the line.

In addition to the quantities F, $\mathcal{J}$, K, we now introduce a corresponding set of quantities F_ν', $\mathcal{J}_\nu'$, K_ν' defined in exactly the same way but with the I_ν''s replacing the I's in the respective integrals.

The equation of transfer is (*cf.* Eddington, *loc. cit.*, equation (4))

$$\cos\theta\frac{\partial I_\nu'}{\partial r} - \frac{\sin\theta}{r}\frac{\partial I_\nu'}{\partial\theta} = -\rho(\kappa_\nu+s_\nu)I_\nu' + \rho(1-\epsilon)s_\nu\mathcal{J}_\nu' + \epsilon\rho s_\nu B_\nu + \rho\kappa_\nu B_\nu, \tag{74}$$

* *Cf.* E. A. Milne, *M.N.* (1), **88**, 493, 1928 ; (2), **89**, 3, 1928 ; A. S. Eddington, *M.N.*, **89**, 620, 1928.

where ϵ is the fraction of the absorbed scattered radiation which is lost in collisions of the second kind, and B_ν as usual corresponds to the Planck-function.

Multiplying (74) by $\frac{1}{2}\sin\theta d\theta$ and $\frac{1}{2}\sin\theta\cos\theta d\theta$, and integrating between 0 to π, we have (*cf.* equations (14), (15) and (38))

$$\frac{1}{4r^2}\frac{d}{dr}r^2F_\nu' = -\rho(\kappa_\nu+\epsilon s_\nu)(\mathcal{J}_\nu'-B_\nu), \tag{75}$$

$$\frac{dK_\nu'}{dr}+\frac{1}{r}(3K_\nu'-\mathcal{J}_\nu') = -\tfrac{1}{4}\rho(\kappa_\nu+s_\nu)F_\nu'. \tag{76}$$

Let

$$\eta = s_\nu/\kappa_\nu, \tag{77}$$

and defining the optical thickness τ_ν by

$$d\tau_\nu = -\kappa_\nu\rho dr, \tag{78}$$

we have our fundamental system of differential equations

$$\frac{1}{4r^2}\frac{d}{d\tau_\nu}r^2F_\nu' = (1+\epsilon\eta)(\mathcal{J}_\nu'-B_\nu), \tag{79}$$

$$\frac{dK_\nu'}{d\tau_\nu} = -\frac{1}{\rho\kappa_\nu r}(\mathcal{J}_\nu'-3K_\nu')+\tfrac{1}{4}(1+\eta)F_\nu'. \tag{80}$$

Our approximation is now to set $\mathcal{J}_\nu' = 3K_\nu'$. Hence

$$\frac{1}{4r^2}\frac{d}{d\tau_\nu}r^2F_\nu' = (1+\epsilon\eta)(\mathcal{J}_\nu'-B_\nu), \tag{81}$$

$$\frac{d\mathcal{J}_\nu'}{d\tau_\nu} = \tfrac{3}{4}(1+\eta)F_\nu'. \tag{82}$$

§ 15. Assume now that η and ϵ are both constants as a function of τ_ν. It is doubtful whether this approximation can be justified to the extent to which it can be justified in the case where the matter is stratified in parallel planes (*cf.* Milne (2), *loc. cit.*, p. 5). However, we shall adopt it to see the nature of the results that arise out of this assumption. From (81) and (82) we now have

$$\frac{1}{r^2}\frac{d}{d\tau_\nu}\left(r^2\frac{d\mathcal{J}_\nu'}{d\tau_\nu}\right) = q^2(\mathcal{J}_\nu'-B_\nu), \tag{83}$$

where

$$q^2 = 3(1+\eta)(1+\epsilon\eta). \tag{84}$$

We will now consider the case where B_ν has its "equilibrium value," *i.e.* the radiation just outside the line has its equilibrium density. We have then to adopt our earlier solution in the form (50) for B_ν:

$$B_\nu = \tfrac{1}{2}F_{R,\nu}\left\{1+\tfrac{3}{2}\int_0^{\tau_\nu}\frac{R^2}{r^2}d\tau_\nu\right\}. \tag{85}$$

For the sake of brevity we shall hereafter suppress the suffix ν to F_R, but it

has to be understood that F_R always stands for the net flux of radiation in the frequency range $(\nu, \nu+d\nu)$ at the boundary $(r=R)$ of the star.

From (83) and (85) it follows that

$$\frac{1}{r^2}\frac{d}{d\tau_\nu}\left\{r^2\frac{d(\mathcal{J}_\nu'-B_\nu)}{d\tau_\nu}\right\}=q^2(\mathcal{J}_\nu'-B_\nu), \tag{86}$$

or differently as

$$\frac{d^2(\mathcal{J}_\nu'-B_\nu)}{d^2\tau_\nu}+\frac{2}{r}\frac{dr}{d\tau_\nu}\frac{d(\mathcal{J}_\nu'-B_\nu)}{d\tau_\nu}-q^2(\mathcal{J}_\nu'-B_\nu)=0. \tag{87}$$

It is seen that to solve (87) we need the variation of τ_ν with r. We shall examine the case when τ_ν varies as some inverse power m of r, *i.e.*

$$\tau_\nu=cr^{-m} \text{ (say)}. \tag{88}$$

Consistent with this assumption we should now rewrite (85) in the form

$$B_\nu=\tfrac{3}{4}F_0\int_0^{\tau_\nu}\frac{d\tau_\nu}{r^2}, \tag{85'}$$

where F_0 now stands for $F_{0,\nu}$. Introducing the following new quantities

$$n=\frac{m+2}{2m}, \tag{89}$$

$$\mathcal{J}_\nu'-B_\nu=Q\tau_\nu{}^n\,; \qquad Z=q\tau_\nu, \tag{90}$$

the equation (87) combined with the relation (88) leads to the following differential equation for Q :—

$$Z^2\frac{d^2Q}{dZ^2}+Z\frac{dQ}{dZ}-(n^2+Z^2)Q=0. \tag{91}$$

(91) is just Bessel's equation with the purely imaginary argument *in*. We need a solution of (91) which tends exponentially to zero for large values of Z, since $\mathcal{J}_\nu'$ must tend to its equilibrium value at great distances. Hence the appropriate solution we have to consider is the following :— *

$$Q(Z)=K_n(Z)=\tfrac{1}{2}\pi\{I_{-n}(Z)-I_n(Z)\}\cot n\pi. \tag{92}$$

Hence our solution is

$$\mathcal{J}_\nu'=\tfrac{3}{4}F_0\int_0^{\tau_\nu}\frac{d\tau_\nu}{r^2}+A(q\tau_\nu)^nK_n(q\tau_\nu), \tag{93}$$

where A is a constant at present undetermined. Finally, by (82), we have for the flux $\pi F_\nu'$,

$$F_\nu'=\frac{4}{3(1+\eta)}\left\{\frac{3F_0}{4r^2}-Aq(q\tau_\nu)^nK_{n-1}(q\tau_\nu)\right\}. \tag{94}$$

A is now determined from the boundary condition that at $\tau_\nu=0$, *i.e.* as $r\to\infty$, $F_\nu'-2\mathcal{J}_\nu'\to 0$. From physical considerations both must separately

* *Cf.* Whittaker and Watson, *Modern Analysis* (Cambridge, 1927), p. 373.

tend to zero as $r \to \infty$. We will not go into the details here, but one can easily prove that if $n > \frac{1}{2}$ (*i.e.* if m is finite) then $Z^n K_{n-1}(Z) \to 0$ as $Z \to 0$, while $Z^n K_n(Z)$ tends to some limiting value. Hence our boundary condition can be satisfied if, and only if, $A = 0$, in which case we simply have

$$F_\nu' = \frac{F_0 r^{-2}}{1+\eta}. \tag{95}$$

On the other hand, for the flux F_ν just outside the line,

$$F_\nu = F_0 r^{-2}. \tag{96}$$

Hence

$$\frac{F_\nu'}{F_\nu} = \frac{1}{1+\eta}. \tag{97}$$

For the case where the material is stratified in parallel planes the formula corresponding to (97) is (*cf.* Eddington, *loc. cit.*, equation (17))

$$\frac{F_\nu'}{F_\nu} = \frac{1+\frac{2}{3}q}{1+\eta+\frac{2}{3}q}. \tag{98}$$

Thus for the case we have considered the introduction of the curvature far from introducing complications essentially simplifies the problem. Though the result (97) has been obtained only for a strictly infinite atmosphere, we can expect it to be valid if only the atmosphere be sufficiently extended.

IV. *The Radiative Equilibrium of a Planetary Nebula*

§ 16. This problem has already been considered in some detail by Milne.* But he neglected the curvature of the layers. It is, however, quite easy to find the appropriate solutions, taking into account the curvature as well.

Let πS be the incident flux per cm.^{2} due to the central star on the inner boundary of the nebular shell. The equation of radiative equilibrium then takes the form

$$2\int_0^\pi (B - I) \sin\theta d\theta = \frac{S r_1^2}{r^2} e^{-(\tau_1 - \tau)}, \tag{99}$$

where the optical thickness τ is measured from the outer boundary of the nebular shell the total radial optical thickness of which is taken to be τ_1. Further, let r_1 and r_2 be the inner and the outer radii of the planetary nebula.

The equation of transfer is the same as before (equation (1)). Multiplying the equation of transfer by $\sin\theta d\theta$ and integrating from 0 to π and using (99), we find that

$$\frac{d}{d\tau} r^2 F = -S r_1^2 e^{-(\tau_1 - \tau)}, \tag{100}$$

which on integration yields

$$r^2 F = \text{constant} - S r_1^2 e^{-(\tau_1 - \tau)}. \tag{101}$$

* E. A. Milne, *Zeits. f. Astro. Physik*, 1, 98, 1930.

At $\tau = \tau_1$, $r = r_1$ we have $F = 0$. This is precisely equivalent to the boundary condition discussed by Milne (*loc. cit.*, p. 102). From this we deduce that

$$F = \frac{Sr_1^2}{r^2}(1 - e^{-(\tau_1 - \tau)}), \tag{102}$$

which is now our flux integral. Multiplying the equation of transfer by $\frac{1}{2} \sin\theta \cos\theta d\theta$ and integrating from 0 to π and setting $3K = \mathcal{J}$, we have

$$\frac{dK}{d\tau} = \frac{Sr_1^2}{4r^2}(1 - e^{-(\tau_1 - \tau)}), \tag{103}$$

which leads to

$$\mathcal{J} = \tfrac{3}{4}\int_0^\tau \frac{Sr_1^2}{r^2}(1 - e^{-(\tau_1 - \tau)})d\tau + K_0, \tag{104}$$

where K_0 is a constant of integration to be determined from our usual boundary condition that at $r = r_2$, $\tau = 0$, $F = 2\mathcal{J}$. We find that

$$K_0 = \tfrac{1}{2}\frac{Sr_1^2}{r_2^2}(1 - e^{-\tau_1}). \tag{105}$$

We finally obtain from (99), (104) and (105) that

$$B = \tfrac{1}{2}S\left\{\frac{r_1^2}{r_2^2}(1 - e^{-\tau_1}) + \tfrac{1}{2}\frac{r_1^2}{r^2}e^{-(\tau_1 - \tau)} + \tfrac{3}{2}\int_0^\tau \frac{r_1^2}{r^2}(1 - e^{-(\tau_1 - \tau)})d\tau\right\}. \tag{106}$$

If the radius of curvature be neglected, *i.e.* $r_1 = r_2 = r = \text{constant}$, then we easily derive from (106) that

$$B = \tfrac{1}{2}S\{1 + \tfrac{1}{2}e^{-\tau} - e^{-(\tau_1 - \tau)} + \tfrac{3}{2}\tau\}, \tag{107}$$

which is Milne's result (*loc. cit.*, equation (28)). The ratio of the boundary temperatures at $r = r_2$ given by (107) and (106) is seen to be $\sqrt{r_1/r_2}$, which might be appreciable for many planetaries.

Summary

In this paper the standard problems in the theory of radiative equilibrium which arise in the theory of stellar atmospheres are rediscussed without neglecting the curvature of the outer layers of the star.

The solution for the Schuster problem shows that the residual intensity depends not only on the optical thickness of the scattering material but also on the extent to which it is spread out. For a given optical thickness the minimum absorption ratio occurs when the tangent cone from a point on the boundary of the scattering atmosphere has a semivertical angle of 60°.

The formation of absorption lines has also been discussed in detail for the case when τ_ν varies as some inverse power m of r. It is shown that if m is finite then we always have

$$\frac{F_\nu'}{F_\nu} = \frac{1}{1 + \eta},$$

(F_ν' being the flux of radiation in the line, while F_ν is the corresponding flux just outside the line and $\eta = s_\nu/\kappa_\nu$).

Finally, the radiative equilibrium of the planetary nebula is briefly considered. It is shown that if r_1 and r_2 are the inner and the outer radii of the nebular shell, then the temperature at the boundary is $\sqrt{r_1/r_2}$ times the value that would be predicted if we had neglected the curvature.

Trinity College, Cambridge :
1934 *March* 2.

THE CONTOURS OF THE POTASSIUM RESONANCE LINES IN ABSORPTION.

J. F. Heard, Ph.D., 1851 *Exhibition Student.*

(Communicated by Prof. A. Fowler, F.R.S.)

Introduction

Minkowski * and Korff † have shown that, neglecting second order quantities, the classical dispersion theory of Lorentz ‡ and Voigt § for the distribution of energy within a spectral line which has arisen from absorption by a finite thickness of vapour at a moderate temperature yields an expression, the form of which, as given by Korff, is

$$(\Delta\lambda)^2 \log_e I/I_0 = -\frac{2\pi e^4 \lambda^2}{3m^2c^4} N \qquad (1)$$

where $\Delta\lambda$ is the distance of a given frequency within the line from the resonance frequency and

I is the intensity of light transmitted at the given frequency,

I_0 is the intensity of light transmitted at a frequency far from resonance, *i.e.* the intensity of the continuous background,

e is the charge of the electron,

λ is the wave-length of the line under consideration,

m is the mass of the electron,

c is the velocity of light,

N is the number of linear oscillators in 1 sq. cm. section in the line of sight.

The resonance lines of alkali arc spectra lend themselves to a test of the classical theory. The number of linear oscillators corresponding to each member of the doublet may be taken as $N = nzf$, where n is the number of atoms per c.c., z the length of the absorbing column, and f the oscillator strength or the proportion of atoms being raised by absorption to the particular doublet state involved. From a consideration of the statistical

* *Zeit. f. Phys.*, **36**, 839, 1926.
† *Ap. J.*, **76**, 124, 1932.
‡ *Proc. Amst. Acad.*, **8**, 591, 1905.
§ *Münch. Ber.*, p. 603, 1912.

weights of the doublet states, $2P_{\frac{1}{2}}$ and $2P_{\frac{3}{2}}$, the values of f for the alkali resonance lines are 1/3 and 2/3.

Minkowski * and Korff † both have examined the contours of the sodium D lines, and for small values of n have obtained agreement with theory. For larger values of n, and when foreign gas was present in the absorption tubes, their lines were broadened beyond the theoretical widths.

The contours of the resonance lines of the other alkali metals have not previously been examined under conditions which would be expected to yield results comparable with theory. The results of an investigation upon the potassium resonance lines in absorption are presented here. These

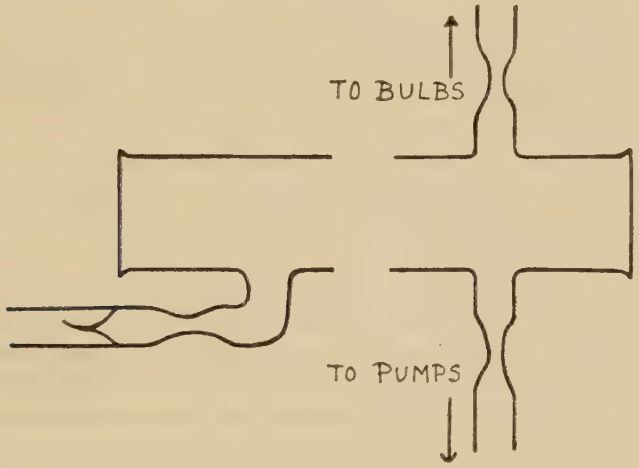

FIG. 1.—*Absorption tube.*

results provide a further verification of the classical theory and certain facts about the departure from theory for values of n above a critical value.

Experimental

The absorption cells consisted of tubes of Pyrex glass, 3 cm. in diameter and of different lengths, on to which Pyrex end windows had been sealed. In introducing the potassium the following procedure was adopted. By side tubes possessing constrictions for sealing off, the absorption tube was connected on one side to a mercury diffusion pump backed by a Hyvac, and on the other side to a series of Pyrex bulbs separated by constrictions. (A third side tube on the absorption tube had sealed inside it a fragile tip which could be broken later by a magnetic hammer.) Fig. 1 is a sketch of the absorption tube. Into the Pyrex bulb furthest from the absorption tube a small quantity of freshly cut potassium, obtained from Messrs. Kahlbaum, was introduced. Commercial nitrogen was passed over the potassium and the latter was heated gently ; the nitrogen contained sufficient oxygen for this procedure to oxidise much of the hydrocarbons in the potassium without oxidising the potassium too much. Then the system was sealed

* *Loc. cit.* † *Loc. cit.*

up and evacuated. During the evacuation the absorption tube was kept at a temperature of about 500° C. to drive occluded gases from its walls. After several hours it was allowed to cool, and the potassium was distilled slowly from one bulb to another and finally into the absorption tube, the empty bulb being sealed off after each distillation. Then the absorption tube was sealed off from the pumps and placed in a furnace, where it was kept for a day at a temperature of about 250° C. to drive any hydrogen from the potassium. (At temperatures higher than this the potassium produced serious discoloration of the Pyrex.) When the tube had cooled it was again sealed to the pumps at the third side tube, the internal tip was broken by means of a magnetic hammer and the tube was evacuated again. As a final precaution towards removing hydrogen the potassium "mirror" was driven from place to place in the tube by means of a Bunsen-burner for several hours with the pumps still running. Then the tube was sealed off from the pumps and was ready for use.

The electric furnace used in the absorption experiments was based on an iron pipe 80 cm. long and 15 cm. in diameter. There were three windings of nichrome resistance wire, one winding uniform along the whole length of the furnace and a winding of 10 cm. extent at each end. By adjusting the currents through these latter windings the temperature of the furnace could be made uniform along nearly its whole length. The furnace was surrounded with steam-pipe lagging, and each end was stopped with two uralite discs with central glass windows 1 inch in diameter. The absorption tube was supported centrally in the furnace and two small auxiliary heaters maintained the ends of the tube at a temperature a few degrees higher than that of the furnace, in order to prevent the deposition of potassium on the windows. The temperature of the absorption tube could be measured at intervals along its length by means of a mercury thermometer which had been calibrated against a platinum resistance thermometer. The temperature of the furnace when it had become steady could be kept constant within about 1 degree.

The light source was a 500 c.p. Pointolite lamp. A lens formed a parallel beam in which the absorption tube was placed, and a second lens formed an image of the light source upon the slit of the spectrograph. The spectrograph was a 10-foot concave grating in an Eagle mounting. It was used in the first and second orders. In the required region (λ 7700) the dispersion was 5·5 A/mm. in the first order and 2·4 A/mm. in the second order, and the theoretical resolving powers, 50,000 and 100,000, were approximately attained in practice. Slit widths ranging from 0·03 to 0·04 mm. were used. The second was the highest order which could be used with this grating for the above-mentioned region, and, as it will appear later, the dispersion and resolving power there were hardly sufficient to obtain the complete contours of the fines corresponding to the lowest temperatures. On the other hand, little might be gained by using a much larger dispersion, for the exposure time would then be unreasonably long.

Ilford Infra-red plates were used. These plates are quite well suited for photography at the region λ 7700; but all infra-red sensitive plates

have comparatively large grain and a tendency to uneven chemical fog, and these factors make for difficulty in photographic photometry. The exposure time for the absorption lines in the first order was about one hour ; in the second order, to obtain sufficiently short-exposure time ($2\frac{1}{2}$ hours), the plates were bathed for about 30 seconds in a 4 per cent. ammonia solution and quickly dried immediately before exposing. This procedure, indeed, increased the grain effect and the chemical fog, but reasonably consistent results could be obtained, and the sources of error so introduced were less formidable than those which would have resulted from very long exposures with unbathed plates. The plates were developed for 8 minutes in borax "fine-grain" developer.

The intensity calibration of the plates was effected by means of a stepped slit placed at the opened slit of a small transmission grating spectrograph and exposed to white light from a small diffuse source placed at a large distance. The "steps" of the stepped slit were eight in number and ranged in width from 0·19 mm. to 1·43 mm.

A Wratten No. 70 filter placed before the slit for all exposures served to cut out other grating orders and to reduce the effects of scattered light within the spectrographs.

The photometry was done with a Cambridge Instrument Company's recording microphotometer. Runs were made across the two absorption lines and across the calibration marks at the mean wave-length of the two absorption lines. From the record of the deflections corresponding to the calibration marks a deflection-intensity curve could be drawn for each plate, and from this the relative intensities of all parts of each absorption line could be determined.

A number of tests were made to justify certain assumptions regarding the photometry. For example, it was determined that, although the plate sensitivity varied somewhat in the region between the absorption lines, the plate characteristic did not vary, and so it was justifiable to use the same deflection-intensity curve for both lines. Again, it was determined that the characteristic of bathed plates did not change during a three-hour period after bathing, and therefore it was permissible to make the calibration exposure either before or after the exposure to the absorption lines.

Results

From the microphotometer record for each absorption line, measurements of the half-width, $\Delta\lambda$, have been made for various values of the intensity, I. These values plotted give the contour of the line. In fig. 2 the results for the wider line, λ 7665, are shown in this way for four different temperatures. In the case of the two lowest temperatures the contours are incomplete because the resolving power of the spectrograph was not sufficient to resolve the component parts of the narrowest portions of fine lines. That is to say, the tip of the line shows itself blunted off at a finite value of the intensity, and the half-width at this point is comparable with the smallest interval which the spectrograph is expected to resolve. It is

clear also that with imperfect resolution the lines will be measured too broad at large values of I. Knowing the degree of imperfection of the resolution and the approximate shape of the lines it is possible to estimate roughly the

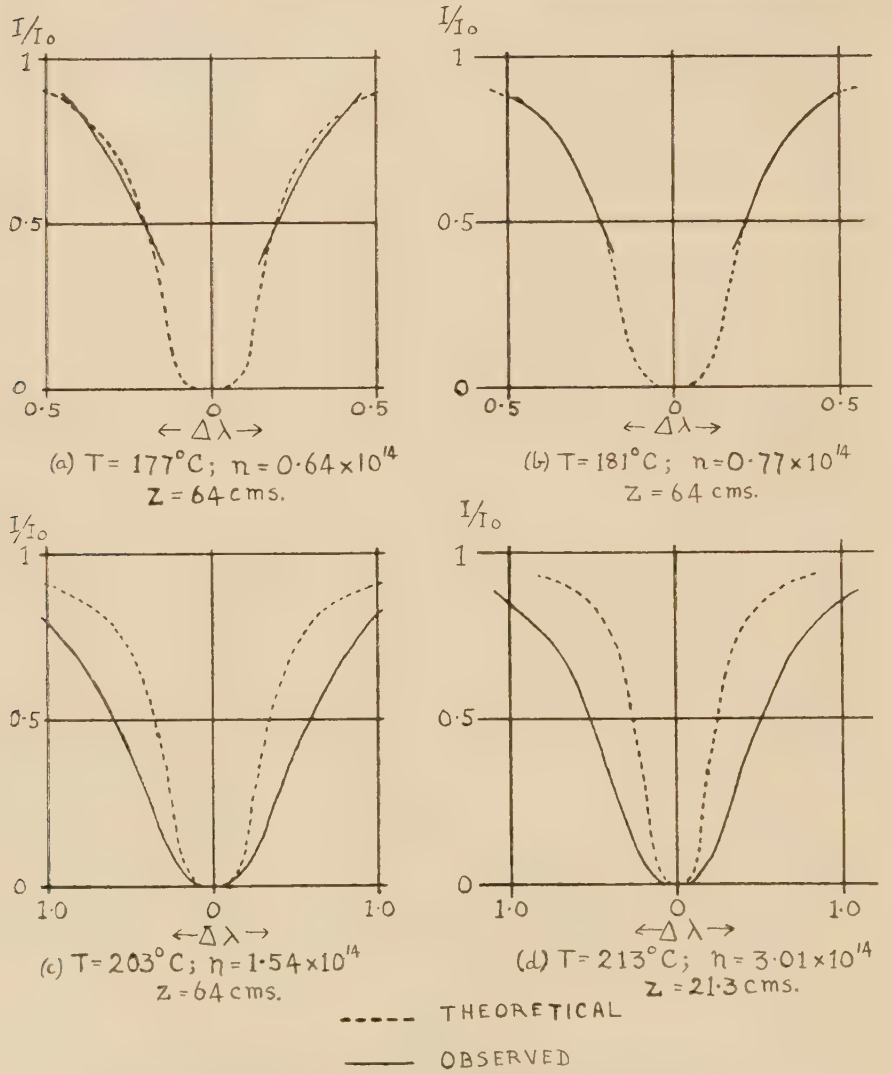

FIG. 2.—*I/I_0 plotted against $\Delta\lambda$ for potassium absorption line λ 7665.*

broadening to be expected from this cause. For the lines here examined it has been concluded that this error is within the errors of photometry.

To derive the theoretical contours given by equation (1) it is necessary to know the values of n, the number of atoms per c.c. These have been calculated from the vapour pressure data of Weiler.* The theoretical contours of λ 7665 for the appropriate temperatures have been drawn in fig. 2 for comparison with the measured contours. (It should be observed

* *Annalen der Phys.*, **1**, 385, 1929.

that the scale of $\Delta\lambda$ for (*a*) and (*b*) is different from that for (*c*) and (*d*), and that the tube length corresponding to (*d*) is 21·3 cm.) The theoretical contours of λ 7699 would be narrower than those of λ 7665 by a factor of $\sqrt{2}$. The comparison of the theoretical with the measured contours for λ 7699 is not shown here, but it is much the same as for λ 7665 at corresponding temperatures (*vide infra*).

A more convenient method of presenting the results is that used by Korff.* Writing B for the quantity $-\dfrac{(\Delta\lambda)^2 \log_e I/I_0}{nzf}$ we see from equation (1) that the theoretical value of B is $\dfrac{2\pi e^4\lambda^2}{3m^2c^4}$, which, with λ expressed in angstroms, gives $0{\cdot}97 \times 10^{-17}$ for λ 7665 ($f = 2/3$) and $0{\cdot}98 \times 10^{-17}$ for λ 7699 ($f = 1/3$). The experimental results are given in Table I, and a comparison of the tabulated results for B with those just stated indicates the extent of agreement, at various atomic densities, between observation and theory. The values of B are given for $I/I_0 = 0{\cdot}75$ and for $I/I_0 = 0{\cdot}50$, except for a few cases, corresponding to low temperatures, in which the resolution at $I/I_0 = 0{\cdot}50$ was insufficient.

TABLE I

T ° C.	n atoms/c.c.	z Tube Length (cm.)	I/I_0	λ 7665 ($f = 2/3$)		λ 7699 ($f = 1/3$)	
				$\Delta\lambda$	B	$\Delta\lambda$	B
173	$0{\cdot}528 \times 10^{14}$	64	0·75	0·292	$1{\cdot}17 \times 10^{-17}$	0·200	$1{\cdot}17 \times 10^{-17}$
175	0·582	64	0·75	0·294	1·00	0·194	0·92
			0·50	0·193	1·08	...	...
176	0·609	64	0·75	0·305	1·02	0·202	0·90
			0·50	0·192	0·98	...	...
177	0·638	64	0·75	0·324	1·10	0·221	1·06
			0·50	0·214	1·16	0·143	1·06
179	0·700	64	0·75	0·315	0·96	0·228	1·07
			0·50	0·194	0·88	0·134	0·88
181	0·773	64	0·75	0·337	0·99	0·242	1·03
			0·50	0·216	0·98	0·148	0·99
182	0·804	64	0·75	0·382	1·32	0·271	1·23
			0·50	0·237	1·15	0·161	1·07
183	0·840	64	0·75	0·400	1·29	0·286	1·29
			0·50	0·231	1·06	0·146	0·90
185	0·923	64	0·75	0·454	1·51	0·312	1·43
			0·50	0·282	1·40	0·183	1·17

* *Loc. cit.*

T ° C.	n atoms/c.c.	z Tube Length (cm.)	I/I_0	λ 7665 ($f=2/3$)		λ 7699 ($f=1/3$)	
				$\Delta\lambda$	B	$\Delta\lambda$	B
186	0.964×10^{14}	64	0·75	0·437	1.34×10^{-17}	0·307	1.34×10^{-17}
			0·50	0·273	1·36	0·184	1·16
192	1·26	21·3	0·75	0·34	1·90	0·24	1·88
			0·50	0·21	1·73	0·14	1·56
194	1·37	64	0·75	0·65	2·10	0·38	1·44
			0·50	0·39	1·64	0·21	1·01
198	1·65	64	0·75	0·80	2·6	0·54	2·4
			0·50	0·47	2·2	0·31	1·9
201	1·84	21·3	0·75	0·52	3·0	0·35	2·7
			0·50	0·30	2·4	0·19	2·0
203	2·01	64	0·75	0·92	2·8	0·59	2·4
			0·50	0·58	2·7	0·37	2·3
204	2·09	21·3	0·75	0·53	2·7	0·37	2·6
			0·50	0·33	2·5	0·22	2·3
211	2·80	64	0·75	1·30	4·1	0·80	3·2
			0·50	0·83	4·0	0·51	2·9
213	3·01	21·3	0·75	0·77	4·0	0·50	3·3
			0·50	0·50	4·0	0·32	3·2
220	4·05	64	0·75	1·70	4·8	1·12	4·2
			0·50	1·07	4·6	0·69	3·8

The range of temperatures in Table I is about the greatest range for which the absorption lines could be satisfactorily examined in this investigation; at temperatures below 173° C. the detail of the lines was insufficiently resolved and at temperatures above 220° C. absorption bands caused trouble.

It is estimated that the possible experimental error in the determination of the quantity B is about 10 per cent. Bearing this in mind, it will be observed from Table I that the value of B is independent of the number of atoms per c.c. for values of n less than about 0.80×10^{14}. For such densities the average value of B is, for λ 7665, 1.03×10^{-17} and, for λ 7699, 1.01×10^{-17}, as compared with the theoretical values, 0.97×10^{-17} and 0.98×10^{-17} respectively.

For values of n greater than 0.80×10^{14} the values of B increase as n increases and, moreover, the values of B for λ 7665 become appreciably greater than those for λ 7699. These facts are shown in fig. 3 where, for both lines, the values of B at $I/I_0 = 0.75$ have been plotted against the values of $\log_{10} n$.

No asymmetry of the broadened lines was observed.

Discussion of the Results

Within the limits of experimental error, for both lines the values of B for various values of the intensity, I, are in agreement with the theoretical values for numbers of atoms per c.c. less than $0{\cdot}80 \times 10^{14}$. This observation represents a verification of the classical theory of line width.

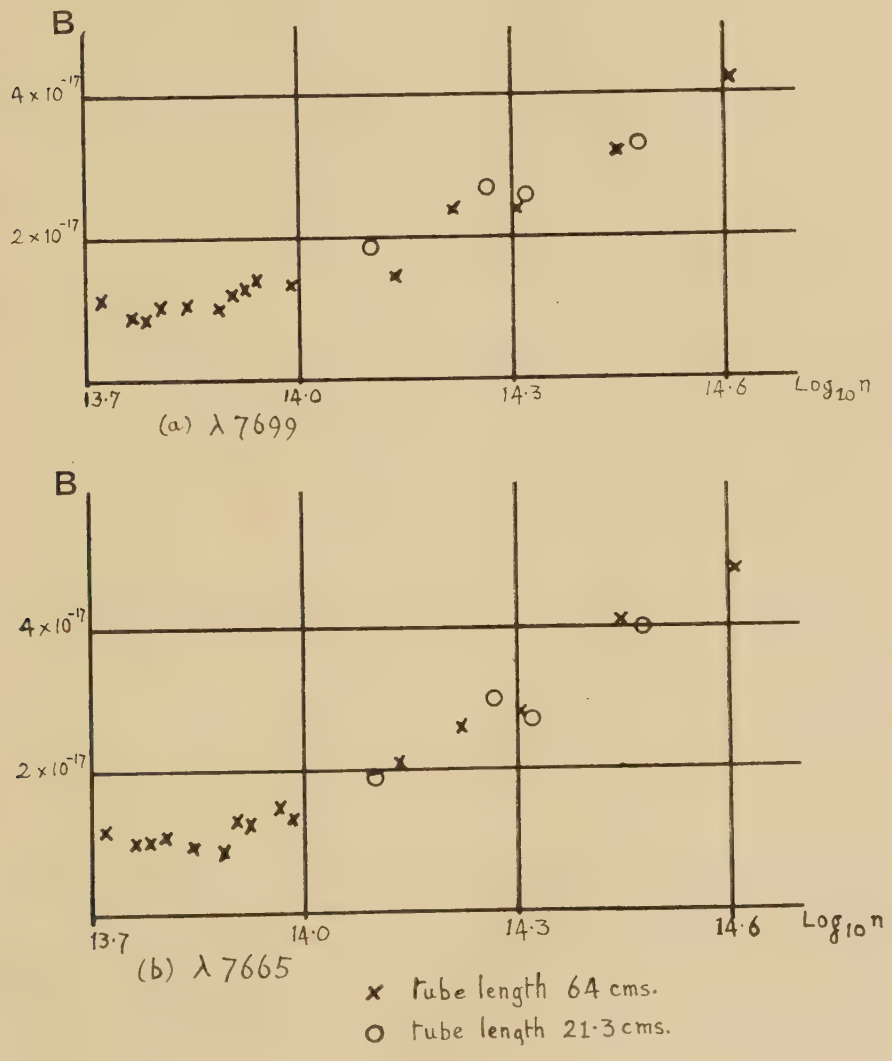

FIG. 3.

In fig. 3 the circles indicate tube lengths of 21·3 cm. and the crosses tube lengths of 64 cm. The fact that these points lie roughly on the same curve is a further verification of the theoretical dependence of line width upon abundance of atoms, *i.e.* that the half-width, $\Delta\lambda$, at any value of I/I_0 is proportional to the square root of the number of atoms in the line of sight.

The departure of both lines from their theoretical widths takes place

at $n = 0{\cdot}80 \times 10^{14}$ atoms per c.c. (temperature = 182° C.). Korff * found that for the sodium D lines the broadening began at $n = 0{\cdot}61 \times 10^{14}$ atoms per c.c. The accepted explanation of this type of broadening is that the higher atomic levels are perturbed during collisions, so that broadening is observed when the atoms are sufficiently abundant for collisions to take place during the lifetime of the excited state.

The comparatively close agreement between the values of B for the two lines before pressure broadening begins supports the theoretical assumption that the f values of the two lines are in the ratio 1 : 2. For the pressure-broadened lines the values of B for λ 7665 are greater than those for λ 7699, the ratio increasing as n increases. This does not necessarily indicate that the f values have changed. A more probable interpretation is that at a given pressure the effect of collisions upon the state $2p_{\frac{3}{2}}$ is greater than that upon the state $2p_{\frac{1}{2}}$.

There appears to be some uncertainty regarding the vapour-pressure data for potassium. Besides that of Weiler,† the results of which have been used here, other recent investigations regarding potassium vapour-pressures are those of Edmondson and Egerton,‡ Mayer,§ and Killian.‖ Of the four investigations, those of Edmondson and Egerton and of Weiler are the only ones in which the ranges of temperature include the temperatures of the present experiments ; and the formula given by Edmondson and Egerton gives vapour-pressures (and hence values of n) about 30 per cent. lower than those given by Weiler's formula. However, at lower temperatures included in the ranges of all four investigations, the results given by Mayer and Killian are in better agreement with those of Weiler, being respectively 3 per cent. and 7 per cent. higher than his, while those of Edmondson and Egerton are still 30 per cent. lower. This seems sufficient reason for using Weiler's formula rather than that of Edmondson and Egerton. If, however, the latter were used, the values of B in the present investigation would be about 35 per cent. higher than the theoretical values.

Summary

The contours of the resonance lines of potassium, λ 7665 and λ 7699, have been examined in absorption by a method of photographic photometry, using a 10-foot concave grating in the first and second orders. The results verify the classical dispersion theory of line width for numbers of atoms per c.c. less than $0{\cdot}80 \times 10^{14}$. For greater atomic densities the lines are broadened beyond their theoretical widths, and the theoretical relation between the widths of the two lines no longer holds.

In conclusion, the writer wishes to acknowledge with thanks the kind interest and helpful criticisms of Professor A. Fowler, F.R.S., in whose laboratory this work was carried out.

Imperial College of Science,
London.

* *Loc. cit.* † *Loc. cit.* ‡ *Proc. Roy. Soc.*, A, **113**, 530, 1927.
§ *Zeit. f. Phys.*, **67**, 261, 1931. ‖ *Phys. Rev.*, **27**, 587, 1926.

THE LUMINOSITIES OF K STARS: A REPLY TO DR. STRÖMBERG'S CRITICISM.

L. Gratton, D.Sc.

(Communicated by W. M. Smart)

A paper by G. Strömberg in *M.N.*, **94**, 68, 1933, contains a criticism of my note on the luminosities of K stars published in *B.A.N.*, 248.* A short answer to Strömberg's criticism seems to be appropriate.

1. I agree with Strömberg that there is no great advantage in taking into account the ellipsoidal character of the distribution of stellar velocities. The asymmetry of high velocities is accounted for in Strömberg's method † as well as in mine, so that little or no difference may arise from this.

2. The use of the logarithms of v and τ instead of the natural values is not questionable from a merely theoretical point of view. I wish only to observe that there is some danger in this; for instance, Strömberg divides the inverval between $-1{\cdot}0$ and $-4{\cdot}0$ of his quantity x_2 into 30 parts. If we take stars of, say, 5th magnitude, this is equivalent to dividing the interval between $|\,0{\cdot}010\,|$ and $|\,0{\cdot}000\,|$ of v in the same number of parts. This is possible because x_2 depends also on the apparent magnitudes, but it is clear that such a division is quite illusory so far as the dynamical variables are concerned.

Using the natural values I could quite naturally discriminate between negative and positive values of v, a factor of importance in showing the true character of the distribution of this quantity. This is perhaps the most important difference between the two methods, a slight improvement of mine with respect to Strömberg's.

3. When comparing the luminosity curves derived by Strömberg and by myself, of course, I examined the difference which arises from my using only stars between $5^{m}{\cdot}0$ and $5^{m}{\cdot}8$. Using Oort's factors in order to take into account the decrease of star density with the distance from the Sun, I found the correcting factors so little different from unity that it was quite useless to consider them.

4. A rather unsatisfactory feature of Strömberg's work is the simultaneous use of two spectral classifications. Putting two stars at the same time into two spectral classes increases illusorily the material, which is not without danger when dealing with frequency curves.

5. I believe it much better to solve such equations as are common in statistical astronomy by trial and error instead of using a purely numerical

* See also *Mem. Soc. Astr. It.*, **7**, 239–257 and 281–301, 1933.

† G. Strömberg, *Mt. Wilson Contr.*, 395, 410, 411, 418; *Ap. J.*, **71**, 163; **72**, 111 and 117; and **73**, 40, 1930–31.

method. This is the only way to get quickly a good result. Of course it may be that the computer is influenced by his preconceived ideas about the result, although nobody would say so. Yet I do not know whether this is worse than puzzling results, like finding negative frequencies, such as those which are obtained by entirely numerical solutions. In my case, after the error curve, my second trial was the very curve of Strömberg, which I found in disagreement with the data. So that my curve is almost surely an improvement with respect to Strömberg's.

6. As it is acknowledged by Strömberg himself, nothing can be said by our statistical methods about the "dips" on either side of the group of normal K giants. Such dips as these are probably illusory, due to the fact that Strömberg gives his result in very great detail, greater perhaps than what is allowed by his method.*

Generally the true statistical functions, viz. the curves we obtain by counting directly the individuals, which have a given character among the totality considered, are rather irregular; of course, when dealing with the characters of importance of the distribution, the small irregularities must be smoothed out. How much is more or less a question of personal taste, and it greatly depends on the accuracy of the counting. In our case we must not forget that our luminosity curves are derived by means of indirect methods like Strömberg's and mine; the chance of finding spurious irregularities is thus rather great. It is very probable that there is really a small group of stars of very high luminosities in each spectral class (supergiants), but whether their luminosities are all grouped together or scattered over a large interval is quite another question.

But there is another difference between Strömberg's result and mine, which Strömberg seems to have overlooked. The dispersion of the distribution is about $1^{M}\cdot1$ in my case and only $0^{M}\cdot5$ in Strömberg's. Now the dispersion is a character of a frequency curve of the highest importance and it is rather difficult to "adjust" it, because it comes almost at first from the data. My belief is that such a difference cannot be explained by the lack of data. The maximum of Strömberg's curve is almost surely too sharp; a dispersion of at least about $1^{M}\cdot0$ seems to be required by the observations. Incidentally, it may be noted that Strömberg derives from trigonometric parallaxes † a dispersion of more than one magnitude in much better agreement with my result than with his own.

7. Finally, I did not conclude, as Strömberg says, that there is no gap in the luminosity function between giants and dwarfs; I merely suggested that there might not be. My luminosity function is derived from trigonometric parallaxes as well as from radial velocities and proper motions; the agreement between the two methods makes it probable that we have there a rather good approximation. But, as it is possible to see from my figures, the uncertainty of the result is very great. According to Strömberg the deficiency of stars of intermediate luminosity would be found between $M = +4\cdot0$ and $+5\cdot0$. This is what we obtain from stars brighter than

* See also Öpik, *Harv. Circ.*, 381.

† Strömberg, *Ap. J.*, **78**, 178; *Mt. Wilson Contr.*, 473, 1933.

a given apparent magnitude without applying any correction for selection. We get a very different result if we consider the luminosity curve per unit volume. Here the minimum lies according to Oort, from Strömberg's data, at about $M = +1{\cdot}5$ and according to van Rhijn between $M = +2{\cdot}5$ and $3{\cdot}5$ approximately. As a matter of fact, two points in my computed curve between $M = +4{\cdot}0$ and $+5{\cdot}0$ lie rather below the adopted curve, but these are the very points for which the effect of the selection of the observing lists is the greatest, as it is possible to see from the great probable errors. Another point in the same interval and with much smaller probable error lies above the curve.

A general belief is that stars in Russell's diagram are distributed along the two branches of dwarfs and giants with a deficiency in the middle. I believe that this is by no means proved, and that astrophysicists must not forget that a gapped curve fits the observations as well as an ungapped one. As the real luminosity curve is doubtless different on different parts of the galactic system, it is possible that both curves are present at the same time. It is perhaps interesting to note that we have in the galactic clusters examples of both types of luminosity curves.

The suggestion is rather tempting that here we are in presence of two "races" of stars which differ by the form of the luminosity function. If this is true, my luminosity curve merely indicates that the majority of the stars belongs to the race with ungapped luminosity curve.* But, as I concluded in my quoted paper, my result and all the other ones hitherto obtained are too uncertain to allow any definite conclusion. At present the best is perhaps to consider both types of luminosity function as equally possible and to wait for more data or more refined computations.

THE MAGNETIC FIELD OF SUNSPOTS.

Sir Joseph Larmor, F.R.S.

In *M.N.* for 1933 November (pp. 39–48) there is a paper by Dr. T. G. Cowling on "The Magnetic Field of Sunspots." The Summary appended to it is brief and reads as follows :—

"The theory proposed by Sir Joseph Larmor, that the magnetic field of a sunspot is maintained by the currents it induces in moving matter, is examined and shown to be faulty : the same result also applies for the similar theory of the maintenance of the general field of Earth and Sun. The possibility that the sunspot field may arise as a disturbance in the general field is examined, and it is shown that several of the properties of the spot field are explicable on this hypothesis. Observation, however, must ultimately decide on its validity."

* According to Trumpler (*Lick Bull.*, **14**, 154, 1930) the majority of the galactic clusters belongs to the types with very few or no yellow and red giants.

The view that I advanced briefly and tentatively long ago,* which has come to be referred to as, perhaps too precisely, the self-exciting dynamo analogy, is still, so far as I know, the only foundation on which a gaseous body such as the Sun could possess a magnetic field : so that if it is demolished there could be no explanation of the Sun's magnetism even remotely in sight. I am, however, not ready to accept the present adverse decision : and a restatement, not so condensed, perhaps with rather different emphasis, may be permitted.†

Let the diagram represent a conceivable rough scheme of circulation within the fluid mass of the Sun. It expresses flow near the axis from both poles N and S towards the equator, continued by equatorial outward flow, and completed by a return flow toward the poles in the outer regions. This circulation amounts formally to two stout vortex rings, with vanishing apertures, in the N and S hemispheres, the cyclic flow being in meridian

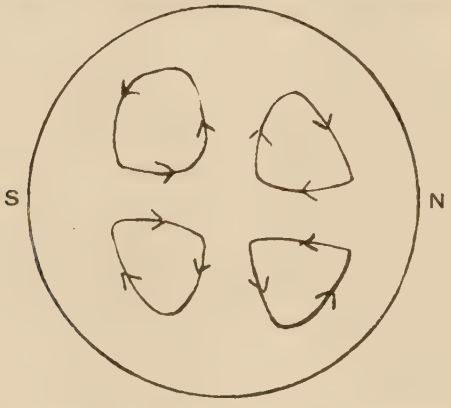

planes. The drift towards the poles may be more concentrated to the outer surface. If the gas is partially ionized, and there happens to be a magnetic field however small, in the direction of the axis, it will exert a force driving the electric ions round the axis, in different ways according to their signs, with velocity increasing continually as the force is permanent, and so will augment the existing axial magnetic field, provided the direction of the vortical circulation is the suitable one, until a limit is imposed by frictional agencies. This suitable direction would be, if I am not mistaken, that described above, with outflow in outer regions toward the poles. The limiting finite field thus produced by this cyclic flow of ions round the axis, from slight accidental beginnings, would be the Sun's magnetic field, as brilliantly determined from its Zeeman effect. An argument that the ionic circulation round the axis could not be intense enough is not effective : for,

* *Brit. Assoc. Report*, 1919, "Math. and Phys. Papers," 2, 612, also more recently, 2, 615, 1928. In writing this sentence I had been deflected from the memory that I had myself (1927, as in the reference above) developed an alternative view, which traced the magnetic field to dynamical interaction between the rotation of the Sun and the outward stream of radiation within it, without need for internal circulation. This correlation of magnetism with rotation was naturally attractive.

† Especially as the writer finds the adverse decision quoted as authoritative in the "Report of the Council," 1934 February (p. 335) of date subsequent to the communication of this paper.

if not ions, then what can take their place? The energy expended by the force driving the ions, and in the steady state dissipated by friction, must come out of the energy of the vortical circulation. This description appears to be, on broad lines, so far as I can at present see, the inevitable conclusion, intricate enough, but one which mathematics could only obscure. It is a kind of converse of the Faraday rotations. The one conceivable detriment might possibly be instability, as in sunspots, though they are relatively small. I observe that the scheme there broached for the much greater magnetic field of sunspots involved flow inward to the axis at one level compensated by flow outward at another level, which makes the flow local and analogously circulatory. This also provided a natural explanation for the feature of the field that at first proved very puzzling, namely, that observation showed it to be confined to a thin disc-shaped region. As before, for N polarity of the spot, which means a negative pole, the suitable direction would appear to be for the outward flow to be the lower one, which corresponds to the weak drift that is observed. But we are still far from finality in these matters.

If the two opposed hemispherical vortices of the illustration above were replaced by one axial vortex filling the whole sphere, the electric flows induced round the axis would be opposite in the two hemispheres, the inducing field arising from an NS magnetization being in one outward in the other inward. Thus the sphere would tend towards becoming a magnet of different type, with two like surface poles compensated by a double pole at the centre, which is not what is observed.*

In elucidation of a remark above which may appear paradoxical, if the circulation is reversed, with the same inducing field, the induced current is reversed, and therefore, if it augmented the field, it will now tend to destroy it. If both circulation and inducing field are reversed, the march of events will not be altered.

* I have learned recently from G. E. Hale that he encounters some unforeseen difficulties in carrying out his delicate project of a detailed magnetic survey of the Sun; also, as may be convenient here to record (*cf.* my remarks in *Nature*, 1934 February 10), he confirms that there is no trace of the Stark effect of an electric field even in high prominences, which might be regarded as well outside the solar surface-charge and so subject to its attraction while the photosphere is not. This absence of electric effect would be accounted for by electric conductance such as would obliterate an electric field within the prominences; which would perhaps require that the density of ions there is greater than that in a spectral tube which shows the Stark effect, notwithstanding theories that estimate extreme rarity. From the other aspect, if a sharp prominence is thus a conductor, its pointed form must make it a source of intense discharge of electricity—that is, of electrons which have no Stark effect—into the region around it. Here also a distinction may possibly demand attention, between quiescent flat prominences in which the adjustments for obliteration of field by conductance have time to be established, and eruptive masses in violent internal motion which would tend to inhibit convective approach to internal electric equilibrium. The cosmic radiation, though slight electrically, could affect bodily charges if it involved ions of the same sign which were driven deep into the body and experienced high resistance to getting out again, for charge would have to accumulate in the outer layer of the body until it produced an outward field of force large enough to make a balance of electric outflow against inflow; but then the charge not being on the surface should reveal itself.

THE DISTRIBUTION OF RADIAL VELOCITIES OF DARK *Hα* MARKINGS NEAR SUNSPOTS.

H. W. Newton.

(Communicated by the Astronomer Royal)

The radial velocities of *Hα* flocculi on the disc have been regularly observed at Greenwich since 1930 with the spectrohelioscope lent by the Mt. Wilson Observatory. These observations show that the distinction in appearance and position on the Sun's surface between the two main classes of dark flocculi is represented by typical distribution of their respective radial velocities. The two classes of dark flocculi * may be described in general terms as follows :—

(1) Markings that tend to avoid sunspots though not the sunspot zones. These flocculi are usually well-defined extensive filaments, though some are diffused patches. Their duration is of the order of days.

(2) Markings associated with sunspots and with the bright flocculi that accompany spots and outlive them. These markings are smaller than those of class (1), and include straight or curved filaments, as well as tiny dense patches. Their duration is usually of the order of hours or minutes.

The respective characteristics of the radial motions of these two classes given by Table I † are as follows :—

(1) Inappreciable or small radial motions generally, but larger velocities are not entirely absent (column (1)).

(2) Frequent large radial motions, although about 30 per cent. of these flocculi have no appreciable velocity (columns (2) *a* and (2) *b*).

The two classes of flocculi described above have their counterpart ‡ at the Sun's limbs, where (1) is represented by the large massive prominences and allied types, and (2) is represented by smaller type prominences of an eruptive nature. But, in at least one respect, there is a discordance (referred to later) between the "plan" picture given on the disc by the spectrohelioscope and the "elevation" picture given by the prominences at the limbs. It may be remarked that observations with the spectrohelioscope show very clearly the occurrence of active flocculi lasting for $\frac{1}{4}$ or $\frac{1}{2}$ hour in the neighbourhood of sunspots.

* See *Memoirs of the Kodaikanal Observatory*, vol. i, pt. ii, by J. and M. A. Evershed (1917); also "The Spectrohelioscope and its Work", by G. E. Hale, *Ap J.*, **70**, 291, 1929.

† Compiled from "Observations of Solar Flocculi made with the Spectrohelioscope", published in the *Greenwich Photoheliographic Results for* 1930–33, and *M.N.*, **91**, 593, 1931 ; **92**, 438, 1932 ; **93**, 168, 1933.

‡ *Kodaikanal Memoir, loc. cit.*

TABLE I

Percentage Frequency of Measured Radial Velocities of Dark Hα *Flocculi, 1930–33*

(1) Not associated with sunspots.
(2) *a*, Associated with sunspots (centre of disc).
(2) *b*, Associated with sunspots (whole disc).
(2) *c*, Associated with bright flocculi : sunspots absent.

Measured Radial Velocity km./sec.	(1)	(2)		
		a	*b*	*c*
0–4	83	32	27	66
5–9	14	7	6	11
10–19	2	5	6	4
20–29	1	17	20	9
30–39	$<\frac{1}{2}$	24	23	7
40–49	0	8	9	1
50–59	0	3	3	1
60–69	0	2	3	0
70–79	0	1	1	1
80–89	0	$<\frac{1}{2}$	$<\frac{1}{2}$	0
90–99	0	0	1	0
$\geqslant$ 100	0	1	1	0
Number of measures	1388	266	572	129

Note.—(i) The probable errors of the tabulated radial velocities are about 2 km./sec. The systematic error for the smallest velocities observed is less than $\frac{1}{2}$ km./sec., as is shown by measures of the Sun's equatorial rotation taken at the limbs.

(ii) In forming columns (2) *a*, *b* and *c*, when different parts of the same flocculus had differing radial velocities, the maximum radial velocity measured for that flocculus has been tabulated. In the case of the flocculi in class (1) this feature of differing velocities within the same flocculus is rarely observed.

(iii) Data for the centre of the disc given in column (2) *a* refer to flocculi within ± 30° of the central meridian and between latitudes ± 30°.

In view of the theoretical researches on the solar chromosphere by E. A. Milne, S. R. Pike, S. Chandrasekhar and others, the observation of radial velocities of absorption markings in areas containing bright flocculi and sunspots is of interest. Referring to the last three columns of Table I, the following features will be noted :—

1. Of the measured radial velocities of dark flocculi associated with areas containing sunspots, those which are appreciable exhibit a pronounced peak in their frequency distribution, with a maximum between 20 and 40 km./sec.*

2. When no attendant sunspot is present in the bright flocculi the large velocities tend to disappear. This fact suggests that the presence of a sunspot is an important factor directly or indirectly in the occurrence of the

* *Note added March* 9.—Dr. S. Chandrasekhar has drawn my attention to his theory of the solar chromosphere discussed in *M.N.*, **94**, 14, 1933, which includes the possibility of the emission of moderately high-speed particles with a limiting vertical velocity of 30 km./sec [equation (48), p. 25, *loc. cit.*].

large radial velocities observed in these regions. The reservation must be made, however, that the majority of these bright areas observed, not containing sunspots, represent the declining phase of sunspot disturbances.

The distribution of the sign of the velocities $\geqslant 5$ km./sec. corresponding to those in column (2) *b* is given in Table II, where − indicates outward motion from the Sun and + inwards. A feature, observed in nearly 30 per cent. of cases when measuring radial velocities of dark flocculi in the general neighbourhood of sunspots, is a progressive difference of velocity within the flocculus itself from one end to the other. The last five lines of Table II give the signs of these differential velocities.

It will be seen that the number of inward velocities observed exceeds those outwards.

TABLE II

Percentage Distribution of Outward and Inward Radial Velocities of Dark Hα Flocculi near Sunspots and Bright Flocculi, 1930–33

Direction of Motion		Percentage		
		−		+
Common velocity outwards (−) or inwards (+).		31		41
Differential velocities	Wholly −	1		
	Wholly +			10
	+ and − equal		1	
	− greater	2		
	+ greater			14
	Total	34	1	65

Reference may be made to the maximum velocities observed at Greenwich during the four years 1930–33. On two occasions outward velocities of 155 km./sec. and 450 km./sec. were observed in connection with dark markings arising from brilliant eruptions of *Hα* flocculi in the vicinity of sunspots. In both cases absorption markings were observed descending with velocities of 105 and 110 km./sec. respectively. Inward velocities of 90 or 100 km./sec. have also been observed on five occasions in connection with dark flocculi flowing into sunspots.

Flocculi moving into Sunspots.—Records of streams of hydrogen moving with high velocity into sunspots are rare on spectroheliograms, but the spectrohelioscope, which is particularly well-adapted to locate large radial velocities, can be successfully employed in observing this type of flocculus. In *Ap. J.* (71, 73, 1930) Dr. Hale gives the results of measures of a number of these dark flocculi observed from 1926 June to September. The maximum inward velocity observed was 115 km./sec. A significant feature is that the inward radial velocity increases as the sunspot is approached. Under good observing conditions the flocculus at its maximum velocity is often seen reduced to a dot at the outer edge of the penumbra of the sunspot.

The present observations at Greenwich record 49 flocculi of this type. This number represents 9 per cent. of the total number of flocculi measured

in sunspot regions. The percentage distribution of their radial velocities at the ends * coterminous with the associated sunspots is given in column (*a*) of Table III. The contribution of these values to column (2) *b* of Table I is given in column (*b*) of Table III.

TABLE III

Percentage Distribution of Maximum Radial Velocities of Dark Hα Flocculi moving into Sunspots

Velocity km./sec.	Percentage Frequency (*a*)	(*b*)	Velocity km./sec.	Percentage Frequency (*a*)	(*b*)
0–9	0	0	50–59	10	0·9
10–19	2	0·2	60–69	15	1·2
20–29	10	0·9	70–79	6	0·5
30–39	39	3·3	80–89	2	0·2
40–49	6	0·5	90–99	8	0·7
			100	2	0·2

The mean inward radial velocity of these 49 flocculi at the boundary of the sunspot is 48 km./sec. The radial velocities corresponding to the far end of the flocculus show a wide range from −41 km./sec. to +46 km./sec., the mean being −3 km./sec. The average distance over which a flocculus was visible (as shown by progressive settings of the line-shifter) is about 50,000 km.

It should be mentioned that two cases have been observed at Greenwich in which the hydrogen appeared to be flowing out of a sunspot.

The short life of this type of flocculus may partly explain their general absence in prominence records. In *Kodaikanal Memoirs* (*loc. cit.*, p. 106), the statement is made that "No case has been found in which prominences were falling into sunspots, but the reverse has several times been observed." A few typical sunspot prominences have been observed, however, both by Hale and Slocum to give velocities downwards towards spots of the same order of magnitude as the radial velocities measured on the disc with the spectrohelioscope. In addition Pettit † has found from measures of "splash" prominences that streamers were flowing into spots with velocities of the order of 30 km./sec.

A rather infrequent but interesting type of dark flocculus, observed at Greenwich in the general neighbourhood of sunspots, appears as a pair of closely adjacent, dense dots or small patches, possessing similar radial velocities but of opposite sign. In a few other cases a single marking was first observed with an outward velocity, which was replaced within a few minutes by an inward velocity of similar magnitude at, or nearly at, the same place on the Sun's disc. The measured velocities are closely grouped about 30–35 km./sec. These flocculi appear to represent narrow arches and jets

* In *Greenwich Photoheliographic Results* these measures are printed in heavy type.

† *Publications of the Yerkes Observatory*, **3**, pt. iv, p. 227.

respectively. There is, obviously, useful work to be done in co-ordinating limb and disc phenomena.

In conclusion it may be remarked that the Greenwich results of radial measures from 1930–33 (representing about 500 hours of observation) give but a sample of the activity presented on the Sun's disc. Yet the samples from each year are so accordant as to suggest that they are representative of solar activity throughout the 11-year cycle.

Royal Observatory, Greenwich:
1934 *February* 28.

REMARKS ON THE GEODESICS OF EXPANDING SPACE-TIME.

G. C. McVittie, Ph.D.

1. It is well known, chiefly from the work of Robertson,* that the metric of space-time can be determined on the basis of Mach's principle alone, without recourse to field equations, provided that space is isotropic and space-time homogeneous. The resulting possible forms for the metric are

$$ds^2 = dt^2 - \frac{e^{\beta(t)}}{c^2}\left\{\frac{dr^2 + r^2(d\theta^2 + \sin^2\theta d\phi^2)}{\left(1 + \frac{kr^2}{4R^2}\right)^2}\right\}, \qquad (1)$$

where k is either $+1$, 0 or -1 and R is the "radius" of space. The further assumption that the paths of individual particles are geodesics in space-time completely determines the mechanics of moving particles. Assuming these two principles we discuss the motions of particles in space-time of type (1), using as our "distance variable" one chosen in accordance with astronomical methods of distance-determination. We show that the clocks on certain moving particles can be synchronised, and we investigate the "statistical system of particles" of Milne's theory † by relativistic methods.

2. *Distance.*—It has been pointed out by Whittaker ‡ that distance from the origin in (1), as determined by the methods at present used by astronomers for finding the distances of the spiral nebulæ, is given by

$$e^{\frac{1}{2}\beta(t)}r\Big/\left(1 + \frac{r^2}{4R^2}\right)^{\frac{1}{2}}, \qquad e^{\frac{1}{2}\beta(t)}r \quad \text{or} \quad e^{\frac{1}{2}\beta(t)}r\Big/\left(1 - \frac{r^2}{4R^2}\right)^{\frac{1}{2}},$$

according as k is $+1$, 0 or -1. At present, however, observations do not extend to sufficient distances to enable us to decide on the value of either

* H. P. Robertson, *Nat. Acad. Sci. Proc.*, **15**, 822–829, 1929.

† E. A. Milne, *Zs. f. Astrophysik*, **6**, 1–96, 1933; *M.N.*, **94**, 3–14, 1933.

‡ E. T. Whittaker, *Roy. Soc. Proc.*, **133** A, 93–105, 1931; H. P. Robertson, "Relativistic Cosmology," *Rev. Mod. Phys.*, **5**, 62–90, Note E.

k or R. All that can be said is that R must certainly be very large. We adopt, therefore, the expression

$$l(t) = e^{\frac{1}{2}\beta(t)} \int \frac{dr}{1 + \frac{kr^2}{4R^2}} \tag{2}$$

for the distance from the origin. This expression differs from the others proposed only in terms involving $1/R^2$, which are therefore negligibly small from the observational point of view. It has the advantage of enabling us to deal with the geodesics of the three cases ($k = +1, 0, -1$) simultaneously.

We remark that Milne,* in a case for which $e^{\beta(t)} = \left(\frac{ct}{R}\right)^2$ and $k = -1$, uses the co-ordinates r_m, t_m for distance and time respectively, where

$$r_m = \frac{ct}{R} \frac{r}{\left(1 - \frac{r^2}{4R^2}\right)}, \qquad t_m = t \frac{(1 + r^2/4R^2)}{(1 - r^2/4R^2)}. \tag{3}$$

3. *Geodesics through the Origin.*—The geodesics of any manifold are, of course, given by the equations

$$\frac{d^2x^\alpha}{ds^2} + \left\{ \begin{matrix} \alpha \\ \mu\nu \end{matrix} \right\} \frac{dx^\mu}{ds} \frac{dx^\nu}{ds} = 0, \tag{4}$$

where the $\left\{ \begin{matrix} \alpha \\ \mu\nu \end{matrix} \right\}$ are the Christoffel symbols for the metric. The radial geodesics through the origin for the metric (1) have the equations

$$\frac{d^2r}{ds^2} - \frac{1}{2} \frac{kr}{R^2(1 + kr^2/4R^2)} \left(\frac{dr}{ds}\right)^2 + \dot{\beta} \frac{dr}{ds} \frac{dt}{ds} = 0, \tag{5}$$

$$\left(\frac{dt}{ds}\right)^2 - \frac{e^{\beta(t)}}{c^2(1 + kr^2/4R^2)^2} \left(\frac{dr}{ds}\right)^2 = 1, \tag{6}$$

where $\dot{\beta} = d\beta/dt$.

An integral of (5) is

$$e^{\beta(t)} \frac{dr}{ds} = K\left(1 + \frac{kr^2}{4R^2}\right), \tag{7}$$

where K is the constant of integration. Transforming to $l(t)$ by (2), we find that (7) and (6) become

$$\frac{dl}{ds} = \frac{l\dot{\beta}}{2} \frac{dt}{ds} + Ke^{-\frac{1}{2}\beta}, \tag{8}$$

$$\left(\frac{dt}{ds}\right)^2 = 1 + \frac{K^2}{c^2} e^{-\beta}. \tag{9}$$

Hence finally (8) and (9) give

$$\frac{dl}{dt} = \frac{l\dot{\beta}}{2} + \frac{Ke^{-\frac{1}{2}\beta}}{\left(1 + \frac{K^2}{c^2} e^{-\beta}\right)^{\frac{1}{2}}}. \tag{10}$$

* W. O. Kermack and W. H. McCrea, *M.N.*, **93**, 519–529, 1933; H. P. Robertson, *Zs. f. Astrophysik*, **7**, 153–166, 1933.

Whence by differentiation

$$\frac{d^2l}{dt^2}=\frac{l}{2}\left(\ddot{\beta}+\frac{\dot{\beta}^2}{2}\right)+\frac{K^3e^{-\frac{3}{2}\beta}\dot{\beta}}{2c^2\left(1+\frac{K^2}{c^2}e^{-\beta}\right)^{\frac{3}{2}}}. \tag{11}$$

The equation (11) is to be regarded as the equation of motion of the particle. It is clear that the constant K depends on the proper-motion of the particle considered and is not necessarily zero.

The first integrals of the null-geodesics which pass through the origin are easily obtained from (1) by putting $ds=0$. In terms of l we have, therefore, for the velocity of a light-ray

$$\frac{dl}{dt}=\pm c+\frac{l\dot{\beta}}{2}, \tag{12}$$

according as the ray is receding from or approaching the origin.

4. *Synchronisation of Clocks. Cosmic Time.*—A physical meaning can be attached * to the time-variable t by considering the motion of the matter as a whole in the space-time frame (1). Milne,† however, has put forward the objection that the time so defined is not kept by the clock of any observer. We shall now show that the clocks of certain observers in the field (1) do keep time t, and we shall also show how their clocks can be synchronised by means of light-signals so that events can be simultaneous for them.

We recall the familiar meaning attached to the terms "synchronisation" and "simultaneity" in an ordinary Minkowski space-time frame whose line-element is

$$ds^2=dt^2-\frac{dx^2+dy^2+dz^2}{c^2}.$$

Two observers A and B, at some arbitrary distance apart, at rest with respect to each other and to this frame, clearly have the same proper-time ds (or dt). To synchronise their clocks, let A, at time t_0 by his clock, send out a light-signal towards B, who records its arrival at time t_B by his clock. The signal is immediately reflected to A, who records it at time t_2. On communicating this information to B, the latter sets his clock so that the reading t_B on it corresponds to

$$t_B=\frac{t_0+t_2}{2}. \tag{13}$$

Since the velocity of light is assumed by A to be constant, he also supposes that the instant $\frac{1}{2}(t_0+t_2)$ on his clock is that of the arrival of the light-signal at B. The value of this method of synchronisation lies, of course, in the fact that it is reciprocal between A and B. These two observers have thus established a "cosmic time," kept by each of their clocks, in terms of which events can be simultaneous for both of them.

* H. P. Robertson, "Relativistic Cosmology," *Rev. Mod. Phys.*, 5, 62–90, § 2, 1933.

† E. A. Milne, *Zs. f. Astrophysik*, 7, 180–187, 1933.

We now ask what happens when A and B are in a space-time frame (1) instead of in Minkowski space-time. For simplicity we shall illustrate the procedure by using the line-element brought into prominence by Milne's work,* viz.

$$ds^2 = dt^2 - \left(\frac{ct}{R}\right)^2 \frac{1}{c^2}\left\{\frac{dr^2 + r^2(d\theta^2 + \sin^2\theta d\phi^2)}{\left(1 - \frac{r^2}{4R^2}\right)^2}\right\}. \tag{14}$$

In the formulæ of the previous paragraph we have now

$$\beta = 2\log t - 2\log\frac{c}{R}, \tag{15}$$

and we shall now write, in the formulæ obtained from (8), (9), (10) and (11), K instead of KR/c.

Let A be at rest at the origin. Then by (10) $K = 0$ for him, and so by (9) t is his proper-time. Let him emit a light-signal at time t_0, towards B who is at some arbitrary distance, l_1, from him. The equation of motion of the signal is, by (12) and (15),

$$\frac{dl}{dt} = c + \frac{l}{t},$$

whence

$$l = ct(\log t - \log t_0), \tag{16}$$

since $l = 0$ when $t = t_0$. Now B is at l_1 at time t_B by his own clock and at time t_1 by A's clock. The signal, on reaching B, is immediately reflected and travels towards A with velocity

$$\frac{dl}{dt} = -c + \frac{l}{t}.$$

Hence on the return journey

$$l = t\left\{\frac{l_1 + ct_1\log t_1}{t_1} - c\log t\right\}.$$

It therefore reaches A again at time t_2 by A's clock, where

$$c\log t_2 = \frac{l_1 + ct_1\log t_1}{t_1}. \tag{17}$$

But by (16) $l_1 = ct_1(\log t_1 - \log t_0)$. Hence eliminating l_1 from (17) we have

$$t_1^2 = t_0 t_2. \tag{18}$$

This then is the time, t_1, which A assigns for the time arrival of the signal at B. On communicating this result to B, the latter can set his clock so that its reading t_B equals t_1. But, before we can be sure that this synchronisation

* W. O. Kermack and W. H. McCrea, *loc. cit.* We have transformed from χ to r by $R\sinh\chi = \frac{r}{1 - r^2/4R^2}$.

is more than momentary, we must show that B's proper-time is the same as A's, and that B has the same rule (18) for clock-setting as A has.

Now B's proper-time, since he is at some arbitrary distance from the origin and is moving with arbitrary velocity, is s, given by (9) and (15), in terms of A's proper-time, t, as

$$\frac{K^2}{c^2}+t^2=s^2, \tag{19}$$

where an unessential constant of integration has been put equal to zero. Hence

$$\beta=\log\left(s^2-\frac{K^2}{c^2}\right)-2\log\frac{c}{R}. \tag{20}$$

Let B be at l_0 at time s_0 by his own reckoning. Hence by (8), (19) and (20) his position at any subsequent time, s, is

$$l=\left(a+\frac{c}{2}\log\sigma\right)\left(s^2-\frac{K^2}{c^2}\right)^{\frac{1}{2}}, \tag{21}$$

where $\sigma=\left(s-\frac{K}{c}\right)\Big/\left(s+\frac{K}{c}\right)$ and a is a constant of integration given by

$$a=\frac{l_0}{\left(s_0^2-\frac{K^2}{c^2}\right)^{\frac{1}{2}}}-\frac{c}{2}\log\sigma_0. \tag{22}$$

Let B emit a signal towards A at time s_0. By (12), (9), (20) we have, for the motion of the signal,

$$l=\left\{b_1-\frac{c}{2}\log\left(s^2-\frac{K^2}{c^2}\right)\right\}\left(s^2-\frac{K^2}{c^2}\right)^{\frac{1}{2}},$$

where

$$b_1=\frac{l_0}{\left(s_0^2-\frac{K^2}{c^2}\right)^{\frac{1}{2}}}+\frac{c}{2}\log\left(s_0^2-\frac{K^2}{c^2}\right). \tag{23}$$

The signal arrives at A at time s_1 by B's reckoning, where

$$0=b_1-\frac{c}{2}\log\left(s_1^2-\frac{K^2}{c^2}\right). \tag{24}$$

It then returns to B, its position at time s being

$$l=\left\{\frac{c}{2}\log\left(s^2-\frac{K^2}{c^2}\right)-b_1\right\}\left(s^2-\frac{K^2}{c^2}\right)^{\frac{1}{2}}, \tag{25}$$

since $l=0$ when $s=s_1$. It overtakes B at time s_2, where by (21) and (25)

$$a+\frac{c}{2}\log\sigma_2=\frac{c}{2}\log\left(s_2^2-\frac{K^2}{c^2}\right)-b_1.$$

Hence by (22), (23), (24) we get, after some rearranging,

$$s_1^2-\frac{K^2}{c^2}=\left\{\left(s_0^2-\frac{K^2}{c^2}\right)\left(s_2^2-\frac{K^2}{c^2}\right)\frac{\sigma_0}{\sigma_2}\right\}^{\frac{1}{2}}. \tag{26}$$

It is therefore clear that B does not, in general, have either the same proper-time as A or the same rule of synchronisation. But if $K=0$, the proper-times are the same for both observers [by (9)], and (26) is the same function of the "s" as (18) is of the "t." In other words, provided that the velocity of B is l/t in the position l at time t as seen by A, then B will have the same proper-time as A and their clocks can be synchronised by the conventional rule that $t_B = t_1 = \sqrt{t_2 t_0}$.

At first sight this result might appear to contradict the result that two observers in relative motion in Minkowski space-time have neither the same proper-time nor can they synchronise their clocks. But these statements are only true provided the Lorentz transformation holds between the co-ordinate systems of the observers; in other words, provided the velocity of light has the same constant value for both observers and $ds^2 = dt^2 - \frac{1}{c^2}(dx^2+dy^2+dz^2)$. Neither of these conditions holds in the case (14), when t, l are used as co-ordinates, nor do they hold in any co-ordinate-system for the general case (1). In fact, the observers moving with velocity l/t in (14) do not correspond to the moving observers contemplated by the Lorentz transformation in Minkowski space-time, but to the observers at rest whose rule of synchronisation is (13).

We have dealt in detail with the case (14), as the rule of synchronisation is particularly simple. Given the function $\beta(t)$ explicitly in terms of t, the procedure indicated above will give the corresponding synchronisation rule in the general case (1). In each space-time the synchronised clocks are attached to particles whose velocity is $\frac{1}{2}l\dot{\beta}$, when the particle is at distance l from the origin at time t. We call these the "fundamental" particles, following Milne, who studied in particular the fundamental particles of the case (14). In general, a fundamental particle is, by (11), subject to an acceleration $\frac{1}{2}\left(\ddot{\beta}+\frac{\dot{\beta}^2}{2}\right)l$. For the metric (14), this acceleration is always zero owing to the special value (15) of β.

5. *Non-fundamental Particles.*—In Milne's theory,* in addition to the fundamental particles, there occur other particles forming his "statistical system of particles," which are accelerated and which tend to cluster around the fundamental particles. Milne determines the accelerations to within an arbitrary function, ψ, which depends on the distribution of the particles. For a particle near the origin he finds, by a process of averaging and a manipulation of an infinity in ψ of which he does not give full details, the asymptotic formula for the acceleration

$$f_{r,0} \sim \frac{r_m}{t_m^2}\left\{-1+\frac{C}{A}\left(2\log\frac{ct_m}{r_m}\right)^{\frac{1}{2}}\right\}, \qquad (27)$$

the particle being momentarily at rest. We discuss the relation of these "statistical particles" of Milne to the non-fundamental particles of the space-time (14), *i.e.* to those for which $K\neq 0$ in equations (8) to (11).

* E. A. Milne, *M.N.*, **94**, 3–14, 1933.

The acceleration of such a particle is easily calculated in terms of its velocity. For in (14), $\ddot{\beta}+\frac{\dot{\beta}^2}{2}=0$. Hence by (10) and (11) we have

$$\frac{d^2l}{dt^2}=\frac{1}{c^2t}\left(\frac{dl}{dt}-\frac{l}{t}\right)^3, \tag{28}$$

where now, of course, $dl/dt \neq l/t$. Thus the acceleration depends only on the velocity of the particle when its position at time t is given. Again, it is obvious from (10) and (11), with $e^{\beta(t)}=(ct/R)^2$ that the particle will eventually have approximately the same velocity and acceleration as some one of the fundamental particles. In other words, non-fundamental particles will appear to "cluster" round the fundamental particles and to move with them. Thus our non-fundamental particles possess the qualitative properties of Milne's statistical system. But the acceleration laws do not agree. For a non-fundamental particle momentarily at rest we have by (28)

$$\frac{d^2l}{dt^2}=-\frac{l^3}{c^2t^4}. \tag{29}$$

If the particle is near the origin, we have, by (3), that $r_m \doteqdot l$, $t_m \doteqdot t$. Hence we obtain

$$f_{r,0}{}' = -\frac{{r_m}^3}{c^2{t_m}^4}, \tag{30}$$

which differs from (27). It should be remarked that formula (29) is also obtained if the motion of non-fundamental particles whose paths pass near to the origin, but do not go through it, is considered. Since Milne's theory differs essentially from the relativistic one in the use of different co-ordinates, it is difficult to believe that our non-fundamental particles are any other than the particles of Milne's statistical system. We conclude that the discrepancy between formulæ (27) and (30) is to be traced to Milne's new method * of calculating the acceleration of a particle in virtue of which he establishes formula (27).

The discovery of these "statistical" particles has led Milne † to conclude that the values of the cosmical constant, λ, and of the gravitational constant, G, depend on the accelerations of these particles, through formula (27). His argument is that λ and G are introduced in order to describe these accelerations in terms of a "cosmical repulsive force" (involving λ) and a "gravitational attraction" (involving G). This argument appears to be fallacious when λ and G have the meanings attached to them in general relativity. For, reverting to the general case (1) and to equations (10) and (11), it is known ‡ that "cosmical repulsive force" and "gravitational attraction" enter into the accelerations of particles through the term § $\frac{l}{2}\left(\ddot{\beta}+\frac{\dot{\beta}^2}{2}\right)$ of formula (1). But "statistical" particles possess still another contribution to their accelerations, *i.e.* are acted on by

* E. A. Milne, *loc. cit.*, p. 5. † E. A. Milne, *loc. cit.*

‡ See, *e.g.*, W. de Sitter, *Univ. of Calif. Publ. in Maths.*, 2, No. 8, 143–196, § 22.

§ This term also includes the "gravitational" effect of the pressure.

still a third "force," depending on their velocities and represented by the last term of (11). In Milne's case (14), where $\ddot{\beta}+\frac{\dot{\beta}^2}{2}=0$, so that "cosmical repulsion" and "gravitational attraction" are absent, it is only this latter type of "force" that can be said to be operative. In other words, neither λ nor G are in any way involved in the formulæ of Milne's "statistical" system.

The University,
Edinburgh.

PRELIMINARY VALUES OF THE VARIATION OF LATITUDE AT GREENWICH IN 1933

(Communicated by the Astronomer Royal)

This paper contains the preliminary values of the latitude variation derived from observations made with the Cookson floating telescope.

The star places used were those derived from the final discussion of the observations for the period 1919–1926. The number of plates obtained was about the average, but owing to weather conditions there was only a small number of plates in February, November and December.

The following table gives the value of the variation (mean latitude *minus* observed latitude) :—

Date	Variation	Number of Pairs
	″	
1933·033	+·034	100
·161	+·192	84
·230	+·165	99
·294	+·245	90
·390	+·125	100
·459	+·182	87
·539	+·032	93
·620	−·065	92
·684	−·125	90
·780	−·086	93
·918	−·061	80
1934·030	+·071	99

From a curve drawn to represent the observed results as closely as possible, the following corrections, applicable to observed north polar distances, were derived :—

	″		″
1933·0	+·05	1933·6	−·03
33·1	+·12	33·7	−·10
33·2	+·18	33·8	−·09
33·3	+·20	33·9	−·03
33·4	+·18	1934·0	+·04
1933·5	+·08		

Royal Observatory, Greenwich :
1934 *February.*

OBSERVATIONS OF OCCULTATIONS MADE AT TEDDINGTON DURING 1933.

John L. Haughton, D.Sc.

The occultations were observed with a 4-inch refractor mounted on the roof of the Metallurgy Department of the National Physical Laboratory. The co-ordinates of the instrument, determined from a 1-inch Ordnance Survey map, are :—

$$\phi = \text{N. } 51^\circ\ 25'\ 3''{\cdot}6$$
$$\lambda = \text{W. } 0^\circ\ 20'\ 6''{\cdot}6.$$

The time was obtained from a seconds clock mounted in the Metallurgy Department of the Laboratory and checked daily from the B.B.C. time-signals. While the rate of this clock drifted in a curious manner, it never appeared to change suddenly, and it was checked so frequently that any error that it introduced was never as great as 0·5 seconds, and was generally much less. The occultations were observed by means of a split seconds stop-watch, which was started from the clock about 10 minutes before the occultation, one hand stopped when the disappearance or reappearance was observed, and the other hand compared with the clock within 2 minutes of the occultation in order to check the stop-watch.

In all there were 26 occasions when weather conditions made it worth while attempting to observe, but only 13 on which results were obtained. In some cases a correction has been applied to these results when it was considered that the observation was late, but no systematic correction for personal equation has been made.

No.	Date	Star	Mag.	Phase	G.C.T. h	m	s	Prob. Error seconds	Remarks
4	Apr. 4	BD. 24° 1755	6·8	D	1	19	0·0	± 1·0	Slight haze.
7	30	A Geminorum	5·1	D	23	30	44·4	...	D very sharp.
12	Aug. 12	ϵ Arietis	4·6	R	22	49	22·5	± 0·5	R very sharp.
13	Sept. 3	μ Capricorni	5·2	D	2	3	45·0	?	Slight haze. Very uncertain.
15	Oct. 13	η Cancri	5·5	R	1	0	39·5	± 0·5	R very sharp.
16	27	*e* Aquarii	5·4	D	23	22	9·5	± 0·5	D very sharp.
19	Nov. 3	*q* Tauri	4·3	D	19	14	7·0	± 13·0	See below.
20	3	20 Tauri	4·1	D	20	20	33·5	± 2·0	Cloudy. Doubtful.
21	3	17 Tauri	3·8	R	20	41	19·4	?	Probably several seconds late. See below.
22	3	16 Tauri	5·4	R	20	54	0·0	± 2·0	See below.
23	3	*q* Tauri	4·3	R	21	8	17·3	± 2·0	,,
24	3	20 Tauri	4·1	R	21	27	1·2	± 2·0	,,
26	Dec. 6	μ Cancri	5·5	R	5	55	50·9	± 0·5	Slight haze. R very sharp.

No. 19. Clouds passing continuously. Star visible at $19^h\ 13^m\ 55^s$, had disappeared at $19^h\ 14^m\ 20^s$.

Nos. 21 to 24 were reappearances very near the terminator, and in the glare of the Moon it is possible that the stars may have reappeared some seconds before they were seen.

No. 21. J. Cartland (ϕ = N. 51° 24′ ; λ = W. 0° 13′ 45″) reports R at $20^h\ 41^m\ 10^s \pm 1{\cdot}0^s$.

Teddington :
1934 *January* 2.

OCCULTATIONS OF STARS BY THE MOON, OBSERVED AT TOMSK UNIVERSITY OBSERVATORY DURING THE YEAR 1933.

N. Goryatscheff.

($\phi = 56°\ 28'\ 07''$; $l = 5^h\ 39^m\ 47^s{\cdot}1$ East of Greenwich)

Date (G.C.T.) 1933	Local Sidereal Time	Star	Mag.	Δt
	h m s			s
III 1·617532	7 04 51·1	B.D. +18° 305	8·1	+ 6·2
III 2·609427	6 57 05·4	B.D. +22° 457	7·7	+ 2·7
III 3·679609	8 42 22·3	B.D. +25° 678	7·5	+ 5·5
III 5·559675	5 57 04·7	406 B. Tauri	5·6	+ 6·1
III 30·561740	7 38 37·5	21 Tauri	5·8	+ 6·2
III 30·566010	7 44 47·4	22 Tauri	6·5	+ 7·5
IV 1·628444	9 22 49·6	B.D. +27° 799	8·1	+ 1·4
IV 1·654083	9 59 50·9	107 B. Aurigæ	6·5	+ 5·1
IV 1·675864	10 31 17·9	B.D. +27° 811	8·5	+ 6·8
IV 30·709672	13 14 27·0	B.D. +25° 1594	7·0	+10·3
IV 30·712442	13 18 27·0	B.D. +25° 1595	7·7	+ 9·5
IV 30·713615	13 20 08·6	B.D. +25° 1596	8·6	+10·6
V 3·781446	15 09 54·9	ψ Leonis	5·6	+ 8·0
V 28·699082	14 49 33·1	B.D. +24° 1769	7·8	+16·3
IX 12·701433	21 54 48·4	B.D. +27° 923	7·7	+ 5·6
IX 12·754379	23 11 15·5	B.D. +27° 943	7·0	+11·3

Apparent Places of Occulted Stars, 1933

Star	α	δ	Authority
	h m s	° ′ ″	
B.D. +18° 305	2 22 29·99	+18 36 24·1	Abbadia 1086
B.D. +22° 457	3 10 23·20	+22 42 27·5	Abbadia 1421
B.D. +25° 678	4 04 35·72	+25 42 13·8	Gr_{1910} 1819
406 B. Tauri	5 46 46·19	+27 57 09·5	Amer. Ephem.
21 Tauri	3 41 54·91	+24 20 58·0	
22 Tauri	3 42 03·33	+24 19 22·7	
B.D. +27° 799	5 30 26·13	+27 51 17·3	Gr_{1910} 2423
107 B. Aurigæ	5 31 44·09	+27 37 22·4	Amer. Ephem.
B.D. +27° 811	5 32 27·82	+27 52 25·1	Gr_{1910} 2451
B.D. +25° 1594	7 05 29·88	+25 50 31·6	Gr_{1910} 3604
B.D. +25° 1595	7 05 38·14	+25 50 45·8	Gr_{1910} 3606

Star	α	δ	Authority
	h m s	° ′ ″	
B.D. +25° 1596	7 05 42·13	+25 45 19·1	Gr_{1910} 3607
ψ Leonis	9 40 06·98	+14 19 40·4	Amer. Ephem.
B.D. +24° 1769	7 43 08·82	+23 49 52·3	Abbadia 4574
B.D. +27° 923	5 52 56·45	+27 18 40·1	Gr_{1910} 2716
B.D. +27° 943	5 55 57·11	+27 16 20·4	Gr_{1910} 2752

Observer : Prof. N. Goryatscheff.

Instruments : Zeiss telescope, 90-mm. aperture, magnifying power 90.

Observations made with eye and ear.

The time-corrections of the chronometer were found from the Bordeaux, Rugby and Nauen wireless signals.

Tomsk, Siberia, U.S.S.R.,
University Astronomical Observatory :
1934 *February* 22.